UNIVERSITY OF LONDON THESIS

Degree PhD Year 2007 Name of Author THOMAS, Richard Mark

COPYRIGHT

This is a thesis accepted for a Higher Degree of the University of London. It is an unpublished typescript and the copyright is held by the author. All persons consulting this thesis must read and abide by the Copyright Declaration below.

COPYRIGHT DECLARATION

I recognise that the copyright of the above-described thesis rests with the author and that no quotation from it or information derived from it may be published without the prior written consent of the author.

LOANS

Theses may not be lent to individuals, but the Senate House Library may lend a copy to approved libraries within the United Kingdom, for consultation solely on the premises of those libraries. Application should be made to: Inter-Library Loans, Senate House Library, Senate House, Malet Street, London WC1E 7HU.

REPRODUCTION

University of London theses may not be reproduced without explicit written permission from the Senate House Library. Enquiries should be addressed to the Theses Section of the Library. Regulations concerning reproduction vary according to the date of acceptance of the thesis and are listed below as guidelines.

A. Before 1962. Permission granted only upon the prior written consent of the author. (The Senate House Library will provide addresses where possible).

B. 1962-1974. In many cases the author has agreed to permit copying upon completion of a Copyright Declaration.

C. 1975-1988. Most theses may be copied upon completion of a Copyright Declaration.

D. 1989 onwards. Most theses may be copied.

This thesis comes within category D.

☐ This copy has been deposited in the Library of _____

☑ This copy has been deposited in the Senate House Library, Senate House, Malet Street, London WC1E 7HU.

Csk is an important negative regulator of phagocyte responsiveness in vivo:

Characterisation of myeloid cell-specific Csk deficiency in mice by conditional mutagenesis (cre/loxP).

Communication submitted for Doctor of Philosophy

2004

Richard Mark Thomas

Molecular Genetics and Immunity

Windeyer Instiitute for Medical Sciences

University College London.

ProQuest LLC
789 East Eisenhower Parkway
P.O. Box 1346
Ann Arbor, MI 48106-1346

ABSTRACT

Whilst the recruitment of phagocytic leukocytes is fundamental to the innate response against pathogenic infection, the inappropriate mobilisation of their cytotoxic potential can also lead to fatal tissue injury. To determine the contribution of Csk, a negative regulator of Src family kinases, to the regulation of phagocyte recruitment and activation *in vivo*, mice lacking Csk in the myeloid lineage were generated using conditional mutagenesis (cre/loxP). This Csk deficiency resulted in acute multifocal inflammation in skin and lung, accompanied by extramedullary haematopoiesis in the spleen and liver, and increased myelopoiesis in bone marrow. Animals were protected from the disease in a microbiologically controlled environment, but remained hypersensitive to LPS-induced shock. Csk-deficient granulocytes showed enhanced spontaneous and ligand-induced degranulation accompanied by hyperinduction of integrins. Hyperresponsiveness was associated with hyperadhesion and impaired migratory responses *in vitro*. Biochemical studies revealed spontaneous accumulation of tyrosine-phosphorylated proteins, including hyperphosphorylation of key signalling proteins including Syk and paxillin. These data support a breakdown of the activation threshold set by Csk. Thus, Csk is critical in preventing premature granulocyte recruitment through enforcing the requirement for ligand engagement while supporting the migratory capacity of activated cells through negative regulation of cell adhesion. To address the incomplete Cre mediated deletion of floxed genes *in vivo*, a genetic approach to elevate Cre recombinase gene expression was developed. Whilst manipulation of regulatory elements including promoter, enhancer, and untranslated regions has yielded enhanced and sustained expression *in vitro*, this has been difficult to achieve *in vivo*. Here, it is reported that construction of artificial exons through insertion of short heterologous intron sequences into the open reading frames of the Cre recombinase and enhanced green fluorescent protein results in functional expression accompanied by a 30-fold increase in transcription levels *in vitro*. Furthermore, green fluorescence levels were enhanced five-fold in cell lines and enhanced considerably in the rat brain after transduction with a herpes simplex virus-based vector. These data define a method of improving both the level and duration of recombinant gene expression, in addition to and independently of surrounding regulatory elements. Significantly, the method should help to increase Cre recombinase expression from weak or transiently expressed promoters thus overcoming an important limitation of Cre/loxP technology – incomplete deletion. Furthermore, this method may also be applicable in gene therapy to obtain sustained and effective expression of recombinant proteins *in vivo*.

Abbreviations.

bp	base pair
BrdU	Bromo-2'-deoxyuridine
BSA	Bovine serum albumin
Cbp	Csk binding protein
Csk	C-terminal Src kinase
CD	Cluster of differentiation
DMEM	Dulbecco's Modified Eagles's Medium
eGFP	enhanced Green Fluorescent Protein
ELISA	Enzyme-linked Immunosorbent Assay
FACS	Flow Activated Cell Sorting
Fc	Fragment of crystallisation
fMLP	formyl-Methionyl-Leucyl-Phenylalanine
GCSF	Granulocyte Colony Stimulating Factor
GFP	Green Fluorescent Protein
HBSS	Hanks Buffered Saline Solution
HUVEC	Human Umbilical Vein Endothelial Cell
ICAM	Intercellular Adhesion Molecule
Ig	Immunoglobulin
IL-	Interleukin-
kD	kilo Dalton
LAD-1	Leukocyte Adhesion Deficiency-1
LPS	Lipopolysaccharide
MACS	Magnetic Activated Cell Sorting
MAdCAM	Mucosal Addressin Cell Adhesion Molecule
MAPK	Mitogen-Activated Protein Kinase
NPF	Nucleation Promoting Factor
Ntk	Nervous tissue and T-lymphocyte Kinase
PAG	Phosphoprotein Associated with Glycosphingolipid-enriched microdomains
PBS	Phosphate Buffered Saline
PECAM	Platelet-Endothelial Cell Adhesion Molecule
PKC	Protein Kinase C
PMA	Phorbol Myristate Acetate
PTPα	Protein Tyrosine Phosphatase-alpha
PMN	Polymorphonuclear cell
ROI	Reactive Oxygen Intermediate
SCAR/WAVE	Suppressor of cAMP receptor/WASP family verprolin homologous
SH2/3	Src Homology 2 or 3
SHP1	Src homology 2-containing tyrosine phosphatase 1
TLR4	Toll-like Receptor
TNFα	Tumor Necrosis Factor-alpha
UTR	Untranslated Region
VCAM	Vascular Cell Adhesion Molecule
WASP	Wiskott-Aldrich Syndrome Protein

Table of Contents

For Minor Corrections: Please see Addendum on inside back cover.

Table of Figure Headings

INTRODUCTION

Chapter 1: The Src family of protein tyrosine kinases

1.1 Src family of protein tyrosine kinases

Phosphorylation of proteins on tyrosine residues represents a specific and reversible molecular switch that allows the formation or disruption of regulatory connections between cell signalling components (Pawson and Scott, 1997). Hence, a balance between protein tyrosine kinase and protein tyrosine phosphatase activity is required for appropriate specificity and intensity of cellular signalling.

The Src family of non-receptor protein tyrosine kinases (Src-fk) has nine members: c-Src, c-Yes, c-Fgr, Fyn, Lck, Hck, Lyn, Blk, and Yrk. The family's founding member, c-Src, was originally identified after a causal relationship between viral infection and sarcomas in chickens by Peyton Rous. Stehelin et al. later identified the gene responsible required for transformation, v-src, as derived from the normal cellular gene c-src (Stehelin *et al.*, 1976). The majority of Src-fk members have restricted patterns of expression, particularly in the hematopoietic system. For example, Lck is found exclusively in the lymphoid compartment, in T lymphocytes and natural killer (NK) cells (Marth *et al.*, 1985). Blk is found exclusively in B-lymphocytes (Dymecki *et al.*, 1990). Furthermore, c-Fgr, Hck and Lyn are expressed in varying amounts in B-lymphocytes, platelets, and in the myeloid compartment. c-Src, c-Yes and Fyn are expressed more generally, with elevated expression in the brain (Soriano *et al.*, 1991).

1.2 Primary Structure.

All Src-fk have a highly conserved primary structure. The primary structure is characterised by:

An N-terminal myristoylation signal at glycine 2 allowing attachment to the cytoplasmic face of the plasma membrane (Buss and Sefton, 1985), followed by palmitoylation at cysteine positions 3 and/or 5 and/or 6, and a cluster of basic residues that in total mediate interaction with acidic phospholipids in the membrane (reviewed in Resh, 1994).

A 'unique' domain of 50 to 80 amino acids distal from the N-terminal myristoylation signal at glycine 2, where Src-fk diverge.

A Src homology 3 domain (SH3) – a proline rich sequence possibly involved in signal amplification (reviewed in Pawson and Gish, 1992)

A Src homology 2 domain (SH2) – mediates interaction with phosphorylated tyrosine residues in proteins (reviewed in Pawson and Gish, 1992)

The catalytic domain – a region containing the sites for autophosphorylation (tyrosine 416 in c-Src, tyrosine 394 in Lck), ATP binding and phospho-transfer (lysine 295 in c-Src, lysine 273 in Lck)

The C-terminal negative regulatory domain – region containing the major site for tyrosine phosphorylation *in vivo* (tyrosine 527 in c-Src (Cooper *et al.*, 1986) and tyrosine 505 in Lck (Bergman *et al.*, 1992).

For a diagrammatic representation, see figure 1.2.

Figure 1.2. Src and Csk family protein tyrosine kinase primary structures

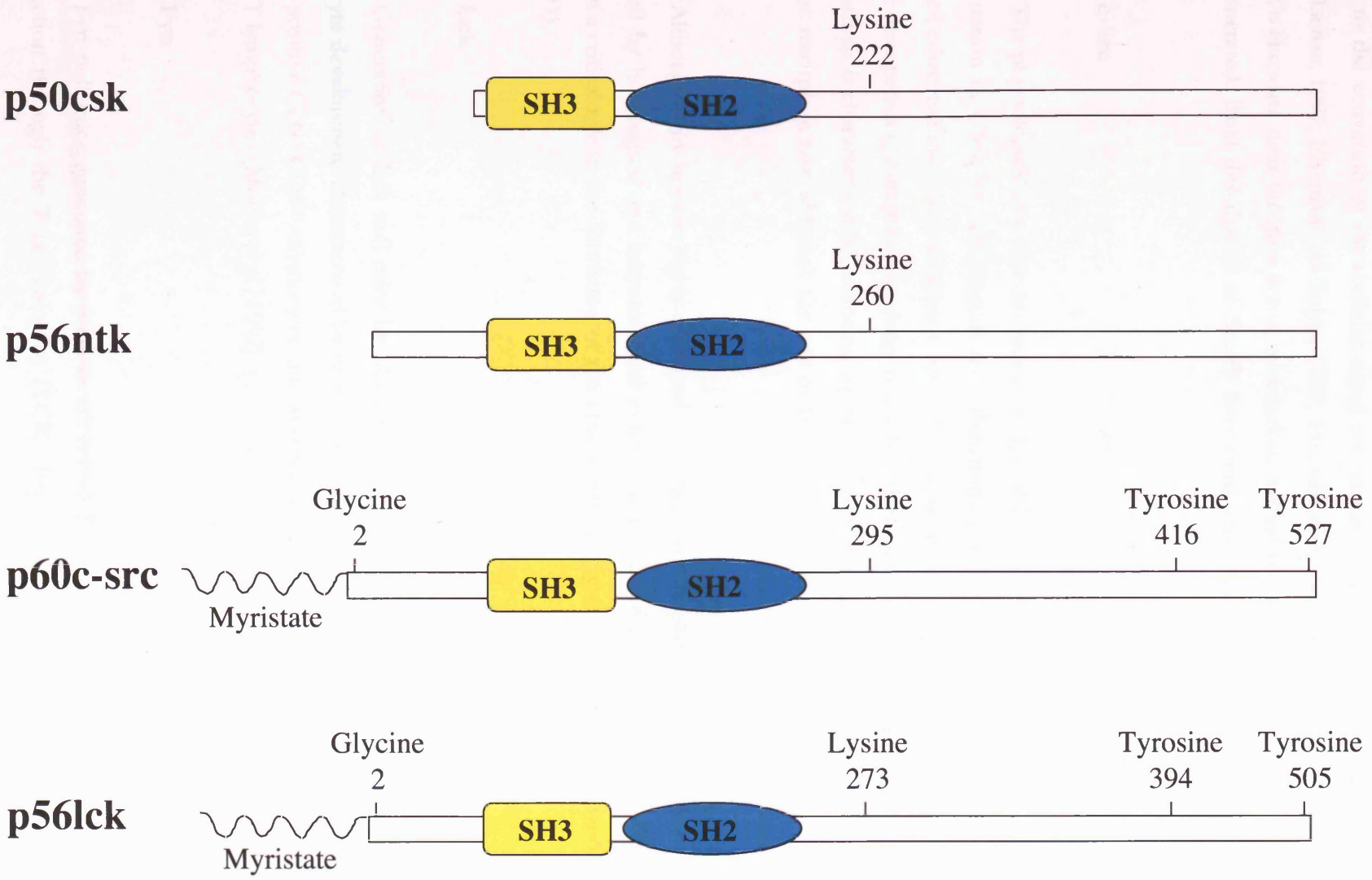

1.3 Function of Src family protein tyrosine kinases *in vivo*. An overview.

Src-fk associate with cell receptors, and are rapidly activated upon ligand binding, leading to the activation of intracellular signal transduction pathways (Courtneidge *et al.*, 1993; Daeron, 1997; Eiseman and Bolen, 1990; Eiseman and Bolen, 1992; Yamamoto *et al.*, 1993). To elucidate their function *in vivo*, mice lacking individual members of the Src-fk have been generated. Brief description of Src-fk knockouts and their phenotypes are outlined below:

1.3.1 c-Src

The physiological role of c-Src was investigated by Soriano et al., who introduced a null mutation in c-Src by homologous recombination in embryonic stem cells, and thus generated c-Src null mice. The resultant c-Src null mice are live-born but develop a recessive form of osteopetrosis, commonly resulting in death within the first few weeks of birth. The osteopetrosis is characterised by osteoclast dysfunction resulting in a significant decrease in the bone resorption rate, although the rate of bone formation hardly differs (Soriano *et al.*, 1991).

Although c-Src in most highly expressed in the brain and in platelets, no defects were observed by histological and hematological examination, indicating that c-Src does not perform a critical role in the formation of the central nervous system or platelets (Soriano *et al.*, 1991).

1.3.2 Lck

Generation of Lck null mice by Molina et al. revealed a critical role for Lck in thymocyte development characterised by profound thymic atrophy, significant reduction in double positive CD4+CD8+ thymocytes, and absence of mature single-positive CD4+ and CD8+ T lymphocytes (Molina *et al.*, 1992).

1.3.3 Fyn

Fyn null mice generated by Stein et al., revealed a critical role for Fyn in signal transduction through the T cell receptor (TCR). Fyn null thymocytes showed reduced

proliferation in response to Thy-1 cross-linking, and abrogated proliferation in response to TCR-CD3 cross-linking. Splenocytes exhibited normal proliferation in response to both stimuli (Stein *et al.*, 1992).

Furthermore, defective TCR signalling was confirmed in mice lacking the thymic isoform of Fyn generated by Appleby et al. Here, thymocytes were refractory to stimulation with PMA, in conjunction with TCR-CD3 complex or concanavalin A, and showed a significant reduction in calcium fluxes and proliferative responses (Appleby *et al.*, 1992).

Grant et al demonstrated the involvement of Fyn in the development of the hippocampus. Fyn null mice revealed impaired long-term potentiation, characterised by impaired spatial learning (Grant *et al.*, 1992).

1.3.4 c-Fgr

c-Fgr null mice are born at the expected Mendelian ratio and show no overt phenotype. Total cell numbers and percentages of cell types in the myeloid and lymphoid compartments are normal. Furthermore, normal histology was displayed in bone marrow, spleen, thymus, liver, lymph nodes, and peripheral blood cells. Macrophages phagocytosed latex beads and soluble IgG coated sheep erythrocytes normally indicating no dysfunction of Fc-receptor signalling. Resting, primed, or activated macrophages revealed no difference in the expression or kinase activity of c-Src, Hck, or Lyn, indicating no compensation for c-Fgr deficiency (Lowell *et al.*, 1994).

1.3.5 Hck

Hck null mice are born at expected Mendelian ratios and show no overt phenotype. Like c-Fgr null mice, total cell numbers and percentages of cell types in the myeloid and lymphoid compartments were normal, and normal histology was displayed in bone marrow, spleen, thymus, liver, lymph nodes, and peripheral blood cells from c-Fgr null mice. Unlike c-Fgr null mice, thioglycolate-induced inflammatory macrophages derived from Hck null mice reveal reduced phagocytosis of soluble IgG coated sheep erythrocytes, and albumin-coated latex beads, indicating defects in both Fc-receptor dependent and independent phagocytosis. Resting and activated Hck null macrophages compared to wild-type macrophages revealed no significant difference in Lyn expression. However, a 2-3-fold increase in Lyn kinase activity

was observed in Hck deficient macrophages suggesting functional compensation for the loss of Hck (Lowell *et al.*, 1994).

1.3.6 Lyn

Lyn mice are viable and fertile and born at the expected Mendelian ratios. Leukocyte development in mice lacking Lyn is essentially normal with the exception of abnormalities in the B-lymphocyte lineage and in mast cell function. Lyn null mice have reduced numbers of recirculating B cells which demonstrate impaired proliferation to cross-linking of surface immunoglobulin. Lyn null mice also demonstrate elevated levels of serum IgM indicating an elevation in the total number of IgM-producing plasma cells in these mice. These mice also show impaired immune responses to both T-dependent and T-independent antigens. Mast cell function abnormalities became apparent when Lyn null mice demonstrated defective IgE-mediated anaphylaxis indicating an essential role for Lyn in FcεR1 signalling. Lyn null mice also develop severe glomerulonephritis as a result of IgG immune complex deposition in the kidney. These reported data demonstrate a critical role for Lyn in immunoglobulin-mediated signalling (Hibbs *et al.*, 1995).

1.3.7 Hck/Fgr

Hck/c-Fgr null mice develop normally and are born at the expected Mendelian ratios. Again like the c-Fgr null mice, Hck/c-Fgr null mice presented no abnormalities in the numbers or percentages of cells in the myeloid and lymphoid compartments, and histology of the bone marrow, spleen, liver, thymus, lymph nodes, and peripheral blood cells was normal. However, Hck/c-Fgr null mice demonstrated an increased susceptibility to infection with Listeria monocytogenes (Lowell *et al.*, 1994). Purified bone marrow PMN from Hck/c-Fgr null mice adherent to fibrinogen, fibronectin, or collagen coated surfaces do not produce reactive oxygen intermediates (ROI) in response to tumor necrosis factor (TNFα) or formyl-methionyl-leucyl-phenylalanine (fMLP) but respond normally when stimulated with immune complexes or PMA indicating a specific defect in integrin signalling (Lowell *et al.*, 1996). Additionally, PMN from Hck/c-Fgr null mice directly cross-linked upon anti-β2 and anti-β3 antibody coated surfaces, or TNFα-primed PMN plated upon endothelial leukocyte integrin counter-receptor ICAM-1 coated surfaces failed to produce ROI. In contrast, single mutant c-Fgr null or Hck null PMN responded as wild-type PMN under these conditions (Lowell *et al.*, 1996). Hck/c-Fgr null mice also exhibit hypo-responsiveness to lipopolysaccharide (LPS)

demonstrated by resistance to the high dose model of endotoxemia (Lowell and Berton, 1998). PMN from Hck/c-Fgr mice also demonstrate defective adhesion-dependent degranulation in response to TNFα (Mocsai *et al.*, 1999). Impaired integrin-mediated signal transduction, and reduced motility accompanied with altered cytoskeletal structure is observed in Hck/c-Fgr null macrophage (Suen *et al.*, 1999).

1.3.8 Hck/Fgr/Lyn

Hck/Fgr/Lyn null mice develop normally and are fertile. Bone marrow derived and peritoneal elicited triple mutant macrophage do not demonstrate any defects in LPS-induced activation showing normal levels or moderately enhanced levels of nitrite, interleukin-1, interleukin-6, and TNFα. Moreover, activation of extracellular signal-related kinases 1 and 2, Jun N-terminal kinase, and the transcription factor NF-κB are equivalent in normal and mutant macrophages after LPS stimulation. Importantly, this study demonstrates that Src-fk Fgr, Hck and Lyn are not requisite for LPS-induced signal transduction in macrophages (Meng and Lowell, 1997). Fcγ-receptor mediated phagocytosis is defective in Fgr/Hck/Lyn null mice demonstrated by diminished or delayed phagocytosis of opsonised erythrocytes, actin cup formation, respiratory burst, and activation of extracellular signal-related kinases 1 and 2, phosphatidylinositol-3-kinase, and p72Syk (Fitzer-Attas *et al.*, 2000). Furthermore, p38 MAP kinase activation by fMLP was abrogated by the Hck/Fgr/Lyn mutation resulting in decreased exocytic activity in granulocytes (Mocsai *et al.*, 2000).

In summary, five of the Src-fk (Lck, Fyn, Hck, Fgr, and Lyn), participate in signalling events in lymphocytes, macrophage and granulocytes. Src appears not to be clearly associated with these processes. Additionally, it is clear that impairment of signalling processes in the absence of specific Src-fk leads to altered cellular function. This demonstrates a critical role for Src-fk in governing cellular responses. However, the information gained from loss of function studies although important, is limited to the cellular response in the absence of specific Src-fk, and does not contribute to our understanding of the regulatory processes which govern the activity of Src-fk. How is Src family protein tyrosine kinase activity regulated?

Chapter 2 Regulation of Src family protein tyrosine kinase activity

The regulation of Src-fk activity is largely dependent on the phosphorylation of the C-terminal tyrosine residue (tyrosine 505 in Lck and tyrosine 527 in c-Src). Phosphorylation at this site results in attenuation of enzymatic function, whilst dephosphorylation at this site results in functional activation. Consistent with this observation, dephosphorylation of the C-terminal residue by acid phosphatase treatment results in a 10-20-fold increase in kinase activity (Cooper and King, 1986). Furthermore, over-expression of the protein tyrosine phosphatase PTPαwhich similarly dephosphorylates the C-terminal residue, results in elevated c-Src kinase activity, cell transformation, and tumorigenesis (Zheng *et al.*, 1992). Indeed, the PTPα knockout mouse generated by Ponniah et al. revealed reduced activity of c-Src and Fyn, associated with enhanced levels of phosphorylation at the C-terminal residue (Ponniah *et al.*, 1999). Moreover, direct mutagenesis of the C-terminal tyrosine residue to phenylalanine, results in constitutive activation in Src family members. This mutation in c-Src, c-Fgr, Lck, Fyn, and Hck results in the ability to transform fibroblasts (Amrein and Sefton, 1988; Cartwright *et al.*, 1987; Davidson *et al.*, 1994; Kmiecik and Shalloway, 1987; Piwnica-Worms *et al.*, 1987; Ziegler *et al.*, 1989).

Due to intrinsic low-level auto-phosphorylation of the C-terminal tyrosine residue, it was thought that phosphorylation was mediated by a distinct protein tyrosine kinase. Okada and Nakagawa identified a novel protein tyrosine kinase that specifically phosphorylated the C-terminal tyrosine residue in c-Src (Okada and Nakagawa, 1989). Later, using a probe constructed from a set of isolated cDNA's encoding novel protein tyrosine kinases, a gene designated *cyl* for consensus tyrosine-lacking kinase was isolated from the K562 human leukaemia cell line (Partanen *et al.*, 1991). During the same year, Nada et al, purified a protein-tyrosine kinase that specifically phosphorylates tyrosine 527 of c-Src from neonatal rat brain (Nada *et al.*, 1991) designated *csk* for C-terminal src kinase. Both groups identified a novel primary structure not found in other known subfamilies of cytoplasmic protein tyrosine kinases, and thus a novel protein tyrosine kinase family was born.

2.1 The Csk family of regulatory proteins

As outlined above, Csk was co-identified by Nada et al and Partanen et al. Analysis of the primary structure revealed similarities with the Src-fk, in that it possessed both a SH2 and SH3 domain, and a tyrosine kinase domain. However, in contrast, Csk lacks a membrane association domain, including both the myristoylation signal and palmitoylation sites allowing attachment to the cytoplasmic face of the cell membrane. Furthermore, the major tyrosine autophosphorylation site, and the C-terminal negative regulatory tyrosine residue are absent in Csk (Figure 1.2) (Nada *et al.*, 1991; Partanen *et al.*, 1991).

Analysis of Csk tissue distribution revealed the highest expression in the spleen, with high levels also identified in the thymus, neonatal brain, lung and liver. Other tissues including the heart, kidney, and testis showed limited expression of Csk (Okada *et al.*, 1991).

The C-terminal regulatory tyrosine residue, Y527, in c-Src was shown to be directly phosphorylated by Csk, and was associated with a reduction in c-Src activity indicated by a decrease in enolase phosphorylating activity (Okada and Nakagawa, 1989). The C-terminals of Src-fk are conserved, suggesting that Csk may exert an effect on other Src-fk in addition to c-Src. Okada et al demonstrated that Csk phosphorylated the C-terminal tyrosine residue in Lyn and Fyn, and this was again associated with a reduction in kinase activity reflected in a decrease in enolase phosphorylating activity (Okada *et al.*, 1991). Furthermore, Bergman et al demonstrated Csk mediated phosphorylation of Lck at the C-terminal tyrosine residue, Y505. Suppression of Lck catalytic activity was also demonstrated with decreased ability to phosphorylate enolase (Bergman *et al.*, 1992).

A Csk homologue, Ntk (for nervous tissue and T lymphocyte kinase) possesses both a SH2 and SH3 domain and lacks the membrane association domain present in Src-fk. Unlike the ubiquitous expression reported for Csk, analysis of the tissue distribution of *ntk* revealed a restricted pattern of expression. *ntk* mRNA was most abundant in the brain, with high levels additionally expressed in the spleen and thymus. Low levels of *ntk* transcripts were additionally identified in the testis, ovary, and intestine. No expression of *ntk* was documented in the kidney, liver, and muscle. Ntk was shown to phosphorylate a Lck derivative specifically at the C-terminal tyrosine residue confirming that Ntk was a Csk-related enzyme (Chow *et al.*, 1994b). Furthermore, two distinct *ntk* cDNA's were isolated from two independent groups differing by the absence or presence of a proximal insertion of

a 136 base pair sequence. Characterisation of both cDNA's revealed the 136bp sequence was most likely an entire exon and the difference in transcript length was due to alternative splicing. Two distinct protein isoforms, p52ntk and p56ntk, are generated which are both localised in the cytoplasm. The extended amino terminus present in the p56ntk isoform is believed to provide additional sequences that may direct cellular localisation or to mediate distinct protein-protein interactions (Chow *et al.*, 1994a).

2.2 Csk binding protein (CBP)

Src-fk's are membrane associated via N-terminal myristoylation, and are proposed to transduce intracellular signals from associated transmembrane receptors. Csk, a negative regulator of Src-fk is a mainly cytoplasmic protein, which mediates protein tyrosine kinase activity through phosphorylation of a conserved C-terminal tyrosine residue. This presented a paradox – how could Csk, a cytoplasmic protein, exert its negative regulatory function upon Src-fk activity without a localisation signal that would target it effectively to its substrate?

A novel transmembrane protein designated Csk binding protein, Cbp, has been identified by Okada et al from rat neonatal brain, and shown to bind the SH2 domain of Csk and mediate its localisation to the cell membrane where it exerts its function upon Src-fk's (Kawabuchi *et al.*, 2000).

Cbp, a 46kDa protein (deduced molecular weight), is exclusively localised in the GM1 glycosphingolipid-enriched microdomain, also known as the detergent-insoluble glycolipid-rich membrane domain or lipid/membrane rafts. These structures are important in receptor-mediated signalling (reviewed in Langlet *et al.*, 2000). The expression profile of Cbp is very similar to Csk in that it is expressed ubiquitously, with expression most prominent in the neonatal brain, thymus, spleen, lung and testis. The primary structure of Cbp possesses a short extracellular domain (residues 1-17), a putative transmembrane domain (residues 18-38), putative myristoylation sites (residues 39 and 42), and a long cytoplasmic domain containing nine putative tyrosine phosphorylation sites.

Site directed mutagenesis of specific tyrosine residues in the cytoplasmic tail of Cbp identified Y314 that is critical for binding to Csk and consequent localisation of Csk to the plasma membrane. Elegant transfection experiments using COS7 cells showed that in the absence of Cbp, exogenous Csk was diffused within the cytoplasm. In the presence of Cbp,

the majority of Csk was co-localised to the cytoplasmic face of the plasma membrane. Site-directed mutagenesis of the tyrosine residue at position 314 to phenylalanine abrogated Csk co-localisation with Cbp (Kawabuchi *et al.*, 2000).

Further work from Takahashi et al., revealed that phosphorylated Cbp and Csk co-purified as a large protein complex consisting of at least 4 Csk-Cbp units. Furthermore, using an *in vitro* reconstitution Csk assay, this study demonstrated that the addition of phosphorylated Cbp, but not unphosphorylated Cbp, stimulated Csk activity towards Src. This work not only reconfirms that Cbp is involved in the regulation of Src-fk through recruitment of Csk, but also reveals that Cbp exerts its effect through activating Csk directly (Takahashi *et al.*, 1988).

2.3 Phosphoprotein associated with glycosphingolipid-enriched microdomains (PAG)

The predicted molecular weight of PAG is 47kD, and reveals an almost identical primary structure to Cbp. PAG consists of a short extracellular domain (PAG residues 1-16; Cbp residues 1-17), a putative transmembrane domain (PAG, residues 17-36; Cbp, residues 18-38), a putative myristoylation site, and a long cytoplasmic domain containing ten tyrosine residues, nine of which are putative tyrosine phosphorylation sites. Further assessment of PAG demonstrated that it is identical to the glycosphingolipid-enriched microdomain (GEM)-associated and Fyn-associated pp80, and to the major leukocyte tyrosine-phosphorylated 80kD polypeptide. Comparison between untreated and pervanadate treated Jurkat T cells revealed that similar to Cbp, the electrophoretic mobility of PAG depends on the level of phosphorylation - 68-70kD and 85kD respectively. The involvement of PAG in $\alpha\beta$T lymphocyte activation was shown through stimulation of $\alpha\beta$T lymphocytes with CD3/CD28, which resulted in rapid dephosphorylation of PAG and concomitant dissociation from Csk, presumably allowing activation of Src-fk and signal amplification (Brdicka *et al.*, 2000).

2.4 Csk knockout model

The role of Csk in development has been examined by two groups; Nada and co-workers, and Imamoto and Soriano. Both groups employed knockout technology to develop Csk null mice, but used different methods of targeting the csk gene. Both studies revealed a

recessive lethal phenotype at mid-gestation, characterised by growth retardation and necrosis in the notochord and neural tube (Nada *et al.*, 1993; Imamoto and Soriano, 1993)).

Genetic analysis of embryos obtained from intercrosses between $Csk^{+/-}$ mice revealed normal Mendelian ratios of expected genotypes (~25% for $Csk^{+/+}$ embryos, ~50% for $Csk^{+/-}$ embryos, and 25% for $Csk^{-/-}$ embryos) up to E10.5. Neither group could recover $Csk^{-/-}$ embryos by E11.5 due to embryonic death and absorbtion. $Csk^{+/+}$ and $Csk^{+/-}$ littermates were born at expected Mendelian frequency (Nada *et al*, 1993; Imamoto & Soriano, 1993).

Analysis of embryos showed that E8.5 $Csk^{-/-}$ embryos could not be distinguished from their littermates. At E9.5, the majority of $Csk^{-/-}$ embryos were from one-quarter to one-half of the size of their littermates and remained at the 10-12 somite stage. Further analysis revealed that the $Csk^{-/-}$ embryos had not turned, a process where the germ layers are reversed, and the lordotic curvature of the trunk turns into a strong dorsal, kypnotic bend. Development of the neural tube appeared to initiate properly, proceeding through the hind-brain, but the anterior and posterior neuropores remained open, preventing normal differentiation. This was evident in the marked number of necrotic cells and decreased number of mitoses in the ependymal layer of the neural tube (Nada *et al*, 1993; Imamoto & Soriano, 1993).

2.4.1 Enhanced kinase activity of Src-fk

To assess the involvement of Csk in the negative regulation of Src-fk activity, two independent groups examined the ability of specific immunoprecipitated Src-fk to phosphorylate enolase, a commonly used substrate for c-Src in *in vitro* kinase assays. Nada's group analysed the kinase activity of c-Src, Fyn and Lyn in E.8.5 to E10.5 Csk null embryos. Imamoto and Soriano immortalised cells from E.9.5 Csk null embryos with SV40 large T antigen and analysed c-Src activity. An 11-fold increase in enolase phosphorylation was reported by Imamoto and Soriano, whereas an approximate 14.7-fold increase was reported by Nada et al (Nada *et al*, 1993; Imamoto & Soriano, 1993). Concomitantly, both groups reported a decrease in c-Src protein expression in the $Csk^{-/-}$ embryos compared to other genotypes. This may be due to ubiquitin-mediated degradation of active Src-fk (Harris *et al.*, 1999). Nada et al further reported an increase in specific kinase activity for Fyn and Lyn, 3.9- and 8.5-fold respectively. Imamoto and Soriano further demonstrated that in the absence of Csk, phosphorylation of Y527 in c-Src was reduced to 20-50% of the level in wild-type cells.

These data are consistent with Cooper and King's report where removal of approximately 80% of phosphate groups from Y527 in c-Src by acid phosphatase treatment yields a 10-20-fold increase in kinase activity (Cooper and King, 1986). Furthermore, replacement of the tyrosine residue at position 527 with phenylalanine in c-Src also results in a 13-fold increase in specific kinase activity (Kmiecik and Shalloway, 1987). Together, these data reveal that reduced phosphorylation of the C-terminal tyrosine residue in the absence of Csk leads to functional activation of Src-fk, Src, Fyn, and Lyn. This identifies Csk as a critical negative regulator of Src-fk in embryo development.

2.4.2 Cortactin, a major hyperphosphorylated protein in Csk-deficient fibroblast-like cells

Due to limited experimental material derived from Csk null embryos, a direct genetic approach was utilised to generate immortalised cells. Mice heterozygous for the Csk allele were mated with p53-deficient mice allowing further characterisation of the Csk null phenotype *in vitro*. Rhodamine-phalloidin staining for F-actin distribution revealed a reduction in the number of stress fibres compared to controls (Nada *et al.*, 1994). Furthermore, this study revealed that culturing of Csk-deficient cells in non-coated dishes revealed lower numbers of focal contacts. However, these cells were able to associate tightly to gelatin-coated plates. Moreover, analysis of Csk-deficient cell monolayer cultures revealed higher cell densities compared to controls. These data imply that Csk-deficient cells exhibit a partially transformed phenotype, most likely as a result of enhanced tyrosine kinase activity. Consistent with previous reports, Csk-deficient cells demonstrated a reduced expression of c-Src, concomitant with a dramatic increase in specific kinase activity. The major tyrosine phosphorylated protein in Csk-deficient fibroblast-like cells was identified as cortactin. Cortactin was found to be directly associated along the stress fibres in control cells, whilst it was dispersed in the cytoplasm in Csk-deficient cells, suggesting that c-Src may control the localisation of cortactin through tyrosine phosphorylation, and maybe additionally involved in the organisation of stress fibres. Other major tyrosine phosphorylated proteins in Csk-deficient embryos resolved to 125kD, 95kD and 58kD. The identity of these proteins is unknown (Nada *et al.*, 1994). These data identify the importance of Csk-mediated negative regulation of Src-fk in stress fibre formation and cell adhesion.

2.5 Lack of regulatory control in the absence of Csk does not lead to cellular transformation.

v-Src, other variants of c-Src that lack the regulatory tyrosine residue at position 527, and constitutive reduction of phosphorylation at Y527 by over-expression of PTPα, are capable of transforming fibroblast cell lines in vitro (Cooper and King, 1986; Courtneidge, 1985; Zheng *et al.*, 1992). However, Nada et al showed that fibroblast-like cells cultured from E9 $Csk^{-/-}$ embryos undergo a limited number of cell division cycles, are not able to grow in soft agar, and were not tumorigenic when injected into nude mice, indicating that a deficiency in Csk is not sufficient for immortalisation, transformation or tumorigenesis (Nada *et al.*, 1994). These data suggest that in the absence of regulatory control by Csk, the reduction in phosphorylation of the C-terminal tyrosine residues in Src-fk is not sufficient for transformation. However, reduced Csk expression had been observed in a number of tumors. Inversely, adenoviral over-expression of Csk in the NL-17 mouse colon cancer cell line down regulated Src kinase activity, and suppressed tumor metastasis *in vivo*, without affecting tumorigenicity (Nakagawa *et al.*, 2000).

2.6 Conditional mutagenesis of Csk in T lymphocytes.

Although the impact of Csk-deficiency in development has been demonstrated, embryonic lethality has prohibited investigations into the importance of Csk and its contribution to the negative regulation of Src-fk in the function of specific cell systems, for example, the immune system. Through exploitation of the Cre/loxP recombination system (see section 3.4), this limitation has been overcome, and furthermore, has provided a powerful tool to investigate the role of Csk in T-lymphocytes (Schmedt *et al.*, 1998).

Using Cre/loxP technology, the role of Csk in T-lymphocyte development and function has been determined. LoxP sites were introduced into the Csk locus by homologous recombination in mouse embryonic stem cells to enable deletion of exons 9 and 10, which encode an essential fragment of the Csk kinase domain, and mice homozygous for the floxed Csk allele were generated ($csk^{fl/fl}$). MX-Cre mice (Kuhn *et al.*, 1995), which carry the Cre transgene under the control of the type I interferon-inducible promoter, were mated with $csk^{fl/fl}$ mice to inactivate Csk in an array of cell types. Resultant mice manifested an impairment of antigen receptor-mediated development and selection of T-lymphocytes. Inactivation of Csk precluded the requirement for the pre- and αβ-T cell receptors, and

major histocompatibility (MHC) class II for the development of double positive CD4+8+ and single positive CD4+ thymocytes, as well as peripheral CD4 αβT-lineage cells (Schmedt *et al.*, 1998). Importantly, bypassing embryonic lethality associated with Csk knockout mice using Cre/loxP conditional mutagenesis has identified a critical role of Csk in adaptive immunity, however, its role in innate immunity remains elusive.

Chapter 3. Conditional mutagenesis of Csk in myeloid cells.

3.1 Inflammation and the innate response – an introduction.

The recruitment of phagocytic leukocytes plays a central role in the immediate response to microbial infection through phagocytosis and destruction of invading pathogens and the elicitation and maintenance of the inflammatory state. Importantly, phagocytic cells recruited to a local site of infection produce inflammatory mediators promoting further recruitment of new phagocytic cells and activation of cell function, which include cytokines such as, IL-1, IL-6, IL-8, Il-12 and TNFα, and other mediators including nitric oxide (NO), leukotriene B4, prostaglandins, peroxides and oxygen radicals. The combined local effects of these mediators include activation of vascular endothelium, increase in vascular permeability, and activation of neutrophils, lymphocytes and natural killer cells.

Under normal conditions, resting post-capillary venule endothelium is relatively inert and does not recognise circulating leukocytes. Stimulation of endothelium with proinflammatory agents including IL-1, TNFα, or lipopolysaccharide (LPS), induces expression of endothelial cell surface molecules which specifically interact with counter-receptors upon activated leukocytes enhancing their interaction and migration across blood vessel walls into the surrounding tissues. The molecules involved in these events belong to three different structural groups; the immunoglobulin gene superfamily, the integrin family, and the selectin family.

3.1.1 The Immunoglobulin superfamily

The counter-receptors for β2 integrins are members of the immunoglobulin (Ig) family which include intercellular adhesion molecules (ICAM's), vascular cell adhesion molecule-1 (VCAM-1) (Elices *et al.*, 1990), platelet-endothelial cell adhesion molecule-1 (PECAM-1) (Newman *et al.*, 1990) and mucosal addressin cell adhesion molecule-1 (MAdCAM-1) (Briskin *et al.*, 1993). They all contain at least one immunoglobulin (Ig) domain, consisting of 70-110 amino acids with a disulphide bridge that spans 50-70 residues that folds the domain in the typical tertiary structure present in antibodies.

Currently, five ICAM's have been identified: ICAM-1 (CD54) (Marlin and Springer, 1987; Rothlein *et al.*, 1986), ICAM-2 (CD102) (Staunton *et al.*, 1989), ICAM-3 (CD-50)

(Fawcett *et al.*, 1992), ICAM-4 (LW – Landsteiner-Weiner red cells) (Hermand *et al.*, 2000), and ICAM-5 (telencephalin) (Tian *et al.*, 2000). Whilst ICAM-2 is consitutively expressed on endothelial cells, ICAM-1 is expressed at relatively low levels upon resting endothelium. Exposure of endothelium to proinflammatory agents induces up-regulated ICAM-1 expression (Dustin *et al.*, 1986; Pober *et al.*, 1986). ICAM-1 and ICAM-2 both bind to LFA-1, whilst ICAM-1 can additionally bind to Mac-1 (see section 3.1.2 for LFA-1 and Mac-1), on neutrophils, macrophages, and T-lymphocytes. VCAM-1 is expressed on the luminal surface of LPS, IL-1 or TNFα activated endothelium. Together, these interactions provide a mechanism for selective recruitment of leukocytes in an inflammatory environment.

3.1.2 The Integrin family

Counter-receptors for ICAM's and VCAM-1 belong to the integrin family. Integrins are heterodimeric transmembrane proteins composed of two covalently linked gene products, designated the α and β chain. There are 18 different integrin α-chains and 8 different β-chains, which couple together in specific combinations dependent on cell type. Importantly, these combinations provide a diversity of integrin receptors, which as a result increases the number of ligands that can be recognised. The cell surface expression of integrins expressed in phagocytic leukocytes is outlined in Table 3.1.2.

Exposure of phagocytic leukocytes to proinflammatory agents dramatically influences cell surface expression of many of the integrins stated in table 3.1.2, in particular, the β2 family of integrins. The majority of β2 integrins in polymorphonuclear neutrophils (PMN) are stored within intracellular vesicles which following activation are mobilised and fuse to the plasma membrane resulting in increased cell surface expression. There are four β2 integrins, each possessing a unique α (CD11a-d) subunit in combination with a common β2 (CD18) subunit. The rapid cell surface exposure of β2 integrins transforms the neutrophil from a quiescent cell compatible with circulation to a fully primed cell compatible with migration into tissues. The importance of β2 integrins in PMN cell function is perhaps best illustrated by the congenital disorder – leukocyte adhesion deficiency-1 (LAD-1), which is characterised by an absence or deficiency of β2 integrin cell surface expression, and is associated with increased susceptibility to bacterial infection and failure of neutrophils to respond normally to chemoattractants, and to bind and migrate across the endothelium at sites of infection (Anderson and Springer, 1987; Kuypers and Roos, 1989).

Integrins	*Counter-receptors*
β1	
α4/β1 (CD49d/CD29; VLA-4)	Fibronectin, VCAM-1
α5/β1 (CD49e/CD29; VLA-5)	Fibronectin
α6/β1 (CD49f/CD29; VLA-6)	Laminin
β2	
αL/β2 (CD11a/CD18; **LFA-1**)	ICAM-1, ICAM-2, ICAM-3
αM/β2 (CD11b/CD18; CR3; **MAC-1**)	ICAM-1, ICAM-2, C3bi, Fibrinogen, Lipopolysaccharide and others.
αx/β2 (CD11c/CD18; gp150/95)	C3bi, Fibrinogen, Lipopolysaccharide
αD/β2 (CD11d/CD18)	ICAM-3
β3	
αv/β3 (CD51/CD61)	Vitronectin, Entactin and other RGD- and KGAGDV containing ECM proteins.

Table 3.1.2 Integrins expressed by phagocytic leukocytes

For more detailed literature concerning the ligands of β1, β2, and β3-integrins, please see references within (Berton and Lowell, 1999).

In the LAD-1 disorder, all mutations are found within the β2 (CD18) chain gene located on chromosome 21 (Weitzman *et al.*, 1991), the consequence of which is an absence, or a deficiency, or an adoption of an abnormal β chain structure which precludes association with the a chain precursor in the endoplasmic reticulum, which is prerequisite for further processing from an immature to mature glycoprotein in the Golgi apparatus. Mice lacking CD18 manifest a similar phenotype to human LAD-1 patients, with the exception of a severe dermatitis restricted to CD18 knockout mice (Scharffetter-Kochanek *et al.*, 1998).

3.1.3 Selectins

There are three types of selectins involved in the attachment of leukocytes to the endothelium, L-selectin (LECAM-1, LAM-1), E-selectin (ELAM-1), and P-selectin (gmp140, CD62). Each of these three selectins has an NH2-terminal carbohydrate recognition domain characteristic of Ca^{2+}-dependent (C-type) lectins, followed by an epidermal growth factor (EGF)-like motif, a series of short concensus repeats characteristic of complement regulatory proteins, a transmembrane domain, and a cytoplasmic tail (Hensley *et al.*, 1994; Moore *et al.*, 1994; Ushiyama *et al.*, 1993).

L-selectin (CD62L) is expressed on leukocytes and is required for binding of carbohydrate ligands that are constitutively expressed on peripheral lymph node endothelial cells, and inducibly expressed on endothelial cells at inflammatory sites (McEver, 1994), associated with the α-granules of platelets, and Weibel-Palade bodies of endothelial cells, is rapidly mobilised to the plasma membrane upon cellular activation by thrombin, histamine, and peroxides (Hattori *et al.*, 1989; Hsu-Lin *et al.*, 1984; Patel *et al.*, 1991). E-selectin (CD62E) is transiently synthesised and expressed on cytokine-activated endothelial cells (McEver, 1994).

Cellular ligands for selectins include sialylated and fucosylated oligosaccharides, the architype of which is sialylated $Lewis^X$ (sLe^X). sLe^X and related structures are linked to glycoproteins and glycolipids on most leukocytes and some endothelial cells. Furthermore, leukocyte cell surface expression of both sialic acid and fucose are required for selectin interaction. Evidence for a role of sLe^X as an important cell ligand for P-selectin was provided by anti-CD15 (which recognises the Le^X blood group) antibody blocking studies that prevented binding of P-selectin to PMN and monocytes (Larsen *et al.*, 1990). Evidence assigning sLe^X as a ligand for E-selectin arose from an elegant transfection study demonstrating that transfection of a human fucosyltransferase cDNA (responsible for expression of the sialylated Lewis x tetrasaccharide) into nonmyeloid cell lines confers E-selectin-dependent endothelial adhesion (Lowe *et al.*, 1990). PMN, but not lymphocyte, L-selectin is modified with the vascular selectin ligand sLe^X and specifically binds E-selectin transfected cells (Picker *et al.*, 1991). Furthermore, mAbs to L-selectin partially inhibit attachment of flowing neutrophils to E- or P-selectin suggesting that L-selectin may be a ligand for vascular selectins under flow (Abbassi *et al.*, 1993; Jones *et al.*, 1993)

The importance of selectin-mediated adhesion is perhaps best demonstrated by the congenital disorder – leukocyte adhesion deficiency II (LADII), which is characterised by a lack of sLe^X ligand as a result of impaired fucose metabolism (Etzioni *et al.*, 1992), and is associated with increased susceptibility to bacterial infection and failure of neutrophils to bind and migrate across the endothelium at sites of infection. Furthermore, the roles of L-, P-, and E-selectins have been genetically defined *in vivo* through generation of knockout mice. Mice lacking L-selectin mainfested delayed neutrophil migration in a sterile peritonitis model, associated with reduced leukocyte rolling (Arbones *et al.*, 1994). Mice lacking P-selectin showed delayed extravasation of neutrophils in a sterile peritonitis model, which was associated with an almost complete absence of baseline leukocyte rolling in mesenteric venules and neutrophilia (Johnson *et al.*, 1995; Mayadas *et al.*, 1993). In contrast to both mice lacking L-selectin or P-selectin, mice lacking E-selectin showed no defect in recruitment in a sterile peritonitis model (Labow *et al.*, 1994). However, mice lacking both P- and E-selectin manifest a more severe phenotype than mice lacking either selectin alone. Similar symtomology to the LADII disorder in humans is demonstrated in the double knockout mice, characterised by augmented susceptibility to opportunistic bacterial infection leading to increased mortality (Bullard *et al.*, 1996).

3.1.4 Molecular interactions between neutrophils and the endothelium

Emigration of neutrophils from the circulation to the sites of infection within tissues is thought to occur in four steps. The first step is mediated by the selectin family (see section 3.1.3). Release and translocation of P-selectin from Weibel-Palade bodies to the endothelial cell surface occurs within minutes of exposure to leukotriene B4, C5a, or histamine. Interaction of endothelial P-selectin with its the carbohydrate ligand, sialyl-Lewis^X (sLe^X), expressed on neutrophils contributes to neutrophil attachment and rolling upon the endothelial wall. However, the expression of P-selectin is short lived and is replaced by E-selectin (whose expression is regulated by TNFα and IL-1 but not IFNγ), which continues the endothelial-leukocyte interaction (Luscinskas *et al.*, 1991). These transient attachments expose the neutrophils to locally expressed signalling molecules.

The second phase involves the interaction between β2-integrins expressed on activated neutrophils (section 3.1.2), and immunoglobulin related intercellular adhesion molecules, ICAM-1 and ICAM-2, expressed on activated endothelium (section 3.1.1). The β2-integrins LFA-1 and Mac-1 (see table 3.1.2) adhere only weakly in quiescent circulating

neutrophils, however, exposure of neutrophils to chemoattractants (Campbell *et al.*, 1998; Gerszten *et al.*, 1999) or other activating agents results in increased affinity of the integrin for its ligand and/or integrin clustering that leads to increased avidity for its ligand, resulting in firm adhesion (reviewed in Stewart and Hogg, 1996 and van Kooyk and Figdor, 2000). Furthermore, evidence indicates that engagement of L-selectin involved in leukocyte rolling also increases the adhesiveness of β2 integrins for ICAM counter-receptors (Crockett-Torabi *et al.*, 1995; Gopalan *et al.*, 1997; Simon *et al.*, 1995; Simon *et al.*, 1999; Tsang *et al.*, 1997).

The third phase involves extravasation and crossing of the endothelial wall known as diapedesis. This process involves neutrophil LFA-1 and Mac-1 (Henderson *et al.*, 2001), in addition to the immunoglobulin-related PECAM-1 (CD31), which is expressed in the lateral borders between endothelial cells and the surfaces of neutrophils, monocytes, platelets, and some T cell subsets (reviewed in Muller, 1995). These interactions permit movement of neutrophils through the endothelium to the basement membrane where neutrophil surface bound proteolytic activity, assigned to granulocyte elastase and cathepsin G (Owen *et al.*, 1995), break down the proteins of the basement membrane, allowing passage to the site of infection in the fourth and final phase through migration towards chemoattractant cytokines.

3.2 Aims of investigation

Recruitment of leukocytes to the site of pathogenic infection requires trans-migration from the peripheral bloodstream into the surrounding tissues. As outlined in section 3.1, phagocyte recruitment and priming may largely be determined by the endothelial cell through expression of ligands for counter-receptors on leukocytes. However, the contribution to this process of cell autonomous negative regulatory mechanisms, which control phagocyte responsiveness remained unclear.

Initiation of intracellular signalling cascades by Src-fk represent a principal event in the adhesion dependent activation of cellular responses in phagocytes (see sections 1.3.7 & 1.3.8). Granulocytes and macrophages lacking Hck and Fgr exhibit impaired actin cytoskeletal remodelling, associated with reduced adhesion dependent mobilisation of the respiratory burst and granule secretion (Lowell *et al.*, 1996; Mocsai *et al.*, 1999). Furthermore, mice deficient in Hck and Fgr are hypo-responsive to LPS, and demonstrate impaired PMN migration into the liver parenchyma (Lowell and Berton, 1998). Src-fk are regulated by the coordinated action of protein tyrosine kinases and protein tyrosine phosphatases. It is

conceivable that deregulation of coordinated activity between these two types of enzymes may result in impaired function of phagocytic leukocytes.

Csk negatively regulates Src-fk activity via phosphorylation of their C-terminal inhibitory tyrosine residue (Nada *et al.*, 1991; Partanen *et al.*, 1991). Csk expression is most prominent in the spleen, with high levels also identified in the thymus, neonatal brain, lung and liver. Other tissues including the heart, kidney, and testis also show limited expression of Csk (Okada *et al.*, 1991). The widespread expression of Csk suggests that it may serve as a master regulator controlling Src-fk activity. Furthermore, Csk homologues, Ntk/Ctk also expressed in hematopoietic cells may contribute to this process (Chow *et al.*, 1994b). Moreover, the inhibitory effect exerted by Csk maybe further reinforced through constitutive association with the protein tyrosine phosphatase, PEP, which selectively dephosphorylates the activating tyrosine residue in the kinase domain of Src-fks (Cloutier and Veillette, 1996; Gjorloff-Wingren *et al.*, 1999; Wang *et al*, 2001).

To address whether Csk and its contribution to the negative regulation of Src-fk is critical in the regulation of phagocyte cellular responses *in vivo*, Csk was inactivated in a cell-type specific manner. Utilising Cre/loxP technology (see section 3.4 for Cre/loxP recombination), embryonic lethality associated with germline mutagenesis of Csk was circumvented, and myeloid cells were targeted for conditional gene inactivation. Myeloid cell specific Cre mice were generated using a targeted knock-in strategy, inserting Cre recombinase within frame to an endogenous coding region juxtaposed to the granulocyte elastase promoter (Tkalcevic *et al.*, 2000). Csk floxed mice were constructed and obtained from Christian Schmedt (Schmedt *et al.*, 1998). By intercrossing these mice, a conditional Csk deficiency restricted to myeloid cells, primarily granulocytes, was generated.

3.3 Problems with previous studies and existing models

Src-fk are intimately associated with cell surface receptors. Upon ligand binding, a rapid transient activation of specific Src-fk occurs, mediated in part by autophosphorylation of the tyrosine residue in the catalytic domain. Activated Src-fk participate in the initiation and/or amplification of cellular signals to the nuclear compartment ultimately resulting in altered gene expression (Daeron, 1997; Eiseman and Bolen, 1990; Eiseman and Bolen, 1992; Yamamoto *et al.*, 1993).

The physiological roles of individual members of Src-fk have been elucidated through production and characterisation of knockout mice (See section 1.3). Furthermore, redundancies particularly between Hck, Fgr, and Lyn kinases have been addressed through the production and characterisation of double and triple knockouts. These studies have demonstrated diverse roles for Src-fk from being involved in osteoclast function (c-Src) to spatial learning (Fyn) to phagocyte responsiveness (Hck, c-Fgr, Lyn). However, these studies do not contribute to our understanding of the negative regulatory processes that dictate Src-fk function *in vivo*.

Recently, research interest towards elucidating the processes involved in the negative regulation of Src-fk has increased. Evidence is accumulating that Src-fk activity is inhibited by complex and highly regulated mechanisms that involves protein tyrosine kinases (Csk; Imamoto and Soriano, 1993; Nada *et al.*, 1993), protein tyrosine phosphatases (SHP-1, CD45; Burns *et al.*, 1994; Cahir McFarland *et al.*, 1993; Somani *et al.*, 1997) and ubiquitin ligases (Cbl; Rao *et al.*, 2002) amongst others. Genetic evidence indicates that negative regulatory machinery is crucial for normal cell function. Indeed, as detailed in section 2.4, mice lacking Csk manifest a recessive lethal phenotype, characterised by growth retardation and necrosis in the notochord and neural tube (Nada *et al*, 1993; Imamoto & Soriano, 1993). The importance of negative regulation of Src-fk is further demonstrated in immune cell function. The protein tyrosine phosphatase, SHP-1, exerts negative control upon Src-fk function via dephosphorylation of the C-terminal negative regulatory tyrosine residue (Somani *et al.*, 1997). Mice lacking catalytically active SHP-1 manifest an acute inflammatory phenotype characterised by accumulation of myeloid cells within the pulmonary compartment leading to interstitial hemorrhagic pneumonia and early mortality (Rossi *et al.*, 1985).

Whilst knockout phenotypes illustrate the requirement of negative regulation in normal cell homeostasis, the contribution of specific cell types to a phenotype is difficult to define. A notable exception arises from mice lacking both catalytically active SHP-1 and rag-1, which manifest identical disease characteristics as mice lacking catalytically active SHP-1 alone, demonstrating that the phenotype is driven entirely by cells of the myeloid lineage (Yu *et al.*, 1996). In order to more accurately define the role of negative regulation in cell function, a strategy is required to inactivate gene function in a cell type specific manner, thus avoiding consequences of gene inactivation in other tissues that could mask a phenotype or

complicate data interpretation. Cell type specific gene inactivation is made possible using the Cre/loxP recombination system.

3.4 The Cre/loxP recombination system

The 1029 bp Cre recombinase nucleotide sequence (EMBL: X03454) derived from P1 phage encodes a 38kD protein of the L integrase family, which includes the yeast derived FLP and R recombinases (Craig, 1988; Sternberg and Hamilton, 1981). The Cre recombinase, herein referred to as Cre, recognises and mediates site-specific recombination at the locus of crossover (x) in P1, referred to as loxP. LoxP sites comprise of two 13bp palindromic inverted repeats interrupted by an 8bp non-palindromic sequence that dictates the overall orientation of the loxP site. Cre mediated recombination occurs between two loxP sites at least 82bp apart, with an outcome dictated by orientation of loxP sites (figure 3.4). Figure 3.4 shows the nucleotide structure and direction of the loxP site with regards to the non-palindromic 8bp sequence (Abremski *et al.*, 1983; Hoess *et al.*, 1982; Kilby *et al.*, 1993).

3.4.1 Generation of mice harbouring loxP flanked alleles

Typically, generation of conditionally gene targeted mice involves the construction of a targeting vector, whereby a selectable marker, typically neomycin, and the target gene of interest or a fragment thereof are both flanked by loxP sites ('floxed') taking caution to prevent interference with normal gene function. Commonly, a negative selection marker such as HSV-TK is additionally incorporated into the target vector construction so as to select against non-homologous recombination events. For an example, the gene targeting strategy for the generation of Csk floxed mice is shown (figure 3.4.1) (Schmedt *et al.*, 1998).

Identified homologous clones transiently transfected with Cre recombinase establish type I and type II Cre-mediated recombination events (figure 3.4.1). Type II recombination results in the removal of the selectable marker only, generating the desired floxed allele, whilst type I recombination additionally removes the floxed allele resulting in non-conditional gene inactivation or modification. Mice produced from ES cell clones with type I deletion harbour the inactivated or modified version of the target gene and clones with type II deletion give rise to mice with the floxed allele for conditional gene inactivation *in vivo*.

I) LoxP nucleotide structure

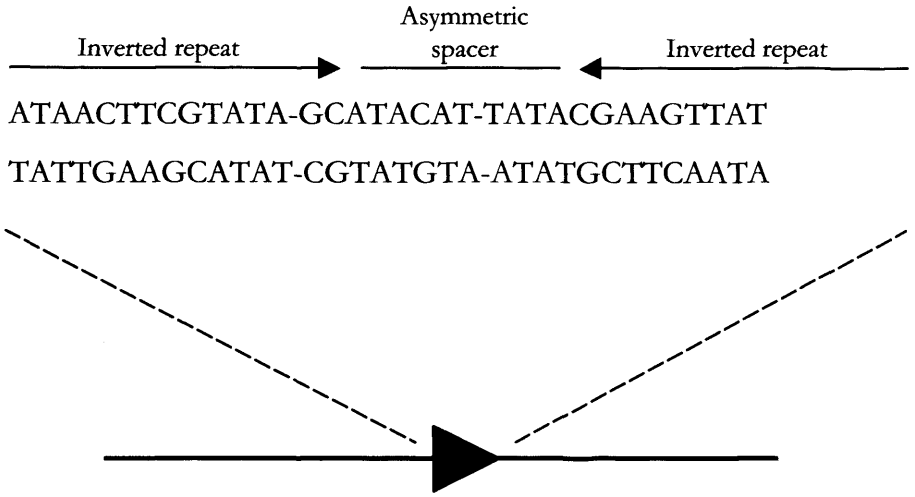

II) Cre mediated deletion and excision

III) Cre mediated inversion

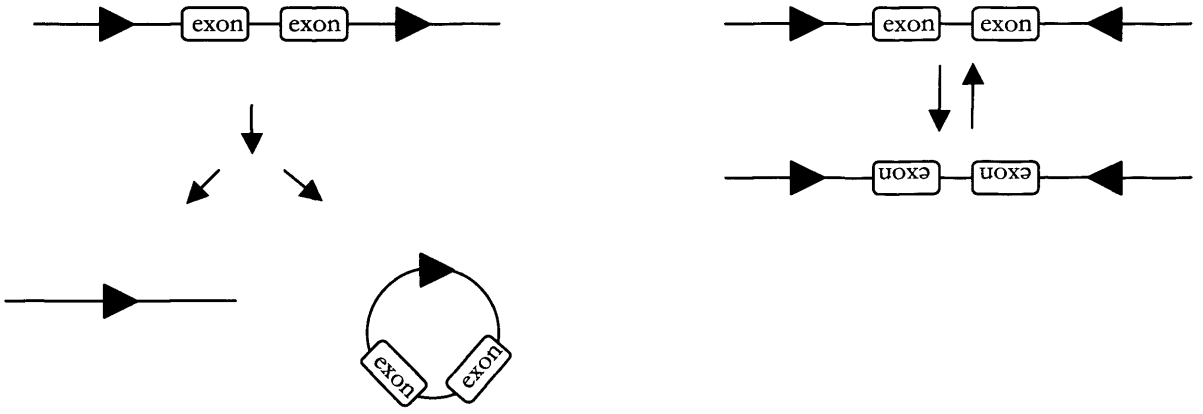

Figure 3.4 (I) LoxP nucleotide structure consisting of two inverted repeats of 13 base pairs and an asymmetric spacer region of 8 base pairs. The asymmetric spacer region determines the orientation of the loxP site typically represented by a filled triangle. Orientation of loxP sites determines type of recombination event. (II) Cre mediated recombination between two loxP sites in the same orientation results in deletion and excision of floxed DNA. (III) Cre mediated recombination between two loxP sites in the opposite orientation results in inversion of floxed DNA.

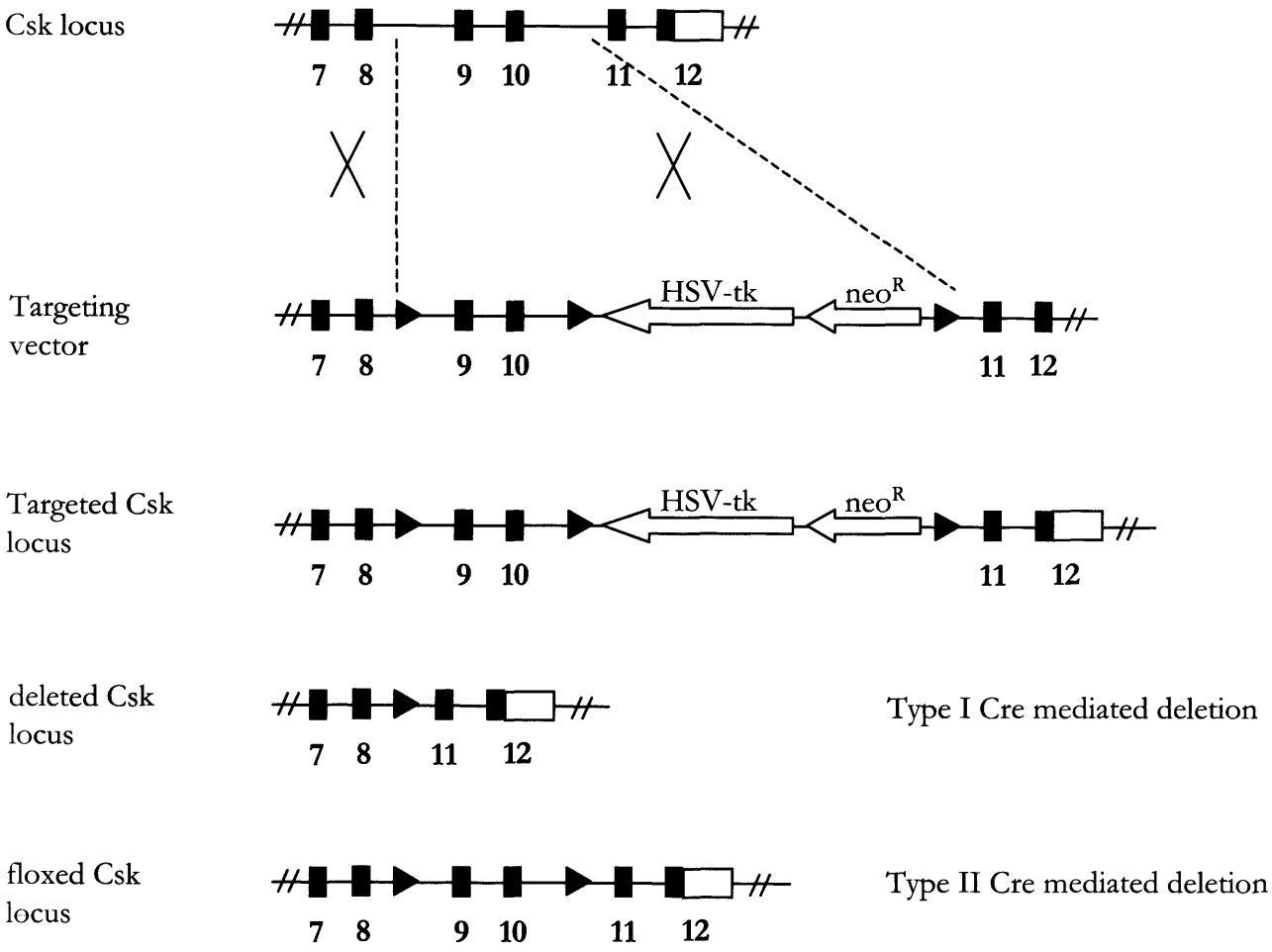

Figure 3.4.1. Gene targeting strategy for the generation of a floxed allele reproduced from Schmedt *et al.*, 1998. Numbered rectangles represent exons. Filled triangles represent loxP sites. The targeting vector is introduced into the embryonic stem cell genome via homologous recombination. Homologous recombinant ES clones transiently transfected with a Cre plasmid results in: Type I Cre mediated deletion which yields a modified or inactivated gene; or Type II Cre mediated deletion which yields the desirable floxed version of the gene. ES clones which have undergone type II Cre mediated deletion maybe used for the generation of floxed mice and conditional gene inactivation by Cre expression *in vivo*.

3.4.2 Cre transgenic mice

Two strategies are available for the production of Cre transgenic mice, either by introduction of Cre via a targeted knock-in strategy within frame to an endogenous coding region juxtaposed to a chosen promoter, or by pronuclear microinjection of conventional, randomly integrating transgene constructs. These strategies have been discussed in detail in Laboratory protocols for Conditional Gene Targeting (Torres M. and Kuhn R. Oxford University Press, 1998) and will not be discussed further.

Production of Cre transgenic mice requires identification and characterisation of a promoter region, to provide essential information on the onset and cell specificity of promoter-driven expression. Furthermore, expression levels from the promoter are important in establishing the level of Cre recombinase activity in a given cell type, and thus the efficiency of gene modification.

Currently, the efficiency of Cre-mediated deletion of a floxed allele and its relationship to the number of Cre molecules per cell has not been determined, but it is likely that a threshold level of Cre molecules per cell is required to obtain complete deletion of the desired floxed allele within a cell population. Incomplete Cre mediated deletion has been observed in conditional mice derived from Lck-Cre mice (Hennet *et al.*, 1995) and granulocyte elastase-Cre mice (this study) amongst others. Incomplete gene inactivation results in a subset of cells retaining functional copies of the targeted gene, which may disguise a potential phenotype and/or complicate data interpretation. Increasing Cre expression and thus the level of Cre molecules per cell may overcome this problem. In support, Gu et al demonstrated that increased Cre expression through introduction of a nuclear-targeting signal (Gu *et al.*, 1993) enhanced Cre recombination efficiencies. We report here a novel approach to increase Cre expression through the insertion of heterologous introns into the open reading frame.

3.4.3 Development of an enhanced Cre recombinase - the effect of introns upon gene expression.

Expression of recombinant genetic material plays a crucial role in elucidating gene function by transgenesis or cell type specific conditional mutagenesis, in recombinant production of therapeutic proteins in cell lines and transgenic animals (Archibald *et al.*, 1990;

Connelly *et al.*, 1996; Wall *et al.*, 1991), and perhaps most significantly, it is crucial to the treatment of genetic disease via gene therapy (Chuah *et al.*, 1995; Clemens *et al.*, 1995; Wang *et al.*, 1996; Yew *et al.*, 1997).

Contribution of promoter, enhancer and untranslated region regulatory sequences to gene expression through direct control of transcription rates or mRNA stability has been extensively reported in the literature and will not discussed further. In addition to these regulatory sequences, it has been shown that inclusion of introns contributes to mRNA stability, processing, and transport of mature mRNA to the cytoplasm. (Brinster *et al.*, 1988; Choi *et al.*, 1991; Palmiter *et al.*, 1991; Whitelaw *et al.*, 1991).

Brinster et al compared four different pairs of gene constructs, each identical apart from the presence or absence of introns, for mRNA expression in transgenic mice derived from pronuclear micro-injected mouse eggs. Analysis of liver and pancreas revealed that the absence of introns resulted in 10-100-fold decrease in the levels of expression compared to their wild-type counterparts. Moreover, frequency of expression was decreased with intronless constructs as indicated by a lower number of transgenic mice showing detectable mRNA levels. Nuclear 'run-on' experiments demonstrated that mRNA levels were proportional to the relative rate of transcription. This data supports the possibility that introns may contain sequences that are important for phasing nucleosomes relative to important promoter elements, so that the position and orientation of introns would be critical (Eissenberg *et al.*, 1985; Richard-Foy and Hager, 1987). Furthermore, introns are reportedly involved in stabilising mRNA's through the association of relatively unstable pre-RNA with spliceosomes, resulting in stabilisation and more efficient transport to the cytoplasm (Neel *et al.*, 1993).

To exploit the beneficial effects of introns on gene expression, using entire genomic loci would be ideal. However, many genomic loci have not been isolated or are simply too large to accommodate into vectors. To circumvent these problems, cDNA is used, but this is typically associated with inadequate gene expression *in vivo.*

Insertion of a heterologous intron or fragment of a genomic gene containing an intron into the 5' or 3' untranslated regions (UTR) of cDNA constructs has been associated with enhanced expression levels. Although these methods take advantage of the reported increase in mRNA stability and processing, the introduction of heterologous intronic sequences into

UTRs may lead to undesirable effects. 5'UTR intron insertion may introduce alternative transcription initiation sites or undesired regulatory sequences that interfere with bonafide recombinant gene transcription and translation, while 3'UTR intron insertion may lead to the normal stop codon becoming operationally redefined as a premature translation termination codon by the presence of a downstream intron, leaving the resultant pre-mRNA susceptible to nonsense-mediated decay (NMD). NMD represents a conserved surveillance mechanism that identifies faulty reading frames that have typically arisen through point or frameshift mutations, and eliminates the resultant imperfect messages that contain mutation-derived premature translation termination codons. (Carter *et al.*, 1996; Cheng *et al.*, 1990; Daar and Maquat, 1988; Hentze and Kulozik, 1999; Neel *et al.*, 1993; Thermann *et al.*, 1998; Urlaub *et al.*, 1989). Introduction of intronic sequences directly into the open reading frames of candidate recombinant genes would remove the potential for these undesired effects. Furthermore, the reported cooperative effect between introns in enhancing gene expression (Neel *et al.*, 1993; Nesic and Maquat, 1994) is not taken advantage of when inserting a single intron into a UTR, while the direct insertion of two heterologous introns into the open reading frame reported below indeed does. Here, a method is reported of creating artificial genes possessing exon/intron topology similar to that observed in normal mammalian genes, through the introduction of two heterologous introns directly into the open reading frames of two naturally intronless genes: the Cre recombinase (see section 3.4), and the red shifted enhanced green fluorescent protein (EGFP), a widely applied reporter gene (see section 3.4.4).

Introns used in this study were derived from the constant region of the immunoglobulin (Ig) IgM and IgE heavy chains. They were selected on the basis that firstly, they are short, thus minimising the size of the resultant construct. Secondly, immunoglobulins can be expressed in large quantities indicating that splicing is effective and compatible with high levels of protein expression. Thirdly, detailed surveys of immunoglobulin loci have provided no indication of detrimental regulatory sequences within these introns for non-B-lymphocytes. Finally, there is no indication that the introns chosen are subject to alternative splicing. These studies provide the foundation for future analysis to further define the importance of splice site recognition, exon definition, exon size, intron co-operation, polyadenylation site recognition and promoter specific effects through the precise insertion of different introns into specific genes.

3.4.4 An Introduction to Green Fluorescent Protein (GFP)

The GFP protein derived from the bioluminescent jellyfish *Aequorea victoria* was discovered by Shimomura et al (Shimomura *et al.*, 1962). The production of fluorescent light results from energy transferred from the Ca^{2+}-activated photoprotein aequorin to the GFP protein, converting the blue emission of the aequorin to green fluorescence of GFP1q.

The cDNA encoding GFP protein has been cloned (Chalfie *et al.*, 1994) and when expressed in heterologous prokaryotic or eukaryotic cells produces green fluorescence upon activation with blue or UV light. Heterologous expression of GFP requires no cofactors, substrates or gene products from *A.victoria* for chromophore activation and is limited only by its requirement for molecular oxygen and excitation light (Heim *et al.*, 1994).

GFP is stable and remains fluorescent after harsh biochemical treatments including SDS treatment, and formaldehyde fixing of cell or tissue samples. Detection of GFP may be performed in living cells and tissues. This has established GFP as an important reporter gene for biomedical research.

The development of enhanced GFP (EGFP), a red-shifted variant which demonstrates a four to thirty five fold increase of fluorescence over wild-type GFP, has improved the versatility of this genetic tool particularly for FACS-based or fluorescent microscopy-based analyses. Application of GFP and EGFP reporter genes in mammalian systems has been facilitated further by the generation of derivatives optimised for mammalian codon usage, aiding translational efficiency (Yang *et al.*, 1996; Zolotukhin *et al.*, 1996). Molecular evolution using DNA shuffling has additionally been utilised to develop a GFP derivative, which has been associated with improved conformational folding at 37°C and increased diffusibility of the resultant GFP within cells (Crameri *et al.*, 1996; Yokoe and Meyer, 1996).

The use of GFP and its variants including EGFP in the development of fusion proteins has provided the molecular tools necessary for study of diverse intracellular processes, including gene expression, subcellular localisation, protein dynamics and the cell cycle. GFP has been successfully targeted to the nucleus (Davis *et al.*, 1995), endoplasmic reticulum (Haseloff *et al.*, 1997), peroxisome (Kalish *et al.*, 1996), mitochondria (Rizzuto *et al.*, 1996), and Golgi body (Cole *et al.*, 1996). Generation of transgenic GFP mice has proved

more difficult. Many attempts of constructing an EGFP transgenic mouse have failed due to pre-natal or post-natal silencing of EGFP protein expression. However, mice which stably express GFP have been constructed through specific 'knockin' stategies, for example, the Oct-4:GFP mice (Yoshimizu *et al.*, 1999) and RAG2:GFP mice (Monroe *et al.*, 1999).

In this study, EGFP represents a useful investigative tool to assess the efficacy of recombinantly introduced heterologous introns on the expression of a naturally intron-less gene, at both the RNA and protein level.

EXPERIMENTAL PROCEDURES

Chapter 4 Methods in Immunological Analysis

4.1 Cytometric analysis

4.1.1 Antibodies used in flow cytometry analysis of mutant mice

Antigen	Antibody	Supplier
CD11b	M1-70/FITC	Pharmingen
CD16/32	2.4G2/Bio	Pharmingen
CD51	H9.2B8/Bio	Pharmingen
CD62L	MEL-14/Bio	Pharmingen
Gr1	RB6-8C5/Bio	Pharmingen
Gr1	RB6-8C5/FITC	Pharmingen
Gr1	RB6-8C5/PE	Pharmingen
B220	RA3-6B2/Bio	Pharmingen
B220	RA3-6B2/PE	Pharmingen
F4/80		Pharmingen
Streptavidin-cychrome	Cy	Pharmingen
Lactoferrin		Sigma
Anti-rabbit IgG	FITC	

4.1.2 Identification of leukocyte subsets through extracellular staining of cell-type specific markers and FACS analysis

Extensive analyses of immunological cell lineages have identified cell surface markers that identify specific leukocyte subsets. Gr1 (Ly-6G) is expressed specifically in granulocytes. The level of Gr1 expression is low ($Gr1^{lo}$) in immature granulocytes and high ($Gr1^{hi}$) in mature granulocytes. B220 is exclusively expressed in B-lymphocytes and F4/80 is exclusively expressed in non-bone marrow macrophages, for example, resident peritoneal macrophages and thioglycollate-induced inflammatory macrophages. CD11b (also known as Mac1 or $\alpha M\beta 2$-integrin) is expressed upon myeloid cells, including both granulocytes and

macrophages. For the purpose of the studies presented herein, mature granulocytes are identified by their $Gr1^{hi}$, $CD11b^{hi}$ characteristics. B-lymphocytes are identified by their $B220^{hi}$ characteristic and inflammatory macrophages by their $F4/80^{+}$, $CD11b^{hi}$ characteristics.

4.1.3 Isolation of bone marrow leukocytes

Animals were killed by CO_2 aphyxiation. Femurs were removed and flushed with PBS, 0.5% BSA with or without 0.01% sodium azide dependent on subsequent manipulation. Cell suspensions were removed leaving large particulate sediment and filtered through 30μm-nylon mesh to remove remaining cell clumps and other particulate matter. Unless otherwise stated, red blood cells were lysed for 1min at room temperature in ACK lysis buffer (0.15M NH_4C1, 10mM $KHCO_3$, 0.1mM Na_2EDTA, pH7.2). Cells were then washed once with PBS, 0.5% BSA with or without 0.01% sodium azide at 4°C.

4.1.4 Induction of sterile peritonitis and recovery of inflammatory granulocytes and macrophages.

Thioglycollate (TG) broth (3%, 0.7ml/20g bodyweight, Difco laboratories) was injected intraperitoneally. Animals were killed by CO_2 asphyxiation, and peritoneal exudates were recovered by peritoneal lavage with 8ml PBS containing 2mM EDTA. Inflammatory granulocytes and macrophages were recovered 4hrs and 4days post-TG administration respectively. Red blood cells were lysed by hypotonic lysis in ACK buffer (see above). No further enrichment was performed. Purity of resultant granulocyte and macrophage populations was confirmed by staining with monoclonal antibodies against Gr1 and F4/80 respectively, and the shared cell surface marker, CD11b. Purity of both populations was determined to be greater than 90%.

4.1.5 Purification of bone marrow granulocytes

Bone marrow leukocyte suspensions were blocked with 10% rat serum for 15min on ice, and subsequently stained with either biotinylated anti-Gr1 antibody (0.5μg/ml, Pharmingen) or biotinylated anti-B220 (0.5μg/ml, Pharmingen) antibody for 30min on ice to identify granulocytes or B-lymphocytes respectively. Selection of biotinylated stained cells was accomplished using a 1/5 volume of anti-biotin magnetic activated cell sorting (MACS;

Miltenyi Biotech) beads (typically 200µl) for a further 30min on ice. Bone marrow granulocytes were purified from cell suspensions by either enrichment of Gr1-Bio stained cells or depletion of B220-Bio stained cells respectively as described in the manufacturers protocol. **Unless otherwise stated depletion purified bone marrow granulocytes were used in all experiments.**

For some experiments, bone marrow granulocytes were stained with anti-Gr1-FITC (0.5µg/ml, Pharmingen) and sorted by fluorescent activated cell sorting (FACS) on a Coulter Epics Elite flow cytometer with Expo software (Applied Cytometry Systems, Coulter Corporation).

Confirmation of cellular purity of cell suspensions derived from either MACS and FACS sorting was determined by extracellular staining with specific cell type markers (See Section 4.1.6). Sorted granulocyte suspensions were stained with both anti-Gr1-FITC (0.5µg/ml, Pharmingen) and anti-CD11b-PE (0.25µg/ml, Pharmingen). Granulocytes were identified by their characteristic CD11b-hi expression and either their Gr1-lo expression (indicating immature granulocytes) or Gr1-hi expression (indicating mature granulocytes). Granulocyte purity was typically greater than 95% by FACS sorting or MACS granulocyte enrichment and greater than 90% by MACS B-lymphocyte depletion. Macrophages were stained with both anti-F4/80-FITC (0.5µg/ml, Pharmingen) and anti-CD11b-PE (0.2µg/ml, Pharmingen), and were identified by their characteristic CD11b-hi and F4/80+ expression. Macrophage purity was typically greater than 90% in cell suspensions recovered from thioglycollate-induced sterile peritonitis.

4.1.6 Extracellular staining for flow cytometry.

Unless otherwise stated, 1 x 10^6 cells were blocked with appropriate blocking agents, either rat, rabbit, or goat serum, in 96-well round bottom micro-titre plates at 4^0C on ice for 15 minutes. Blocked cell suspensions were resuspended in a 1 x antibody mix appropriate for the particular experiment. The following antibodies were used at the stated final concentrations: Gr1-FITC (0.5µg/ml); Gr1-PE (0.25µg/ml); CD11b-PE (0.25µg/ml); CD16/32-Bio (1µg/ml); CD51-Bio (2.5µg/ml); CD62L-Bio (0.5µg/ml); B220-PE (0.20µg/ml); F4/80-FITC (0.5µg/ml); Streptavidin-cychrome (0.25µg/ml); Lactoferrin (0.5mg/µl); Anti-rabbit IgG-FITC (0.5µg/ml). Cells stained with FITC and PE conjugated

antibodies were incubated for 15 minutes on ice. Cells stained with biotinylated antibodies were incubated for 30 minutes on ice followed by washing twice and resuspending in 1x streptavidin-cychrome (0.25μg/ml) and incubated for a further 15 minutes on ice. For analysis of lactoferrin expression, cells were incubated with anti-lactoferrin antibody for 30min on ice followed by washing twice and resuspending in 1x anti-rabbit IgG-FITC for a further 30mins. For binding of fibrinogen-FITC studies, cells were cultured for 30mins in the presence of 50μg/ml fibrinogen-FITC. Stained cells were washed twice immediately before flow cytometric analysis, and resuspended in 200μl of PBS, 0.5% BSA with or without 0.01% sodium azide.

4.1.7 Intracellular staining for flow cytometry

The protocol for extracellular staining was followed, with the exception that cells were permeabilised with 0.5% Triton X-100 in PBS for 5 minutes and subsequently washed extensively with PBS, 0.5% BSA before blocking and incubation with primary antibodies. Stained cells were washed twice with PBS, 0.5% BSA, 2mM EDTA and resuspended in 200μl immediately before flow cytometric analysis.

4.1.8 Examination of cells by flow cytometry

Stained cells were resuspended in 200μl PBS, 0.5% BSA, with oor without 0.01% sodium azide. Cellular fluorescence was quantified using the FL1 detector for FITC labelled cells, the FL2 detector for PE labelled cells, and the FL3 detector for cychrome labelled cells. Where erythrocyte lysis was not performed, a live gate was used in acquisition to exclude these cells. Acquired data was analysed with CellQuest (Becton Dickinson)

4.2 Endotoxic shock induction and analysis.

E.coli LPS 0111:B4 was reconstituted with sterile 1xPBS at 1mg/ml. Mice were challenged intra-peritoneally with either 0.5, 2.5, 5, or 10mg LPS/kg bodyweight and monitored twice daily for at least 10 days. For TNFα and IL-1 levels, mice were challenged with 5mg LPS/kg bodyweight for 90 minutes and 3 hours respectively. Peripheral blood was collected by cardiac puncture. Blood was allowed to clot at room temperature for 2 hours before placing on ice for 15 minutes to allow retraction of the clot. Samples were centrifuged

at 1700rcf and serum removed and stored at -20°C. Serum TNFα and IL-1 levels were analysed by ELISA (according to manufacturers instructions, R&D systems). Liver and lungs were also removed from these mice for histopathological assessment of PMN infiltrate. Extending this part of the study, mice were also sacrificed 8 hours post-endotoxin challenge. Neutrophil numbers were assessed through counting at least five random frames. One histopathologist scored all sections.

4.3 Immunohistochemistry.

All organs with the exception of lungs were immediately placed and fixed in formalin for no less than 24 hours. Lungs were gently inflated with formalin before clamping the trachea and fixing. Kidneys and heart were dissected longitudinally before paraffin embedding. Liver and lungs were embedded as whole organs. Paraffin sections were stained with eosin and haematoxylin.

4.4 Neutrophil apoptosis

1.6 x 10^6 bone marrow leukocytes were seeded into BSA-coated 24 well plates (PBS/1% BSA overnight at 4°C followed by washing with medium) containing 1ml DMEM supplemented with 5% HI-FCS, 20mM HEPES, 0.1mg/ml penicillin and 0.1mg/ml streptomycin. Some wells were further supplemented with 33ng/ml TNFα or 1000ng/ml LPS. These concentrations of TNFα and LPS had been experimentally defined and had shown by FACS analysis to induce maximal CD11b exposure and CD62L shedding in cultured Csk-deficient granulocytes (see figure 9.3d/e). Plates were incubated for 24hr or 48hr at 37°C and 5% CO_2. 1.6 x 10^6 freshly isolated bone marrow leukocytes were placed immediately into 0.5ml of PBS, 0.5% BSA, 0.1% NaN_3 on ice to serve as an uncultured control. At the specified time-points, plates were removed and placed immediately onto an iced water bath. Cells were resuspended by gentle pipetting and placed into 1.5ml eppendorf tubes containing 0.5ml PBS, 0.5% BSA, 0.1% NaN_3 in an iced water bath. Cells were centrifuged in swing-out buckets at 1500rpm for 5min, washed with 1ml PBS, 0.5% BSA, 0.01% NaN_3 and recentrifuged. Cells were stained with 0.25μg/ml Gr1-PE for 15 minutes as outlined in section 4.1.6 and washed. Annexin V-FITC was added at a 1/60 dilution as according to manufacturers instructions in 95μl of ice-cold binding buffer (140mM NaCl, 2.5mM $CaCl_2$, 10mM HEPES pH 7.4, 0.5% BSA). Cells were stained for 30mins before a further 400μl of ice-cold binding buffer was added to each tube. 200μl of stained mixture

was then placed into FACS tubes with propidium iodide (PI) and analysed immediately. A live gate was used in the acquisition of Annexin V positive cells to exclude cells that stained for PI. Each assay was performed in quadruplicate.

4.5 Neutrophil spontaneous priming and shape change

Bone marrow leukocytes were either fixed immediately in 0.5 vol ice cold PBS/12% formaldehyde or incubated in 200µl DMEM supplemented with 5%HI-FCS and 20mM HEPES at a cell density of 1 x 10^6 cells/ml for 30min at 37°C, 5% CO^2 in the presence or absence of 10µM PP2 (4-Amino-5-(4-chlorophenyl)-7-(*t*-butyl)pyrazolo[3,4-d]pyrimidine), a specific inhibitor of Src-fk, and/or 1µM PMA and then fixed. Fixed cells were stained with anti-Gr1-FITC and anti-CD11b-PE to identify granulocytes and were analysed by flow cytometry. To assess the extent of spontaneous priming, $Gr1^{hi}$ cells were gated and analysed for intensity of CD11b cell surface staining. Spontaneous priming becomes apparent in the acquisition of a $CD11b^{hi}$ phenotype. To assess shape change response of spontaneously primed neutrophils, $Gr1^{hi}$ cells were gated and their FSC profiles analysed. An increase of FSC correlates with acquisition of amoeboid morphology and remodelling of the actin cytoskeleton. This assay was performed on at least ten separate occasions.

To further delineate the priming response, bone marrow leukocytes were incubated for 30 minutes in the presence of known priming agents, TNFα, and LPS at different concentrations. Cells were fixed and stained with anti-Gr1-FITC, anti-CD11b-PE, and anti-CD62L-Bio/Streptavidin cychrome. To assess the contributory effect of these priming agents to granulocyte priming, $Gr1^{hi}$ cells were gated and analysed for intensity of CD11b and CD62L cell surface staining. Shedding of L-selectin (CD62L) from the cell surface represents another marker for granulocyte priming. This assay was performed in duplicate.

4.6 Mobilisation of secretory vesicles vs secondary granules.

Mobilisation and fusion of secretory vesicles to the neutrophil cell membrane was assessed by cell surface staining of the secretory vesicle marker CD16 (Fcγ receptor typeIII) (Detmers *et al.*, 1995). Bone marrow leukocytes were either fixed immediately or cultured as outlined in section 4.5 and then fixed. Fixed cells were stained with antibodies to Gr1/Ly-6G and CD11b (MAC1) to identify granulocytes and were further stained with an antibody to CD16/32. $Gr1^{hi}$, $CD11b^{+}$ cells were gated and analysed for intensity of CD16/32 cell

surface staining. Mobilisation and fusion of secondary granules to the neutrophil cell membrane was assessed in a similar fashion using an antibody against the specific granule marker CD51 (the α subunit of the vitronectin receptor) (Borregard *et al.*, 1997).

4.7 Neutrophil degranulation

Determination of lactoferrin release was determined using a modified method from that described in Mocsai et al. (Mocsai et al., 1999). Briefly, femurs were flushed with ice cold Ca^{2+}/Mg^{2+} free HBSS supplemented with 0.1% BSA, followed by hypotonic lysis of erythrocytes. Cells were maintained on ice in Ca^{2+}/Mg^{2+} free HBSS supplemented with 0.1% BSA until use, where cells were resuspended in HBSS containing calcium and magnesium at $4x10^6$ cells/ml. For suspension assays, cell suspensions (100µl/well) were dispensed into plates precoated with 1% BSA overnight at 4°C, and preincubated for 15min at 37°C, 5% CO2 in the presence or absence of 10µM cytochalasin B (CB) and/or 10µM PP2, before stimulation with 1µM fMLP (Sigma) or 100ng/ml PMA (Sigma). Cell suspensions were subsequently incubated for a further 15min before placing plates in an ice water bath for 2min, and centrifuging for 5min at 1800rpm. For adhesion assays, cell suspensions (100µl/well) were dispensed into uncoated, protein-coated or antibody-coated PVC plates (50µg/ml fibrinogen, or 100µg/ml anti-CD11b, or 100µg/ml anti-CD16/32 in 1xPBS overnight at 4°C followed by blocking with PBS, 1% BSA for 30min at room temperature. Serum coated plates were coated with undiluted FCS overnight at 4°C and received no further blocking. All plates were washed with 1xPBS immediately before use), centifuged at 30g for 3min to promote adhesion, and were incubated for 45min at 37°C, 5% CO_2 with or without 10µM PP2. Nunc Maxisorp F96 plates were coated with 50µl of culture supernatant overnight at 4°C or with known concentrations of human lactoferrin. All subsequent steps were carried out at room temperature and were separated by ten washes. Non-specific binding sites were blocked with PBS supplemented with 0.5%BSA and 0.5% Tween 20 (blocking buffer) for 1hr. Plates were then treated with affinity-purified rabbit anti-human lactoferrin (Sigma; 1/500 dilution in blocking buffer. Note, the reactivity of anti-human lactoferrin towards murine lactoferrin had been previously established (Mocsai *et al.*, 1999)) for 2hrs, followed by peroxidase-conjugated swine anti-rabbit (DAKO; 1/2000 dilution in blocking buffer) for 2hrs. Color was developed with TMB (3,3',5,5'-tetramethylbenzidine) liquid substrate (Sigma). Absorbance of wells were measured at 630nm using a Dynex MRX-TC plate reader. The human lactoferrin standard curve was used to determine murine lactoferrin release. Each assay was performed in quadruplicate.

4.8 Adhesion assay

96-well uncoated or serum-coated PVC plates (see section 4.7) containing 150µl of DMEM supplemented with 5% heat-inactivated fetal calf serum and 20mM HEPES (medium) were seeded with $1x10^6$ untreated or β2-integrin 'blocked' depletion purified bone marrow granulocytes in a 10µl volume. Blocking of β2 integrin receptors was accomplished by preincubating granulocytes with both anti-CD11b (100µg/ml) and anti-CD18 (100µg/ml) for 15min on ice in PBS/0.1% BSA followed by washing in medium. A further 150µl of medium was overlaid upon cell suspensions and the plates sealed with adhesive plastic. Cells were sedimented by centrifugation at 30g for 3min. Plates were subsequently incubated in a 37°C water bath for 30min. After incubation, plates were inverted and exposed to a centrifugal force of 755g for 5min. Remaining adherent cells were quantified with microscopy. Each assay was performed in quadruplicate.

4.9 *In-vitro* migration

In-vitro migration was determined by a transwell assay (3µm polycarbonate membrane; Corning) using depletion purified bone marrow granulocyte suspensions. Upper and lower chambers were filled with 100µl and 600µl of HBSS only or HBSS supplemented with 10^{-6}M fMLP respectively. 1 x 10^6 depletion purified bone marrow granulocytes were seeded into the upper chambers and plates were incubated for 45min at 37°C with 5%CO_2. The number of granulocytes that have migrated through the filter into the lower chamber was assessed by microscopy using a haemocytometer. Additionally, individual transwells were removed and their contents aspirated, washed with PBS, and aspirated again. The wells were subsequently placed in a fresh tissue culture plate with 600µl PBS, 10mM EDTA at 37°C for 30min to remove any granulocytes attached to the bottom of the filter. Negligible cell numbers were observed after this treatment. Surfaces of both lower chambers and transwells were checked microscopically after PBS, 10mM EDTA treatment and were demonstrated to be free of cells. Each assay was performed in triplicate.

4.10 Confocal microscopy

Bone marrow leukocytes were collected and either fixed immediately in formalin, or cultured for 30min at 37°C in DMEM, 5% heat-inactivated FCS, 20mM HEPES. For adhesion, cells were incubated for 45min at 37°C with 5% CO_2 on uncoated or fibrinogen-coated glass coverslips (50μg/ml fibrinogen in PBS overnight at 4°C followed by washing and blocking with PBS, 1% BSA for 30min at room temperature followed by washing with PBS) in HBSS medium, and then formalin fixed. Cells cultured in suspension were fixed in formalin and then adhered to polylysine coated glass coverslips before staining. All samples were blocked with 10% rat serum in PBS, 1%BSA for 15min before staining with biotinylated-CD11b (BDPharmingen; 10μg/ml in PBS, 1%BSA for 30min) and subsequently with streptavidin-cychrome (BDPharmingen; 3.3μg/ml in PBS, 1%BSA for 30min). Cells were then permeabilised with 0.1% Triton X in PBS for 5min, washed thoroughly, and stained with 3 units of Texas Red-conjugated phallacidin (Molecular Probes) in PBS, 1%BSA for 20min and washed three times with PBS. Immunofluorescent images were captured sequentially and overlayed using a Leica AOB System.

4.11 Other Neutrophil Assays

Respiratory Burst

Other functional consequences of neutrophil priming include induction of the respiratory burst which results from translocation and assembly of the cytosolic components of the NADPH oxidase enzyme system (p47phox, p67phox, and p21rac) with the membrane-associated flavo-cytochrome, cytochrome b558 (Morel *et al.*, 1991). Flavo-cytochrome b558 located on the membrane of secondary vesicles is translocated to the surface membrane during degranulation (Kjeldsen *et al.*, 1994; Jesaitis *et al.*, 1990). Since an increase in degranulation was observed in Csk-deficient granulocytes (see section 9.5), the ability of Csk-deficient granulocytes to reduce cytochrome c through production of superoxide ions was assessed in adhesion-independent cultures in the presence of 200nM fMLP and 2.5ng/mlPMA, and adhesion-dependent cultures upon tissue culture plastic and fibrinogen-coated plastic. Superoxide release was quantified using a modified previously described method (Lowell *et al.*, 1996). Briefly, uncoated or coated 96-well plates were filled with 50μl of 200mM ferricytochrome c in HBSS and prewarmed to 37°C. 50μl of bone marrow leukocyte suspension ($1x10^6$cells) in HBSS was added to each well, in the addition

or absence of stimuli, and immediately placed into a heated plate reader. Absorbance at 550nm and 490nm was recorded every 10mins. For some experiments, 30units of superoxide dismutase was added to wells to confirm that cytochrome c reduction was due to O_2^- production. For adhesion experiments, cells were centrifuged for 3min at 30g before placing into a heated plate reader. Unfortunately, with the instruments available in our laboratory and in my hands, a plausible positive read-out for respiratory burst could not be produced under any of the above conditions, even with the concentration of materials used.

Phagocytosis

Phagocytosis of microbial pathogens represents another important microbicidal function of granulocytes and is prerequisite for efficient killing. A number of methods exist to measure the rate of phagocytosis in granulocytes and macrophage, including uptake of FITC-labelled, heat killed *Candida albicans*. In this assay, phagocytosis of FITC-labelled, heat killed *Candida albicans* is allowed to procede for an experimentally predetermined time. Phagocytosis is stopped by placing granulocyte/C.albican cultures into prechilled 96-well plates containing a final concentration of 5μM cytochalasin B which inhibits actin polymerisation. The extent of phagocytosis is determined by FACS analysis of granulocytes identified by staining with a biotinylated monoclonal antibody against Gr1 followed by staining with streptavidin-cychrome (Fl3) and by forward/side scatter gating. Non-phagocytosed extracellular *C.albicans* spores are identified by staining with ethidium bromide at a final concentration of 1μM giving red fluorescence (Fl2). Ingested *C.albicans* are protected from ethidium bromide staining while green fluorescence (FITC) remains detectable (Fl1). Unfortunately, although this assay is extremely sensitive, it was decided by mutual discussion with J.Roes that it would be difficult to identify a significant difference in phagocytic potential in granulocytes derived from Csk-GEcre mice over controls since the granulocyte population derived from Csk-GEcre mice consists of approximately half Csk-deficient cells and half Csk-hemizygous cells (80% allelic deletion, figure 8.1c), and thus there would be considerable overlap within the entire Csk-GEcre granulocyte population making a comparison to a pure control granulocyte population unfeasable.

Chapter 5. Methods in Protein Chemistry

5.1 Immunoblot Analysis

Total bone marrow leukocyte and purified granulocyte suspensions were prepared as described. Cells were either maintained in PBS, 0.5% BSA, 2mM EDTA or cultured for 5 minutes at 37oC, 5% CO_2 in DMEM supplemented with 5% heat-inactivated fetal calf serum and 20mM HEPES in the absence or presence of LPS or TNFα. For some experiments, the Src family protein tyrosine kinase inhibitor, PP2 (4-Amino-5-(4-chlorophenyl)-7-(*t*-butyl)pyrazolo[3,4-d]pyrimidine), was used at 10μM. For experiments investigating phosphotyrosine levels, sodium vanadate was added to the culture medium after cell culture at a final concentration of 1mM before placing immediately upon ice. Cells were washed once with PBS or PBS, 1mM Na_3V0_4 for experiments investigating phosphotyrosine levels.

Proteins were solubilised at 95°C for 5 minutes with 16mM Tris-HCl [pH 6.8], 3% glycerol, 1.33% SDS, 0.33M DTT, 0.0033% Bromophenol blue, 25μg/ml TLCK, 1mM PMSF, 5μg/ml Leupeptin, and 5μg/ml Pepstatin. For experiments investigating phosphotyrosine levels, 1mM Na_3VO_4 and 50μM Na_2MoO_4 were additionally included. Solubilised protein lysates were placed on ice, sonicated twice for 10 seconds, and centrifuged at full speed for 10 minutes. Supernatant was removed and subjected to SDS-polyacrylamide gel electrophoresis and electrophoretically transferred to PVDF membrane. Membranes were blocked with PBS, 1% BSA, probed with various antibodies according to manufacturer's instructions, washed, and if necessary further probed with the appropriate peroxidase-conjugated secondary antibody according to the manufacturer's instructions. Immunoreactive proteins were visualised using enhanced chemiluminescence.

Table 5.1 Antibodies used for immunoblot analysis

Antigen	Antibody	Supplier
Goat IgG. Horse Radish Peroxidase (HRP) conjugated		Santa Cruz
Mouse Ig. Horse Radish Peroxidase (HRP) conjugated		Dako
Rabbit Ig. Horse Radish Peroxidase (HRP) conjugated		Pharmingen
Phosphotyrosine	RC20/HRPO	Transduction Laboratories
Cortactin	Rabbit polyclonal (H-191)	Santa Cruz
Phospho specific cortactin Y421	Rabbit polyclonal	Biosource International
Syk		
Phospho specific Syk Y519/520		
Csk	Rabbit polyclonal (C-20)	Santa Cruz
Paxillin	Mouse monoclonal (165)	Transduction Laboratories
Phospho-specific paxillin Y31	Rabbit polyclonal	Biosource International
c-Fgr	Rabbit polyclonal (C-1)	Santa Cruz
Hck	Rabbit polyclonal (M-28)	Santa Cruz
Lyn	Rabbit polyclonal (44)	Santa Cruz

5.2 Immunoprecipitation and kinase assay

Proteins were solubilised from purified granulocytes in modified TNE buffer (10mM Tris-HCl [pH7.5], 1mM EDTA, 150mM NaCl, 1% Nonidet P-40, 1mM Na_3VO_4, 50mM Na_2MoO_4, 1mM PMSF, and 25μg/ml TLCK, 5μg/ml Leupeptin, and 5μg/ml Pepstatin) on ice for 10min. Lysates equivalent to 1 x 10^7 cells were incubated with 1μg of the anti-Hck antibody in 500μl of modified TNE buffer at 4°C for a minimum of 1hr. After adsorbing to protein G sepharose (Pharmacia Biotech), immunoprecipitates were washed three times with lysis buffer and twice with kinase assay buffer (20mM HEPES, 1mM $MnCl_2$, 1mM DTT, 100μM Na_3VO_4). Immunoprecipitates were incubated in the presence of 2.5μg of acid-denatured enolase and 5μM [γ-^{32}P]ATP in 20μl of kinase assay buffer at 30°C for 10min. Phosphorylation was stopped by adding 20μl of ice-cold 2x SDS-PAGE sample buffer and

heating at 95°C for 3min. Phosphoproteins were resolved by SDS-polyacrylamide gel electrophoresis followed by autoradiography or quantification using Storm imager. This assay was performed in duplicate.

Chapter 6. Methods in Molecular Biological Techniques

6.1 Restriction digestion.

Restriction enzymes were purchased from Boehringer Mannheim, Promega, New England Biolabs and Helena Biosciences. Typically, a four to five fold excess of enzyme was used for restriction of plasmids and PCR products.

6.2 Gel electrophoresis.

Agarose gels were prepared with 0.5xTBE at agarose concentrations appropriate for the resolution of specific restriction digests or PCR products. Ficoll loading buffer (Maniatis et al) was used for DNA loading and gels were resolved, at between 80V and 150V, dependent on subsequent application. Gels were visualised on Flowgen video camera apparatus and analysed using AlphaImager software.

6.3 Gel purification.

Required DNA fragments were excised from the agarose gel under short-wave UV to prevent UV induced mutagenesis. Purification of gel slices was performed using QIAQuick DNA purification columns (Qiagen) as according to manufacturers instructions.

6.4 Ligation.

Ligation of DNA fragments was performed using T4 ligase (Gibco BRL) as according to the manufacturers 5min ligation protocol. The quantity of DNA used was determined empirically with respect to the molar quantity of termini per microgram of DNA. This was calculated using the following formula: $2x10^6/(660 \times$ no. of base pairs of fragment). Typically, the vector to insert ratio employed was 10fmol/60fmol respectively. Vector fragments were treated with shrimp alkaline phosphatase (USB technologies) as according to manufacturers instructions, purified and resuspended in dH_2O prior to ligation.

6.5 *E.coli.* Transformation

E.coli DH5α were prepared as according to Hanahan described in Maniatis et al. *E.coli* SCS110 were prepared using $CaCl_2$ as described in Maniatis *et al.* Both were stored in individual reaction aliquots of 50μl at -70°C prior to use. For transformation, aliquots were thawed on ice, supercoiled DNA or ligation mix was added at no more than 10% of cell volume, allowed to incubate on ice for 30min, followed by heat-shock at 42°C for 90 seconds and placed immediately on ice for a further 5min. Recovery medium, typically either 2YT, LB, or SSC medium was added to a final volume of 1.5ml, and the cell suspension transferred to a sterile bijou tube to aid aeration, and placed in a shaking incubator at 37°C for 30min for ampicillin-based vectors and 60min for kanamycin-based vectors. Cells were recovered via centrifugation at 14,000rpm for 1min, resuspended in 100μl of residual medium, plated onto appropriate antibiotic agar plates, and incubated overnight at 37°C.

6.6 Plasmid DNA recovery - plasmid miniprep.

5ml overnight cultures were prepared from single bacterial colony inoculations. Typically, cultures were decanted into 1.5ml eppendorf tubes, the cells recovered via centrifugation at 14,000rpm for 1min and the supernatant discarded. For reasonably pure DNA, a modified alkaline lysis as according to Maniatis was employed. Briefly, cell pellets were resuspended in 100μl Glucose buffer (0.05M Glucose, 0.025M Tris pH8, 0.01M EDTA pH8) followed by the addition of 200μl of freshly prepared cell lysis solution (0.2M NaOH, 1%SDS). Lysates were gently mixed by invertion up to six times. Addition of 150μl high salt buffer (3M KAc supplemented with 28.75ml Acetic acid/250ml) followed by inversion up to six times precipitated proteinaceous material. Supernatant was recovered after centrifugation at full speed for five minutes, and treated with a phenol/chloroform extraction to further removed proteinaceous contamination. DNA was precipitated from resultant supernatant via addition of 1ml 100% ethanol and recovered via further centrifugation at 14,000rpm for 10min. DNA pellets were washed with 70% ethanol, resuspended in ddH_20 supplemented with 20μg/ml RNAase, incubated at 37°C for 20min and studied using restriction digestion and agarose gel analysis. Pure DNA required for DNA sequencing was prepared using Qiagen mini-prep columns as according to manufacturers instructions.

6.7 Cytoplasmic RNA extraction.

CHO cells were harvested at 50% confluency, centrifuged at 1500rpm for 5min, supernatant discarded, washed with ice-cold 1xPBS and re-centrifuged. Cells were treated with ice-cold lysis buffer: 150mM NaCl, 10mM Tris pH7.4, 1mM $MgCl_2$, 0.5% NP-40, 10mM Vanadyl complexes, on ice for 5min prior to extraction and micro-centrifuged at full speed for 5min at 4°C. Supernatants were transferred to independent tubes containing 50µl of 10% SDS and 200µl Tris-buffered phenol, vortexed hard, micro-centrifuged for 2minutes at full speed and re-extracted with Tris-buffered phenol. The aqueous phase was transferred to independent tubes containing 1ml ethanol and 40µl 3M NaAc and micro-centrifuged for a further 15min to pellet RNA. All residual supernatant was removed, the pellet allowed to air-dry for 5min and resuspended in 100µl DEPC treated water. Quantification of RNA was determined using the 1D-MULTI densitometry software from AlphaImager Inc.

6.8 cDNA synthesis.

First strand cDNA synthesis was carried out using Superscript II supplied by Gibco BRL as according to manufacturers instructions using oligo dT primer and 1 µg total RNA derived from CHO cell extractions.

6.9 Slot blot analysis.

Total RNA was denatured using formaldehyde/formamide composition as described in Maniatis. Titrations of denatured total RNA were performed as required, typically five serial 1:2 dilutions from 3.3µg to 0.033µg RNA. Slot blot apparatus was assembled using Genescreen plus (DuPont, NEN Research Products) membrane according to manufacturers instructions. Vacuum was applied to remove excess liquid from membrane and absorbant paper. Wells were washed 3 x 50µl 10xSSC (DEPC treated). Denatured total RNA was loaded into washed wells followed by further washing with 3 x 50µl 5M NH_4Ac (DEPC treated). The slot blot apparatus was dismantled, the membrane removed and placed at 80°C for 1hr before hybridisation.

The resulting membrane was pre-hybridised for at least four hours in 20ml formamide buffer (50% formamide, 5xDenhardt's, 1% SDS, 5xSSPE, 10% Dextran sulphate)

supplemented with 10μg/ml denatured salmon sperm DNA at 55°C. Radio-labelled DNA probes were prepared using ^{32}P-dCTP (Amersham-Pharmacia Biotech) and the random-priming labelling kit (Boehringer Mannheim) as according to manufacturers instructions using 20ng template DNA. Unincorporated nucleotides were removed by passing the resultant probe through a G-50 Sephadex column. Purified radio-labelled probe was eluted in 1 x TE, denatured at 96°C for 10min, and snap-cooled on ice for 5min before addition to freshly prepared formamide buffer without salmon sperm supplementation. Pre-hybridisation solution was decanted from the hybridisation tube, replaced with hybridisation solution and incubated at 55°C overnight. The membrane was washed as described in Genescreen plus membrane protocol booklet for RNA hybridisation. Specific washing conditions was probe dependent and adapted forthwith.

The membrane was wrapped in Saran wrap and exposed to a phosphor-imager cassette (Storm technologies) overnight. The phosphor-imager cassette was analysed using the Storm phosphor-imager and software.

Re-probing was conducted after stripping the membrane of radioactive signal via washing in boiling 0.1% SDS until signal had diminished to background levels as determined with a Geiger counter and re-exposure to a phosphor-imager cassette.

6.10 DNA sequencing.

Template DNA was amplified and purified for sequencing using the protocol and reagents supplied by the DNA sequencing kit (PE Applied Biosystems). Resulting samples were run on the ABI 373 automated sequencer. Acquired sequence data was analysed using Editview (Perkin-Elmer) and GCG (HGMP, Cambridge, UK.) software packages.

6.11 Polymerase chain reaction.

Hot-starts were employed in all PCR reactions to aid sensitivity. Template DNA was prepared in 25μl volume of 1x PCR buffer (500mM KCl, 100mM Tris-Cl, pH 9.0, 0.1% Triton X-100), exposed to a 5min hot-start at 96°C and subsequently paused at 80°C. Remaining PCR constituents were provided in a 2X reaction buffer (20pmoles of each specific primer, 3-5 units Taq polymerase, 1x PCR buffer, 400μM dNTP and 2–6mM

$MgCl_2$). Annealing temperature and extension time were calculated for each PCR as according to the Tm of the primer pairs used and following the dogma of one minute per one kilobase of amplified DNA respectively. Otherwise, a denaturation step at 96°C and annealing step of determined temperature of both thirty seconds was employed, followed by a extension step at 74°C for a determined time. Number of cycles employed was dependent on amount of template DNA or cDNA available.

6.12 Generation of iCre and iGFP vectors.

Precise methodolology for the construction of iCre and iGFP vectors is provided in section 10.1. Oligonucleotide primers used in the generation of these vectors are outlined in table 6.12:

Name	Sequence
	5' 3'
Cre1R	CAG GTA ATC TCT CAC ATC CTC AGG
Cre2F	CTG TAT CTG CAG GCT AGA GGT CTG
Cre2R	GCT GGT GGC AGA TGG AGC AGC AAC
Cre3F	CAG CTG TCC ACT AGA GCC CTG GAA G
Cre3R	CCA GCT CTA GCC ATA TCT CTA GCA GCT C
Cre4F	GAG TTT CAA TCC CCG AGA TCA TGC
Cre141 F	ATA CCT GGA AAA TGC TTC TGT CCG
Cre515F	GGA TTG CTT ATA ACA CCC TGT TAC G
Cre1013R	CAC TAT CCA GGT TAC GGA TAT AGT TC
Cre1045R	ATC TTC CAG CAG GCG CAC CAT TGC
Cre668F	GGG GTA ACT AAA CTG GTC GAG CGA
Cre667R	CAG GCT AAG TGC CTT CTC TAC ACC
ei3fPml	ATA **CAC GTG**[1] AGT ACA GGA GGT GGA GAG T
489mutR	TGG CAG **CGA TCG**[2] CTA TTT TCC ATG AGT GAC CGA ACT TGG
mi1	GTA AGA ACC AAA CCC TCC CAG
mi1R	CTG GAA TGA AAG GTC AAG GTG
ei3	GTG AGT ACA GGA GGT GGA GAG T
ei3r	CTG TGG GAC GAC ATG ACT TAA
eGFP1	GCG **CTC GAG**[3] CCA CCA TGA AAC GCC CCA GGA CCG TGA GCA AGG GCG A
eGFP1R	CTC GG**C CCG GG**[4]T CTT GTA G
eGFP2	GA**C CCG GG**[4]C CGA GGT GAA G
eGFP2R	TGC **GAA TTC**[5] TGG TCG GC**C AGC TG**[6]C ACG C
eGFP3	G**CA GCT G**[6]GC CGA CCA CTA CC
eGFP3R	GCG **AGA TCT**[7] TTA CTT GTA CAG CTC

Table 6.12. Oligonucleotide primers used for amplification and targeted mutagenesis of iCre and iGFP vector components.

Underlined nucleotides represent a transcription start site, whilst bold nucleotides represent enzyme restriction: 1-Pml1, 2-PvuI, 3-XhoI, 4-SmaI, 5-EcoRI, 6-PvuII, 7-BglII.

Chapter 7 Methods for Tissue Culture

7.1 Maintenance of Chinese Hamster Ovary cells

Chinese Hamster Ovary cells (CHO cells) were maintained in DMEM (Gibco/BRL, Paisley, UK) supplemented with 10% fetal calf serum, 0.1 mg/ml Penicillin and Streptomycin, 2 mM Glutamine, 10 mM Sodium Pyruvate, by sub-culturing every two to three days.

7.2 CHO cell stable transfection.

CHO cells were plated at 2 x 10^6 cells per 15cm tissue culture dish. Forty-eight hours later, cells were harvested in mid-log phase via trypsinisation. Using a 0.4cm electroporation cuvette, 8 x 10^6 cells in 800µl (1 x 10^7 cells/ml) culture medium were mixed with 0.1 µg of linearised plasmid, followed by electroporation at 625 V/cm, 500 µF. Cells were plated at a range of densities and selection was initiated after 24-48 hours using culture medium supplemented with 600µg/ml G418. Resistant colonies observed after 10-11 days cells were passaged once before harvesting cells for RNA preparation or flow cytometric analysis. GFP transfected resistant clones were isolated by two consecutive cloning steps, expanded and analysed by flow cytometry using FACSCAN (Becton Dickinson). Analysis of acquired data was performed using CellQuest (Becton Dickinson) software.

RESULTS

Chapter 8 Initial Characterisation of Myeloid Cell Specific Csk Deficient Mice.

Initial characterisation of myeloid cell specific Csk-deficient mice outlined specifically in this chapter was undertaken by Dr. J. Roes, Dr. D. Power and Dr. J. Unger. The results shown in this chapter are included to provide the reader with the foundations upon which my research project was built upon. However, the interpretation and later discussion of these data are my own.

The following genotypes were bred:

$Csk^{+/+}$-$GE^{+/+}$ - Homozygous wild-type at both the Csk and granulocyte elastase locus, to serve as wild-type controls and for breeding stock.

$Csk^{fl/fl}$-$GE^{+/+}$ - Homozygous floxed at the Csk locus and homozygous wild-type at the granulocyte elastase locus, to serve as floxed controls and for breeding stock.

$Csk^{fl/\Delta}$-$GE^{+/+}$ - Hemizygous floxed at the Csk locus and homozygous wild-type at the granulocyte elastase locus, to serve as controls for both floxing and hemizygosity at the csk locus and for breeding stock.

$Csk^{+/+}$-$GE^{cre/cre}$- Homozygous wild-type at the Csk locus and homozygous for Cre recombinase at the granulocyte elastase locus. Used as breeding stock only.

$Csk^{fl/+}$-$GE^{cre/+}$- Heterozygous floxed at the Csk locus and heterozygous for Cre recombinase at the granulocyte elastase locus. **These mice serve as controls for myeloid specific Csk-deficient test group unless otherwise stated.**

$Csk^{fl/\Delta}$-$GE^{cre/+}$ - Hemizygous floxed at the Csk locus and heterozygous at the granulocyte elastase Cre locus. **These mice serve as the myeloid cell specific Csk-deficient experimental test group and are referred to as Csk-GEcre mice from herein.**

All genotypes described above are born at the expected Mendelian ratio and are macroscopically indistinguishable from each other. When the mice are maintained in specific pathogen free conditions, all genotypes survive well into adulthood, although mice were not usually maintained for greater than six months. Due to this time scale, any effect of myeloid specific Csk deficiency upon cellular transformation and/or manifestation of autoimmune disease *in vivo* is unlikely to be observed.

8.1 Cre mediated deletion of the csk^{fl} allele in myeloid cell specific Csk deficient mice.

Cre mediated deletion of the csk^{fl} allele leads to excision of a 400bp fragment carrying exons 9 and 10, which encode part of the kinase domain (figure 8.1a) (Schmedt *et al.*, 1998). The level and specificity of deletion in the myeloid cell specific Csk conditional mutant was determined by Southern blot analysis. Southern blots prepared from genomic DNA isolated from specific cell populations digested with EcoRI were hybridised to a radiolabelled DNA probe spanning exons 9 and 10. This identified Csk^{+} (8.1kb), Csk^{fl} (2.5kb) and Csk$^{\Delta}$ (2.1kb) alleles. Somatic deletion of the Csk allele was determined by calculating the acquisition of the diagnostic Csk$^{\Delta}$ allele against the loss of the Csk^{fl} allele.

In the first instance, levels of deletion in Csk$^{fl/+}$-GE$^{cre/+}$ mice were analysed to eliminate potential selective pressures of a complete loss of Csk expression. Bone marrow and sterile peritonitis induced granulocytes derived from Csk$^{fl/+}$-GE$^{cre/+}$ (heterozygous control) mice revealed 55 ± 1% and 53 ± 3% allelic deletion respectively (figure 8.1b). Splenocytes, thymocytes, and resident peritoneal macrophage demonstrated less than 5% allelic deletion. Intriguingly, inflammatory macrophages recruited to the peritoneum after thioglycollate induction of sterile peritonitis revealed significant deletion at 24 ± 3% (figure 8.1b). To support the generation of Csk-deficient cells, mice carrying only one functional csk^{fl} locus, the second allele having been inactivated in the germline were used. In this genotype (**Csk$^{fl/\Delta}$-GE$^{cre/+}$ referred to forthwith as Csk-GEcre**), every Cre-mediated deletion event generates a Csk-deficient cell. Assessment of *csk* deletion in Csk-GEcre mice revealed 78 ± 6% deletion in bone marrow granulocytes and 63 ± 5% deletion in sterile peritonitis induced granulocytes. The lower level of deletion observed in sterile peritonitis induced granulocytes indicates selection against Csk-deficient cells in the recovered exudates. Again significant deletion was observed in inflammatory macrophages at 59 ± 1% (figure 8.1c).

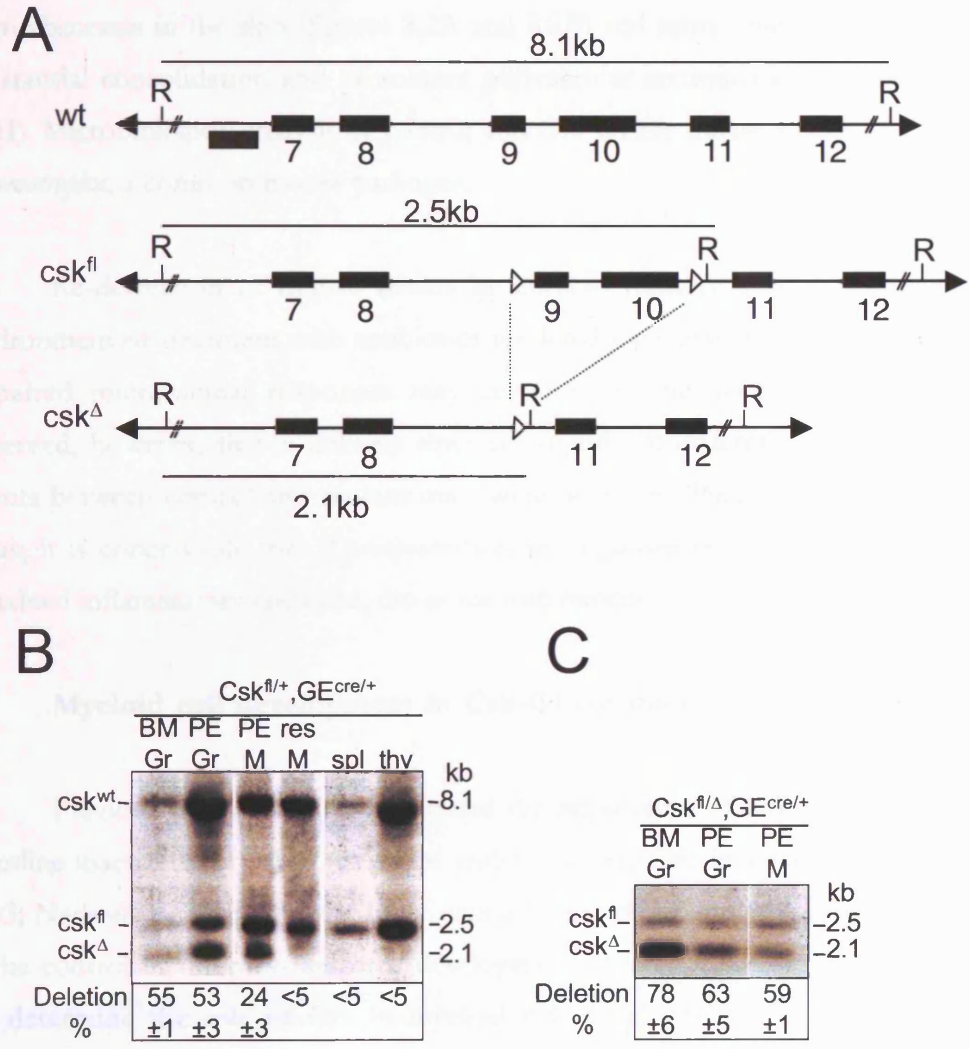

Figure 8.1. Myeloid Specific Inactivation of Csk. (A) Partial structure of the csk locus is shown before and after Cre mediated recombination events. Numbered rectangles represent exons; open triangles represent loxP sites; R, EcoRI. (B,C). Southern blot analysis of EcoR1 restricted genomic DNA from purified leukocyte subpopulations, peritoneal exudates or whole organs (spleen and thymus) from mice heterozygous for the *csk*^{fl} locus (*csk*$^{fl/+}$,*GE*$^{cre/+}$; B) or Csk-GEcre mice 'hemizygous' for csk^{fl} with the second allele already inactivated in the germ line (*csk*$^{fl/\Delta}$, *GE*$^{cre/+}$, C) are shown. Cre-mediated deletion of exon 9 and 10 of the c*sk* gene leads to a 400bp reduction of the 2.5kb restriction fragment (*Csk*^{fl}) and appearance of the 2.1kb fragment (*csk*$^{\Delta}$). Mean deletion levels (%) were determined in three independent experiments. The size of DNA fragment corresponding to wt, csk^{fl}, and csk$^{\Delta}$ and percent deletion are indicated. Gr - granulocyte, M - macrophage, spl - splenocytes, thy - thymocytes, BM - bone marrow, PE - peritoneal exudate, res - resident peritoneal.

8.2 Csk-GEcre mice develop inflammatory disease.

Csk-GEcre mice developed an inflammatory disorder including dermatitis-like symptoms with inflammation of the eyelids and ears. Histopathological analyses revealed microabscesses in the skin (figures 8.2A and 8.2B) and acute pulmonary inflammation with substantial consolidation and prominent perivascular accumulation of PMN (figures 8.2C-8.2H). Microbiological analysis of control and Csk-GEcre mouse strains identified *Pasteurella pneumotropica*, a common mouse pathogen.

Re-derivation of mouse strains by embryo transfer into a specific pathogen free environment or treatment with antibiotics rendered mice essentially free from inflammation. Impaired microbicidal responses may account for the acute, perivascular pneumonia observed, however, this is unlikely since no significant difference in pulmonary microbial counts between control and mutant mice were observed (Personal communication. J.Roes). Thus, it is conceivable that *P.pneumotropica*, an organism that does not normally initiate a sustained inflammatory response, drives the inflammation.

8.3 Myeloid cell development in Csk-GEcre mice.

Previous studies have demonstrated the importance of Csk in development. Indeed, germline inactivation of Csk results in embryonic lethality in mice (Imamoto and Soriano, 1993; Nada *et al.*, 1993). Furthermore, using Cre/loxP technology, Csk has been implicated in the control of receptor-mediated development of T-lymphocytes (Schmedt *et al.*, 1998). To determine the role of Csk in myeloid cell development, bone marrow derived cell suspensions were analysed (figure 8.3). Total numbers of nucleated cells derived from SPF maintained control and Csk-GEcre mouse colonies showed no significant difference (figure 8.3a). Flow cytometric analysis for Gr1 cell surface expression showed no difference in either $Gr1^{hi}$, nor $Gr1^{lo}$ percentages demonstrating no difference in the mature or immature granulocyte populations respectively (figure 8.3b). To assess whether Csk played a role in myeloid cell lifespan and turnover, BrdU incorporation into leukocytes was measured in mice receiving BrdU in their drinking water. No difference was observed in granulocyte turnover between Csk-GEcre and control mice (figure 8.3c). Induction of sterile peritonitis revealed that granulocytes were recruited efficiently into the peritoneal cavity. However, in accordance with the apparent selection against Csk-deficient granulocytes demonstrated in

the deletional analysis (figure 8.1c), Csk-GEcre granulocyte numbers were reduced compared to controls reaching significance at later stages of the inflammatory response (figure 8.3d).

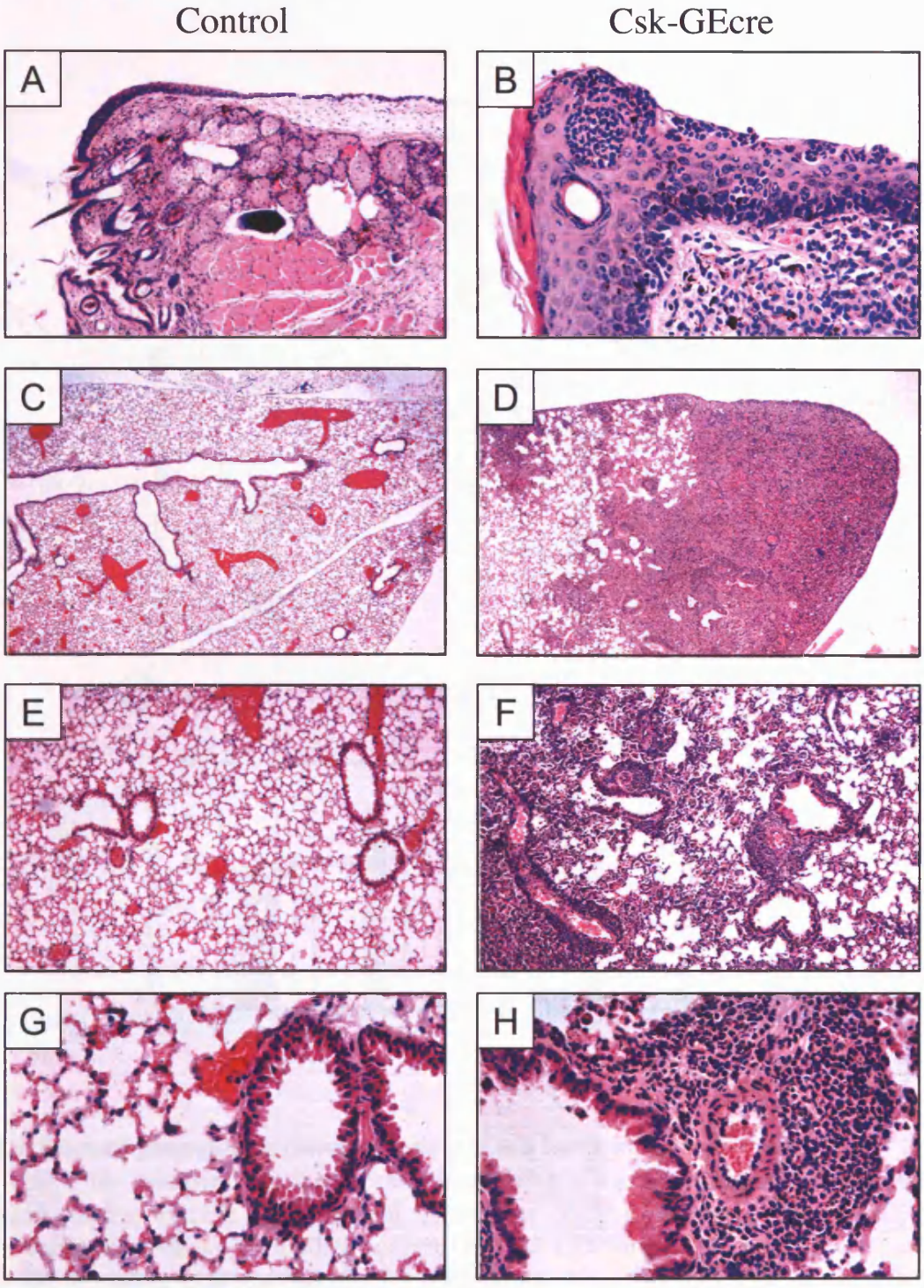

Figure 8.2. Acute pulmonary pneumonia in Csk-GEcre mice maintained under normal housing conditions. Haematoxylin/Eosin stained paraffin tissue sections of control ($Csk^{fl/\Delta}$,GE+/+ ; left column) and Csk-GEcre mice (right column) are shown. (A, B) Sections of eyelids showing microabscess formation with pronounced accumulation of polymorphonuclear granulocytes in the mutants. (C-H) Sections of lung tissue are shown at low (C,D), medium (E, F) and high power (G, H) demonstrating acute lobar pneumonia in the mutants with substantial consolidation of the organ (D). The distinct perivascular accumulation of the polymorphonuclear infiltrate in the mutants is illustrated in (H). Note the large numbers of leukocytes adhering to the blood vessel wall in the centre of the infiltrate indicating a highly active recruitment process.

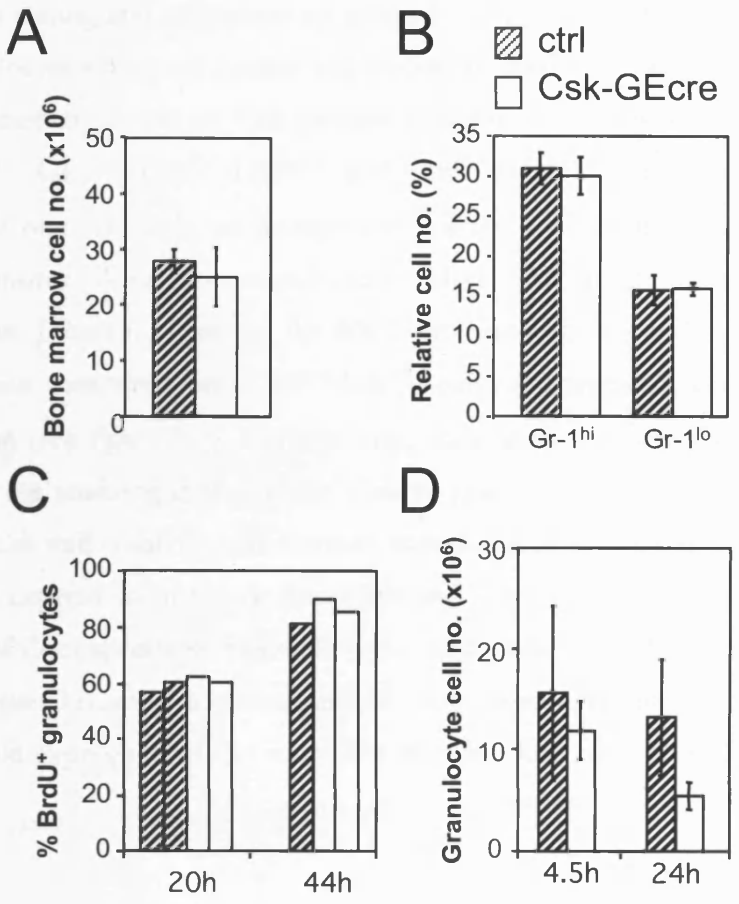

Figure 8.3. Normal granulocyte development and cell turnover in Csk-GEcre mice. Total bone marrow leukocytes numbers (A) were determined using a haemocytometer and percentages of mature granulocytes ($Gr1^{hi}$) and myeloid precursors ($Gr1^{lo}$) (B) were determined by flow cytometry using monoclonal antibodies against Gr1 and CD11b. (C) Bromodeoxyuridine (BrdU) incorporation in mature granulocytes ($Gr1^{hi}$) detected by flow cytometry 20h or 44h after in vivo labelling confirms normal turnover of Csk-GEcre granulocytes. (D) Numbers of granulocytes ($Gr1^{hi}$) recovered from the peritoneal cavity 4.5h and 24h after thioglycollate induction of sterile peritonitis.

Chapter 9 Further Characterisation of Csk-GEcre mice.

9.1 Analysis of Csk and Src-fk expression in bone marrow granulocytes

To complement Southern blot data that determined the specificity and level of allelic *csk* deletion in resting and inflammatory myeloid cells, analysis of enrichment-purified bone marrow granulocyte whole cell lysates was studied to confirm whether somatic Csk deletion was accompanied by a loss of Csk protein expression. Expression of p50Csk is similar between $Csk^{+/+}$-$GE^{+/+}$, $Csk^{fl/+}$-$GE^{cre/+}$ and $Csk^{fl/\Delta}$-$GE^{+/+}$ mice indicating that germline inactivation of one *csk* allele, or juxtaposition of the Cre recombinase to the granulocyte elastase promoter does not significantly alter Csk protein expression (Personal communication. J.Roes.). However, the 50kD immunoreactive band is almost abrogated in Csk-GEcre mice compared with $Csk^{fl/\Delta}$-$GE^{+/+}$ control littermates, consistent with loss of Csk expression (see figure 9.1). Cumulatively, these data validate Csk-GEcre mice as an effective tool for studying deficiency of Csk in granulocytes. Previous studies using cells derived from Csk null embryos have shown a correlation between loss of Csk expression and a reduction in expression of Src-fk (Imamoto and Soriano, 1993; Nada *et al.*, 1993) Does amelioration of Csk expression in granulocytes lead to reduction of Src-fk expression? Whole cell lysates prepared from enrichment purified bone marrow granulocyte populations revealed no difference in expression of the major Src-fk in myeloid cells, Hck, Fgr, and Lyn (figure 9.1).

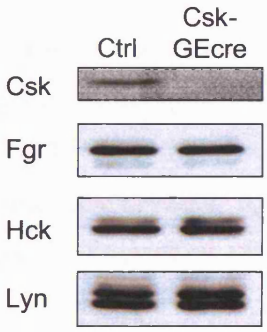

Figure 9.1. Csk-GEcre enrichment purified bone marrow granulocytes show a marked reduction of immunoreactive Csk protein expression compared to $Csk^{fl/\Delta}$-$GE^{+/+}$ control (Ctrl) littermates, whilst expression of other major Src family kinases Hck, Fgr, and Lyn remain unaffected. Granulocytes were enriched from bone marrow derived cell suspensions as described in *Experimental procedures*. Proteins from purified granulocyte whole cell lysates were separated by SDS-PAGE and subjected to immunoblotting with anti-Csk, anti-Fgr, anti-Hck, and anti-Lyn polyclonal antibodies. Equal loading is demonstrated by equal expression of Fgr, Hck and Lyn.

9.2 Csk-GEcre mice are hyper-responsive to lipopolysaccharide.

A strict correlation between myeloid Csk deficiency and an inappropriate sustained inflammatory response associated with acute perivascular pneumonia has been demonstrated (figure 8.2). This phenotype was abrogated upon embryo transfer of the mouse colony into a specific pathogen free environment. Mice deficient for the Src-fk Hck and Fgr are resistant to endotoxin (Lowell and Berton, 1998). If deregulated Src-fk activity caused granulocyte hyperresponsiveness observed in conventionally housed Csk-GEcre mice, this should also affect susceptibility to endotoxin (LPS, lipopolysaccharide). Indeed, Csk-GEcre mice proved hyper-responsive to the high dose model of endotoxemia (figure 9.2a-c). While intra-peritoneal administration of LPS at 10mg/kg induced lethal endotoxic shock in all Csk-GEcre mice (n=6), all control mice were fully protected (figure 9.2a). Extending this study, the rate of mortality at lower doses of LPS was assessed. While controls remained fully protected, Csk-GEcre mice remained hyperresponsive to LPS at 5mg/kg (n=6, figure 9.2b) and 2.5mg/kg (n=3, figure 9.2c), demonstrated by greater than 90% mortality rate. Both experimental groups showed characteristic symptoms of endotoxemia including shivering, piloerection, apathy, and eye secretion. However, these symptoms were more pronounced in the conditional mutants. No deaths were observed at 0.5mg/kg LPS (n=3) in either controls or Csk-GEcre mice indicating that the LD50 for Csk-GEcre mice lies between 0.5mg/kg and 2.5mg/kg. The availability of Csk-GEcre mice and the distress induced by endotoxic shock upon these mice prevented any further titration.

Acute lung injury, a symptom characteristic of acute respiratory distress syndrome (ARDS), develops from the release of proteases and reactive oxygen intermediates (ROI) from PMN sequestered in the pulmonary microvasculature and PMN infiltration into the alveolar airspace (Tate and Repine, 1983). To determine whether acute lung injury may have contributed to the mortality observed in the conditional mutants, lungs were removed from LPS challenged mice for histopathological analysis. Chronic vascular damage and hemorrhagic lesions were indeed observed in lung sections derived from Csk-GEcre mice receiving 10mg/kg LPS, which were not observed in the control group (figure 9.2e/f). Interestingly, LPS-stimulated Csk-GEcre granulocytes demonstrate delayed apoptosis after 48hr culture in vitro (figure 9.2g), suggesting that the functional longevity and cytotoxic potential of these cells at the inflamed site maybe enhanced in vivo during experimental endotoxaemia.

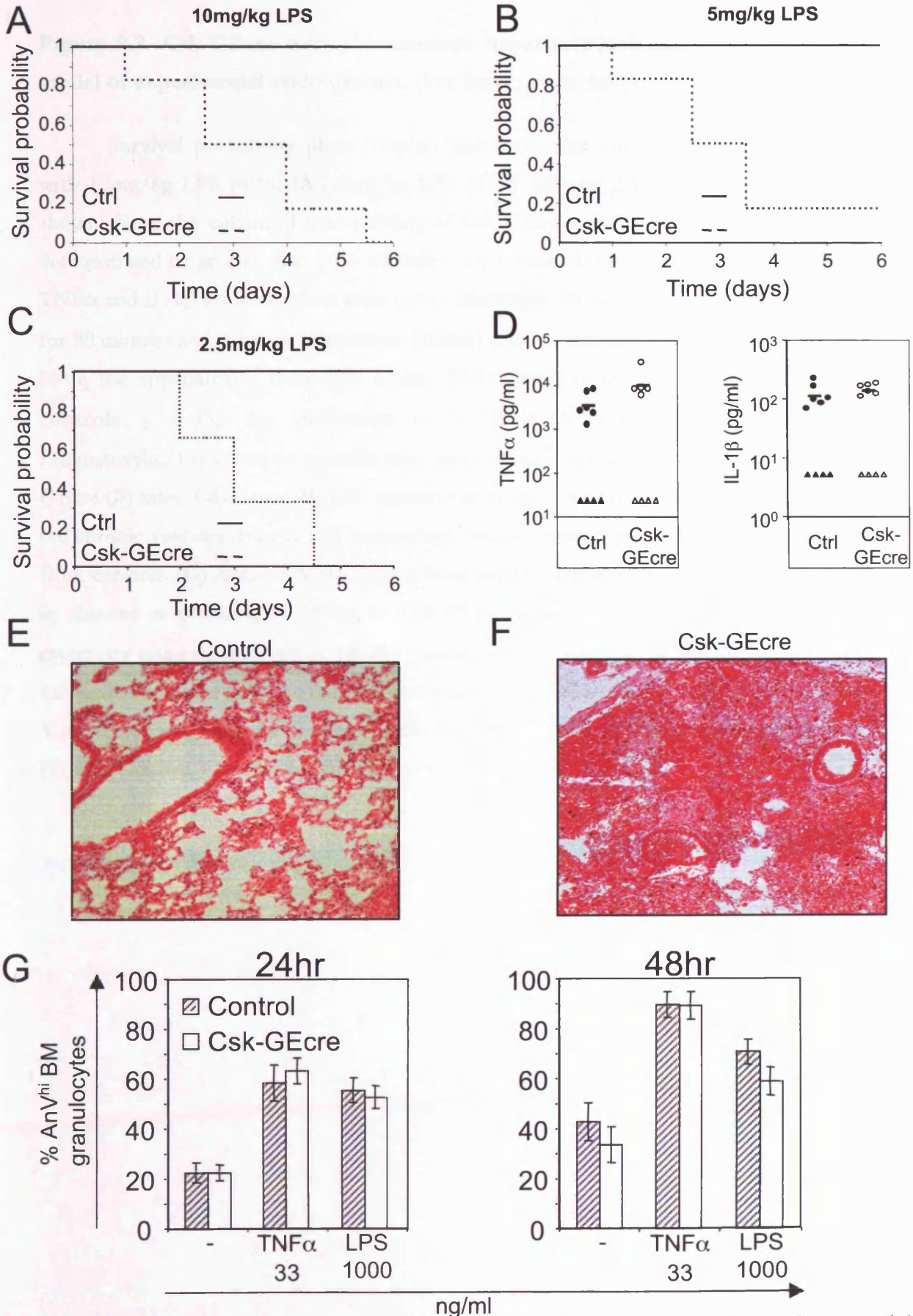

Figure 9.2. Csk-GEcre mice demonstrate hyper-responsiveness to the high dose model of experimental endotoxemia. (For figure legend, please see next page.)

Figure 9.2. Csk-GEcre mice demonstrate hyper-responsiveness to the high dose model of experimental endotoxemia. (For figure, please see previous page.)

Survival probability plots (Kaplan-Meier) of mice injected intra-peritoneally (IP) with 10mg/kg LPS (n=6) (**A**), 5mg/kg LPS (n=6) (**B**) and 2.5mg/kg LPS (n=3) (**C**) are shown. Note the enhanced susceptibility of Csk-GEcre mice to each of these LPS doses demonstrated by greater than 90% mortality while control mice remain fully protected. (**D**) TNFα and IL-1β serum levels in mice (n=6) challenged intra-peritoneally with 5mg/kg LPS for 90 minutes and 3 hours respectively (circles) and for unchallenged mice (n=4, triangles). Note the approximate three-fold higher TNFα levels in the mutants compared to the controls, p=0.05). No difference in IL-1β levels is observed (p=0.21). (**E,F**) Haematoxylin/Eosin stained paraffin lung tissue sections removed from control (**E**) and Csk-GEcre (**F**) mice 3-days post-IP LPS injection at 5mg/kg viewed at 20x magnification. Note the chronic vascular damage and hemorrhagic lesions present in Csk-GEcre mice are absent from controls. (**G**) Annexin V staining on bone marrow granulocytes cultured for 24 or 48hrs in absence or presence of TNFα or LPS at the indicated doses was determined by flow cytometry using monoclonal antibodies against Gr1 and AnnexinV. The bar charts illustrate the relative increase in the proportion of Annexin V^{hi} granulocytes. Cells positive for Annexin V are apoptotic. Note the increased resistance to LPS-induced apoptosis apparent at 48hr (71±5% Control, Csk-GEcre 59±6% AnV+ cells, p=0.01).

Hepatic injury also results from sequestration of PMN to the liver parenchyma. To assess whether deregulated Src-fk activity is associated with hepatic injury, livers were removed eight hours after LPS administration for histopathological assessment. Significantly, substantially enhanced granulocyte recruitment to the liver was observed in Csk-GEcre mice (Control: 5.4 foci/100 fields; Csk-GEcre: 82.5 enlarged foci/100 fields).

TNFα has been identified as a contributing mediator to the endotoxic shock response. This is supported by studies demonstrating reproduction of endotoxic shock symptomology via intravenous administration of recombinant TNFα (Tracey *et al*, 1986), and further confirmed in mice deficient in TNFα or its type I receptor (p55) which are endotoxin resistant (Marino *et al.*, 1997; Pfeffer *et al.*, 1993; Rothe *et al.*, 1993; Tracey *et al.*, 1986). Due to the hyper-responsiveness of the conditional mutants to endotoxin, the possibility was considered that increased serum TNFα levels might have contributed to the susceptibility to endotoxic shock. Intra-peritoneal LPS administration at 5mg/kg indeed showed strong serum induction of TNFα in both conditional mutant and control mice. Interestingly, a discernable three-fold increase in TNFα serum levels was observed in conditional mutant mice (figure 9.2d, p=0.05). Similar levels of IL-1 were found in both genotypes (figure 9.2d, p=0.21). Through a complex signalling mechanism involving TLR4, Myd88 and IRAK, lipopolysaccharide induces nuclear translocation of NF-κB resulting in de novo transcription of NF-kB responsive genes including IL-6, IFNγ and NO, in addition to TNFα and IL1 (Martin and Wesche, 2002). Unfortunately, limited availability of Csk-GEcre mice prevented further serum response studies from being undertaken.

9.3 Enhanced spontaneous priming of Csk-GEcre granulocytes.

Csk-GEcre mice reveal a critical role for Csk in the negative regulation in myeloid cell responsiveness illustrated by inappropriate phagocyte recruitment and a sustained inflammatory response to an inflammatory stimulus (figure 8.2 and 9.2). Neutrophil priming represents one of the key processes regulating functional responsiveness both *in vitro* and *in vivo* (Smedly *et al.*, 1986; Worthen *et al.*, 1987). Mobilisation of intracellular stores augments cell surface expression of β2-integrin transforming the neutrophil from a quiescent cell compatible with circulation, to a highly responsive cell primed for migration into tissues (Crockett-Torabi *et al.*, 1995; Pavalko and LaRoche, 1993; Simon *et al.*, 1995; von Andrian *et*

al., 1991). Is the functional responsiveness of Csk deficient granulocytes a result of spontaneous priming?

Due to considerable selection against recruitment of Csk-deficient granulocytes in sterile peritonitis, bone marrow granulocytes were analysed. Flow cytometric analysis of β2-integrin in quiescent bone marrow granulocytes did not reveal any difference in 'base-line' expression. Upon cell culture without addition of activating stimuli, a sub-population of spontaneous primed granulocytes upregulate cell surface β2-integrin as detected by staining with anti-CD11b antibody. Spontaneous priming is markedly augmented in the Csk-deficient granulocytes compared to controls indicated by a two-fold increase in the $CD11b^{hi}$ population (42 ± 5% Control, 76 ± 6% Csk-GEcre; p=0.002) (figure 9.3a/b). Cells exposed to 10μM PP2, a selective inhibitor of Src-fk, abrogates this effect in the conditional mutants revealing deregulation of Src-fk activity is responsible for augmented spontaneous priming (figure9.3b). Direct activation of protein kinase C (PKC) by PMA induced a similar shift toward the $CD11b^{hi}$ phenotype and similar expression levels in both controls and mutants (figure 9.3b). Although isotype matched antibody controls were not performed in this particular assay and retrospectively should have been included to strengthen the data, these are well known standard reagents that are used routinely in the laboratory. Given the known quality of these reagents and the strength of the signal observed in these data, an argument for their exclusion maybe tentatively made.

The observation of spontaneously increased β2-integrin expression in cultured Csk-deficient granulocytes outlined above was further strengthened by enhanced binding of its ligand, fibrinogen (figure 9.3c). PMA boosted fibrinogen binding and CD11b expression to similar levels in controls and mutants (figure 9.3b/c). This confirms that differences in integrin stores per se do not account for the increased CD11b expression on the cell surface of Csk-deficient granulocytes.

Acquisition of the $CD11b^{hi}$ phenotype was accompanied by a polarisation or shape-change response in the conditional mutants. Shape change typically associated with granulocyte priming represents an adoption of amoeboid morphology, which occurs as a consequence of actin cytoskeletal remodelling and is accompanied by a decrease is cell deformability (Haslett *et al.*, 1985). Using the Forward Scatter Channel (FSC) to assess the extent of cell shape change, it was determined that uncultured control and Csk-GEcre granulocytes showed similar FSC values (378.36 ± 16.96 Control; 404.10 ± 7.25 Csk-

GEcre). However, upon cell culture, *in vitro* spontaneous shape change indicated by an increase in FSC values is considerably augmented in the Csk-GEcre granulocyte population (441.96 ± 1.47 Control; 503.00 ± 12.44 Csk-GEcre, p=0.002). This response was blocked in the presence of PP2 (412.76 ± 1.45 Control; 418 ± 3.94 Csk-GEcre) again confirming that augmented neutrophil priming is due to deregulated Src-fk activity.

The effects of known priming agents, lipopolysaccharide (LPS) and tumor necrosis factor-α (TNFα) (figure 9.3d/e) upon cell surface expression of β2-integrin (CD11b) and L-selectin (CD62L) were also assessed. Csk-deficient granulocytes demonstrate a dose dependent increase in CD11b exposure and CD62L shedding in response to both LPS and TNFα compared to controls.

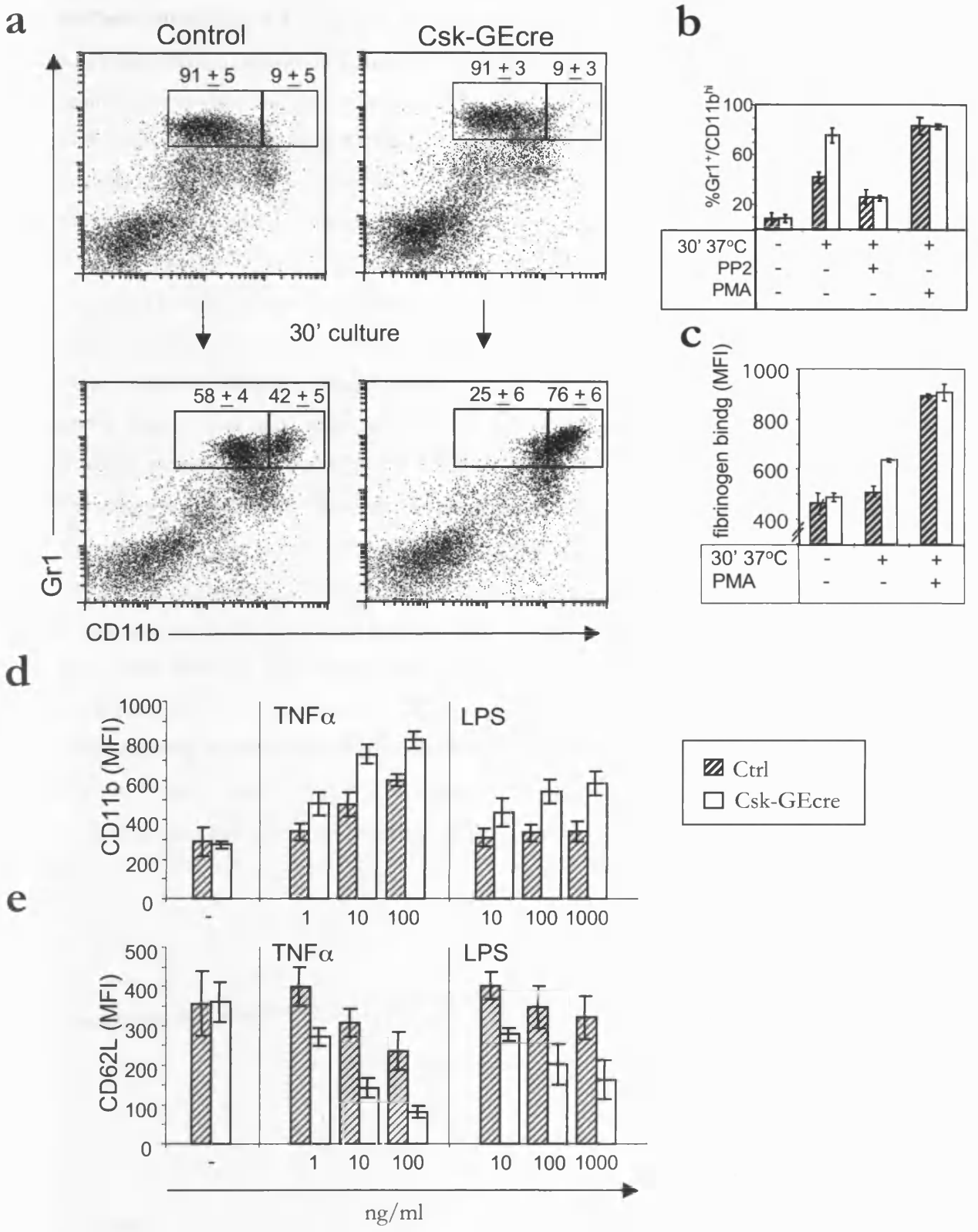

Figure 9.3 Spontaneous priming in Csk deficient granulocytes is associated with augmented responsiveness to inflammatory mediators. For figure legend, see next page.

Figure 9.3. Augmented cell surface expression of β2-integrin (CD11b/18) and cell surface shedding of L-selectin (CD62L) in Csk-deficient granulocytes. β2-integrin and L-selectin expression on bone marrow granulocytes before and after cell culture and/or stimulation in vitro was determined by flow cytometry using monoclonal antibodies against Gr1, CD11b, CD62L (**A,B,D,E**) or by binding of fluorescent fibrinogen. (**A**) Dot plot analysis of bone marrow stained with Gr1 and CD11b show the proportion of granulocytes expressing low and high levels of CD11b before (top panel) and after incubation *in vitro* (bottom panel). Note the relative increase in the proportion of $CD11b^{hi}$ granulocytes (42±5% Control, 76±6% Csk-GEcre, p=0.002) after incubation *in vitro*. The bar charts **B and C** illustrate the relative increase in the proportion of $CD11b^{hi}$ granulocytes (**B**) or level of fibrinogen binding (**C**, mean fluorescent intensity (MFI)) in the controls (hatched bars) and mutants (open bars) after incubation in vitro. Spontaneous induction of CD11b in the mutants is abrogated by the Src-fk inhibitor PP2 (**B**). Binding of the β2-integrin ligand fibrinogen is increased in Csk-deficient granulocytes after incubation in medium (**C,** 511±18 Control, 637±9 Csk-GEcre, p=0.001), in accordance with the spontaneously increased levels of CD11b expression. PMA induces maximal fibrinogen binding in both controls and mutants, in accordance with the maximal CD11b expression observed by direct activation of PKC with PMA in (**B**). Bar charts **D** and **E** illustrate the relative increase in CD11b expression levels or shedding of CD62L (MFI, mean fluorescent intensity) in the controls (hatched bars) and mutants (open bars) after incubation in vitro in the presence or absence of the pro-inflammmatory stimuli TNFα and LPS at the concentrations indicated ($p<0.05$ for all differences observed in the presence of TNFα and LPS).

9.4 Augmented cell surface CD11b is most likely a consequence of enhanced mobilisation and fusion of intracellular granules to the plasma membrane in Csk-deficient granulocytes.

Neutrophil granule membranes serve as a rich supply of receptors. Exocytosis of neutrophil granules leads to extracellular release of granule contents and fusion of the granule membrane into the neutrophil plasma membrane furnishing the cell with new receptors, including β2-integrin. However, β2-integrin can also be incorporated into the neutrophil plasma membrane without corresponding exocytosis of granule content through the rapid mobilisation of secretory vesicles (Borregaard *et al.*, 1987; Borregaard *et al.*, 1990; Sengelov *et al.*, 1992; Miller *et al.*, 1987). In the first instance, it was determined whether augmented CD11b expression in Csk-deficient granulocytes was perhaps due to a shift in subcellular distribution. To explore this possibility, cell surface expression versus intracellular expression of CD11b and lactoferrin (a marker of secondary granules, Cramer *et al.*, 1985) was examined by flow cytometry, using intact and Triton X-100 permeabilised cells with specific antibodies. No difference was observed in intracellular CD11b or lactoferrin levels between controls and conditional mutants (figure 9.4a). Surface staining of CD11b was as previously observed. Lactoferrin surface staining was very low showing no difference between controls and conditional mutants. This clearly demonstrates no difference in subcellular distribution of CD11b between controls and mutants and thus, it seems likely that integrin upregulation in Csk-deficient granulocytes results from enhanced mobilisation and fusion of granules to the granulocyte plasma membrane.

To support this theory, the cell surface expression of granule markers was investigated. It has been previously reported that CD11b is physically associated with CD16 within the plasma membrane (Petty and Todd, 1996; Petty *et al.*, 2002). Studies in human PMN have shown that CD16 is restricted to the secretory vesicles (Detmers *et al.*, 1995). To determine whether enhanced CD11b expression is accompanied by enhanced expression of CD16, and by association enhanced mobilisation of secretory vesicles, cell surface expression of CD16 was analysed in cultured Csk-deficient bone marrow granulocytes using flow cytometry with anti-CD16/32 antibody (figure 9.4b). Intracellular stores of CD11b are not restricted to only secretory vesicles, but are also located in secondary granules (Sengelov *et al.*, 1993). To assess whether mobilisation of secondary granules contributed to the enhanced CD11b expression observed in the conditional mutants, cell surface expression of the vitronectin receptor reportedly confined to the secondary granule compartment was analysed

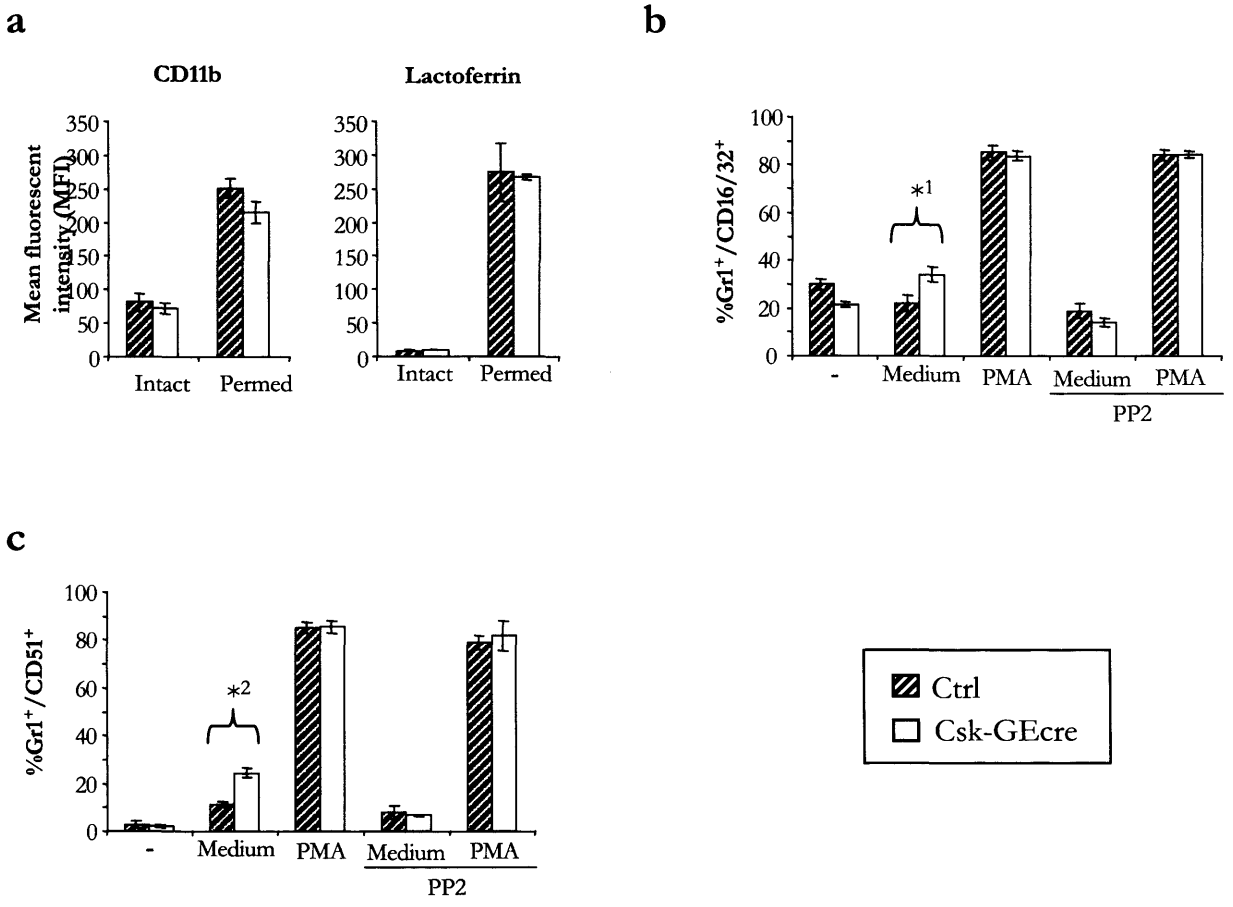

Figure 9.4. A role for Csk in the regulation of intracellular granule mobilisation and subsequent fusion to the granulocyte plasma membrane. a, Integrin and lactoferrin extracellular and intracellular expression on bone marrow granulocytes was determined by flow cytometry using antibodies against Gr1, CD11b and lactoferrin. Bar charts show the mean fluorescent intensity of CD11b and lactoferrin expression levels upon Gr1-hi (mature granulocytes) gated cells from freshly isolated unpermeabilised and permeabilised bone marrow leukocytes. Intact cells reflect cell surface expression of CD11b or lactoferrin, whereas permeabilised cells reflect the total cellular stores of CD11b or lactoferrin. **b,c**, Mobilisation and membrane fusion of secretory vesicles or secondary granules in bone marrow granulocytes was determined by flow cytometry using monoclonal antibodies against Gr1, CD11b, and CD16/32 (a secretory vesicle marker) or CD51 (a secondary granule marker) before and after 30min incubation with/without stimulation with PMA (10^{-6}M) and/or PP2 (10^{-5}M). Bar charts illustrate the relative increase in the proportion of granulocytes expressing CD16/32 (**b,** ^{*1} p=0.002) or CD51 (**c,** ^{*2} p=0.0001) in the mutants after incubation in vitro. The spontaneous augmentation of cell surface CD16/32 or CD51 expression is abrogated by Src-fk inhibitor, PP2. Direct activation of PKC by PMA induces maximal cell surface expression of both CD16/32 and CD51 in both controls and mutants.

via a specific antibody to the CD51 subunit (Singer *et al.*, 1989) (figure 9.4c). Cultured Csk-GEcre bone marrow granulocytes revealed an increase in the percentage of cells acquiring a CD16/32^{hi} phenotype (22.0 ± 3.5% Control; 34.0 ± 3.0% Csk-GEcre, p=0.002) and a CD51^{hi} phenotype (11.1 ± 1.2% Control; 24.5 ± 2.2% Csk-GEcre, p=0.0001) compared to control bone marrow granulocytes, which was abrogated in the presence of the Src-fk inhibitor PP2. PMA boosted CD51 and CD16/32 binding to similar levels in both controls and mutants indicating that differences in CD51 and CD16/32 intracellular stores per se do not account for the increased expression of these markers on the cell surface of Csk-deficient granulocytes. Together, these data support augmentation of both secretory and secondary granule mobilisation in Csk-deficient cells.

9.5 Csk-deficient granulocytes demonstrate enhanced adhesion-independent and dependent degranulation in vitro.

To further verify whether membrane fusion and subsequent exocytosis (degranulation) of neutrophil secondary granules contributed to CD11b cell surface expression in Csk-deficient granulocytes, the release of lactoferrin, a secondary granule marker, into the culture supernatant was measured by ELISA. Cells were cultured in either medium alone, or in the presence of the biological activating bacterial formylated peptide, N-formylmethionyl-leucyl-phenylalanine (fMLP) which signals via Src-fk (Mocsai *et al.*, 2000), in the presence or absence of cytochalasin B, an inhibitor of actin polymerisation which dramatically augments degranulation in granulocytes. The maximal degranulatory response was also determined by direct activation of protein kinase C (PKC) with phorbol myristyl acetate (PMA).

Lactoferrin release in cells cultured in medium revealed a subtle but never the less significant increase in degranulation in conditional mutants over control cells (1.00±0.21rel.U Control; 1.43±0.17rel.U Csk-GEcre, p=0.01) strengthening the position that exocytosis and membrane fusion of secondary granules contributes to the augmented CD11b cell surface expression observed in the conditional mutants as demonstrated by FACS analysis (figure 9.5a). Upon addition of the biological activating bacterial formylated peptide, N-formylmethionyl-leucyl-phenylalanine fMLP, Csk-deficient granulocytes revealed a significant increase in lactoferrin release compared to control cells (1.69±0.21rel.U Control; 3.36±0.33rel.U Csk-GEcre, p=0.003) (figure 9.5a). Inhibition of actin polymerisation through the addition of cytochalasin B to cell cultures markedly enhanced the degranulatory

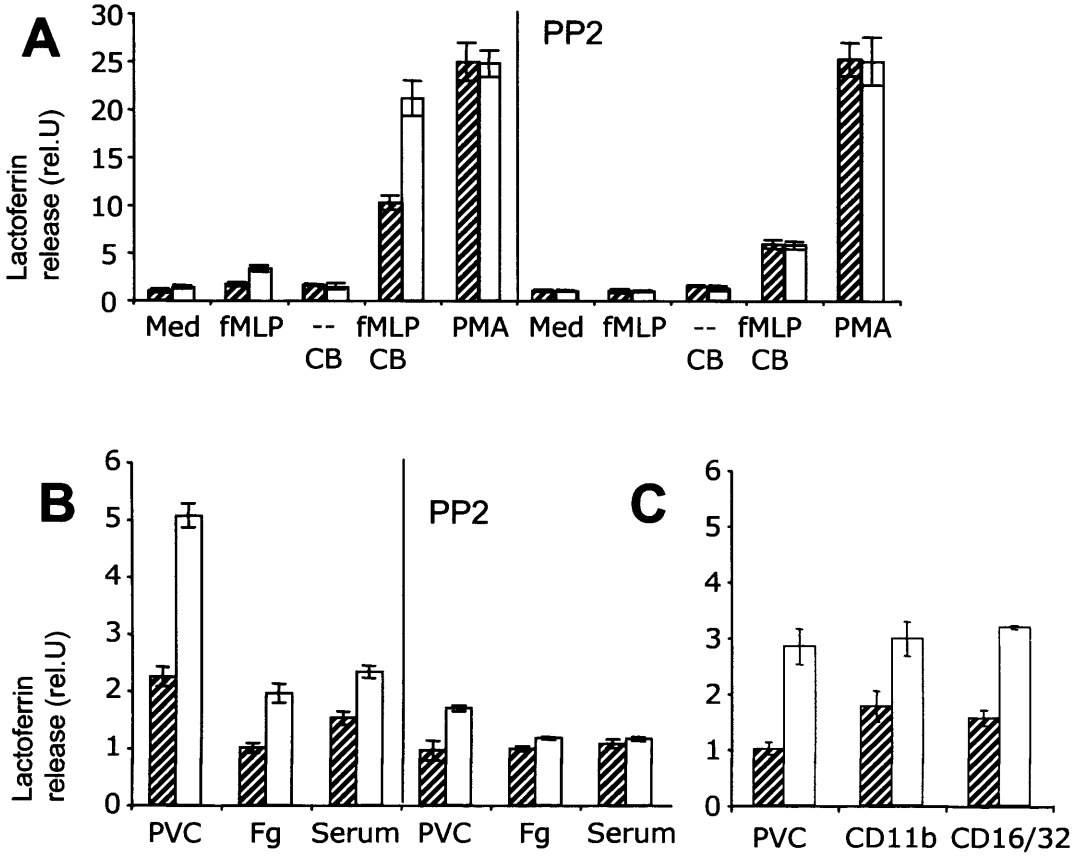

Figure 9.5 Augmented degranulation in Csk-deficient granulocytes. Degranulation as assessed by release of the secondary granule marker lactoferrin, of granulocytes in suspension (**A**) or after adhesion to PVC, fibrinogen (Fg), serum (**B**) or anti-CD11b or anti-Fcγ receptor (CD16/32) (**C**) coated wells without further stimulation is shown. Note that significantly increased degranulation of Csk-deficient granulocytes is apparent in medium alone ($p=0.01$) and after stimulation with fMLP alone ($p=0.003$). Cytochalasin B (CB) maximises degranulation through inhibition of actin polymerisation induced by fMLP. Csk-deficient granulocytes treated with both fMLP and CB almost reach the maximal level of degranulation induced by direct activation of PKC by PMA. This enhanced degranulation demonstrated in Csk-deficient granulocytes is completely suppressed by PP2 indicating its dependence of Src-fk activity. (**B**) Adhesion-dependent induction of degranulation is augmented in Csk-deficient granulocytes adhered to PVC or, Fg-, and serum-coated tissue culture plates and is again suppressed by PP2. (**C**) Direct crosslinking of integrin and Fcγ-receptors also leads to augmented degranulation in Csk-deficient granulocytes. The effect of PP2 on this method of degranulation induction was not experimentally defined. 1 relative unit (rel.U) represents the amount of lactoferrin released by control granulocytes in medium alone (A) or after adhesion to fibrinogen (B) or PVC (C). Spontaneous degranulation on BSA-coated surfaces was less than 0.25 rel.U's.

effect in both conditional mutant and control cells in response to fMLP. However, while the degranulatory response in the control cell population reached only 20% of the maximal response induced directly by PMA, degranulation in the conditional mutant cells is close to this level even in the absence of PMA. This enhanced degranulation is completely suppressed by PP2 indicating its dependence of Src-fk activity.

Impaired adhesion-primed degranulation has been reported in mice lacking Src-fk, Hck and Fgr (Berton and Lowell, 1999). To assess the impact of Csk deficiency upon adhesion-primed degranulation under different physiological conditions, cells were plated onto a non-specific matrix (organic polymer, PVC), or fibrinogen-, or serum-coated tissue culture plates. Csk-deficient granulocytes demonstrated an augmented degranulatory response compared to control cells when plated upon tissue culture plastic, fibrinogen, or serum, which was ameliorated in the presence of PP2, again indicating the dependence of Src-fk (figure 9.5b). To further demonstrate the inappropriate degranulatory response in Csk-deficient granulocytes initiated by deregulated β2-integrin or Fc-receptor signalling, cell surface receptors for CD11b and CD16/32 were directly crosslinked by plating cells upon tissue culture plastic coated with anti-CD11b and anti-CD16/32 (FcRII/III) respectively. Again, degranulation was enhanced in Csk-deficient cells compared to controls (figure 9.5c).

Taken together, these inhibitory effects of Csk reveal a central role of this cell autonomous inhibitory kinase in the negative regulation of the granulocyte activation threshold. Furthermore, the threshold imposed by Csk is apparently not specifically restricted to β2-integrin mediated granulocyte activation but is also involved in other activation pathways.

9.6 Hyper-adherence of Csk-deficient granulocytes is accompanied by impaired migratory responses in vitro.

A strict correlation between myeloid cell specific Csk-deficiency and an inappropriate sustained inflammatory response to an inflammatory stimulus *in vivo* has been demonstrated. Furthermore, augmented integrin expression in Csk-deficient granulocytes *in vitro* has been shown. Integrins are linked with regulation of cell activation and adhesion through a complex bi-directional signal transduction system (Schoenwaelder and Burridge, 1999). To investigate the contribution of Csk in the regulation of leukocyte adherence, the ability of depletion-

purified bone marrow granulocyte populations to adhere to organic polymer (PVC) or serum-coated tissue culture plastic was determined in a centrifugal force assay.

Csk-deficient granulocytes were significantly more resistant to detachment under centrifugal force from PVC (figure 9.6a, $p<0.001$) and serum-coated plastic (figure 9.6b, $p<0.01$) compared to control cells. Preincubation of granulocytes with anti-CD11b and anti-CD18 blocked adhesion to serum protein indicating that this interaction is β2-integrin dependent (figure 9.6b). Remarkably, adhesion to PVC is augmented under these experimental conditions indicating that the establishment of non-specific, charge-dependent cell-substratum interactions is facilitated by antibodies towards β2-integrin suggesting that a similar or perhaps identical cell signal to the one causing hyperadhesiveness in Csk-deficent granulocytes is triggered (figure 9.6a).

To assess the impact of hyperadhesiveness demonstrated in Csk-deficient granulocytes upon cell motility, granulocyte migration was measured. Several assays exist to analyse granulocyte migratory capacity including the under-agarose chemotaxis assay, the bridge chemotaxis assay, the transendothelial migration assay under laminar shear flow, and the filter assay.

In the under-agarose chemotaxis assay, wells are cut into the agarose approximately 2mm apart and chemoattractant is added to one well, which establishes an approximate exponential gradient as it diffuses into the agarose. Cells are then placed in an adjacent well, and their ability to migrate in the small space between the agarose layer and the culture dish is quantified. The major drawback of this assay is the reproducibility of assay conditions, since the distance between wells is wholly dependent of the investigator. This is critical since even slight differences in inter-well spacing will affect the exponential gradient of the chemoattractant and thus the migratory capacity of experimental cell populations. Another drawback of this assay lies in the potential introduction of scratches to the culture dish plastic by apparatus used to generate wells, for example a steel punch. These become barriers to cell migration and thus would additionally affect migratory capacity of experimental cell populations.

In the bridge chemotaxis assay, cells are adhered to glass coverslips and then exposed to a chemotactic gradient formed between two wells on a 1mm wide bridge. The drawback of this assay is that cell migration is quantified by morphological criteria. Normal migrating

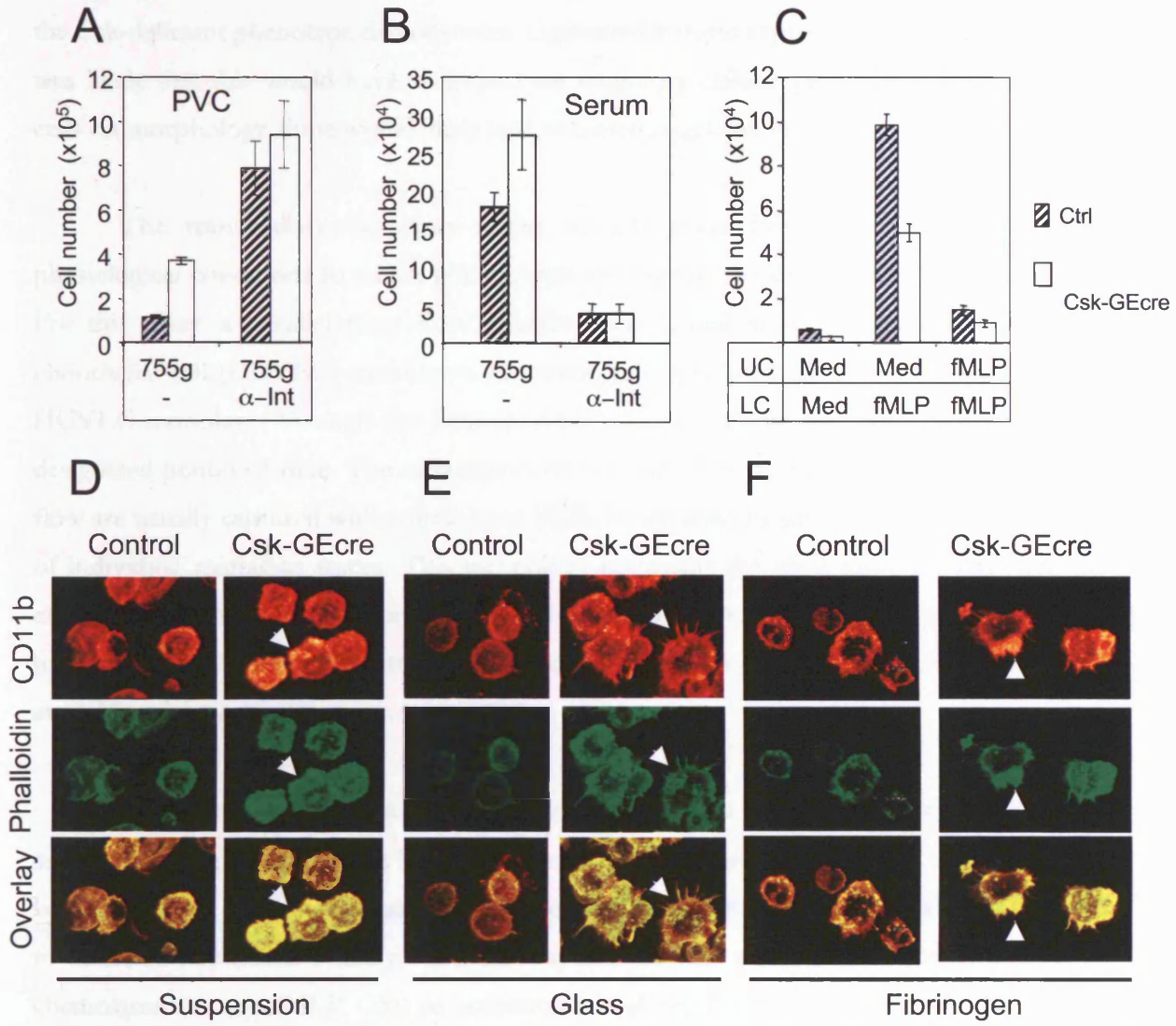

Figure 9.6 Enhanced Adhesion and Impaired Migration of Csk-deficient Granulocytes. (A, B) Csk-deficient depletion purified granulocytes show enhanced resistance to detachment under centrifugal force (-755g) after adhesion to organic polymer (PVC, A) and serum (B). Preincubation with antibodies to CD11b and CD18 (anti-β2 integrin) blocks adhesion to serum showing this interaction is β2-integrin dependent. Conversely, anti-β2 integrin antibodies stimulate adhesion to PVC indicating priming for adhesion through non-specific interactions with the PVC surface. (C) Impaired migratory responses of Csk-deficient granulocytes becomes apparent in a transwell migration assay. Mutant granulocytes show not only reduced chemotactic activity, but also reduced chemokinesis as indicated by the lower cell counts obtained in the absence of a chemotactic gradient (med/med; fMLP/fMLP). UC, upper chamber; LC, lower chamber. (D-F) Morphology is shown of bone marrow granulocytes either incubated in suspension for 30 min, fixed and plated on poly-lysine (C), or adhered to uncoated glass (D) or glass coated with fibrinogen (E), before 30 min incubation. Cells were fixed and stained with anti-CD11b-Biotin/Strepavidin-Cychrome and phalloidin-TexasRed, and DAPI. Polymorphonuclear granulocytes were identified by nuclear morphology. Confocal analysis confirmed not only the increased levels of CD11b (top) in the mutants, but also enhanced formation of integrin clusters and actin polymerization (middle) after incubation in suspension (C), on glass (D), or fibrinogen coated surface (E). Pronounced formation of brightly stained filopodia on glass distinguishes the mutant cells from the controls (B), while cells on fibrinogen show distinctive brightly stained lamellipodia. CD11b staining colocalises with polymerized actin as indicated by the overlay of CD11b and phalloidin staining (bottom).

cells show broad lamellipodia at the leading edge, followed by a thinner tail. However, since the Csk-deficient phenotype demonstrates augmented integrin expression and adhesiveness, it was likely that this would have an impact on migratory cellular processes and thus scoring cells on morphology alone would likely lead to biased migratory values.

The transendothelial assay under laminar shear flow closely reproduces the physiological conditions to which granulocytes are exposed to during cell migration *in vivo*. For this assay, a parallel plate flow chamber is mounted upon a human umbilical vein endothelial cell (HUVEC) monolayer. Granulocyte suspensions are then perfused over the HUVEC monolayer through the flow chamber using an automated syringe pump over a designated period of time. The movements of cells adherent to the HUVEC monolayer in flow are usually captured with a time-lapse VCR. Image analysis software allows observation of individual migration traces. This technology represents the ideal assay for analysing the effects of enhanced integrin expression and adhesion upon Csk-deficient granulocyte cell migration in a physiological setting, however, the technical expertise or facilities were not available to carry this assay out.

The filter assay measures migratory capacity across a thin (10μm) porous membrane and is routinely used across the literature. The main advantage of this assay is that is allows a large number of different materials and concentrations permitting many different parameters to be tested in parallel. These parameters may include pore size, different concentrations of chemoattractant (eg. fMLP, C5a) or activating stimuli (eg lipopolysaccharide or TNFα). For these reasons, the Transwell assay (Corning) was employed to measure migratory capacity of Csk-deficient granulocytes.

Migration of Csk-deficient granulocytes in response to fMLP was indeed impaired (figure 9.6c), indicating that the hyper-adhesiveness was accompanied by deregulation of the dynamic remodelling process, which involves not only establishment, but also resolution of cell/substratum interaction to enable locomotion of the cell.

To more closely analyse the effect of Csk deficiency upon cell/substratum interactions, bone marrow leukocytes were cultured in suspension, fixed and adhered to polylysine-coated glass slides or were adhered to uncoated or fibrinogen-coated glass slides. Confocal microscopy analysis was subsequently employed to visualise the extracellular distribution of β2-integrin and the extent of intracellular actin polymerisation in cultured

granulocytes via staining with anti-CD11b and phalloidin respectively. The increased level of β2-integrin expression demonstrated previously by FACS analysis in suspension-cultured Csk-deficient granulocytes when compared to control cells (figure 9.3) was further corroborated by confocal analysis of CD11b distribution. Csk-deficient granulocytes showed greater staining intensity with CD11b when compared to control cells (figure 9.6d). Remarkably, Csk-deficient granulocytes also showed substantially enhanced formation of integrin clusters (figure 9.6d) which are central for effective cell adhesion and signalling (reviewed in Hogg *et al.*, 2002) when compared to control cells. Furthermore, extensive staining for polymerised actin at these sites of integrin clustering indicates augmented cytoskeletal remodelling in suspension-cultured Csk-deficient granulocytes independent of adhesion.

The effects of Csk deficiency became increasingly striking when granulocytes were adhered to glass (figure 9.6e) or fibrinogen (figure9.6f). Csk-deficient granulocytes cultured either on the non-specific substrate glass or the β2-integrin counter receptor – fibrinogen, extended cellular processes in the form of pronounced filopodia or lamellipodia respectively, which are largely absent in the control granulocyte population. These data support the hypothesis that Csk negatively regulates granulocyte adhesion by suppressing both spontaneous cytoskeletal remodelling and the establishment of cellular processes that form focal contacts and adhesions.

9.7 Spontaneous Tyrosine Hyperphosphorylation of Src-fk Substrates in Csk-Deficient Granulocytes.

To determine whether the negative regulatory effect of Csk upon granulocyte adhesion and migration is reflected at the level of signal transduction, the levels of tyrosine phosphorylation of key signalling components involved in these cellular processes were examined.

In the first instance, total cellular protein tyrosine phosphorylation was examined in flow-sorted control and Csk-deficient bone marrow granulocyte lysates. Quiescent bone marrow granulocytes showed similar baseline tyrosine phosphorylation in both controls and conditional mutants. However, a rapid accumulation of tyrosine-phosphorylated proteins was observed in both genotypes after culture in suspension for five minutes (figure 9.7a). Notably, an 85kD protein was consistently hyper-phosphorylated in the conditional mutants. Furthermore, hypo-phosphorylation of proteins in the 60kD range is observed in the

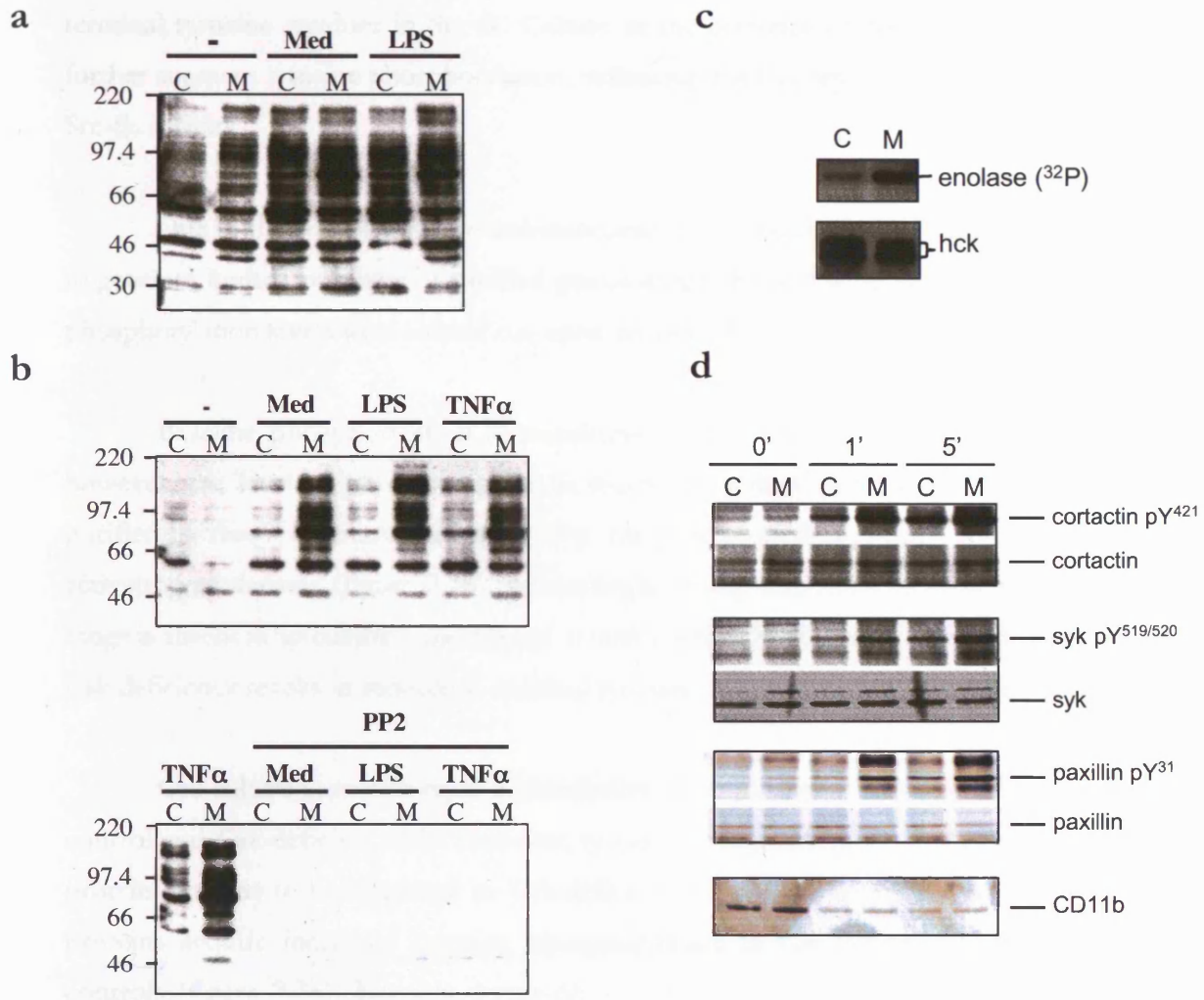

Figure 9.7. Csk deficiency in cultured granulocytes is associated with augmented accumulation of tyrosine phosphorylated proteins, enhanced Hck kinase activity, and hyperphosphorylation of integrin signalling component - Syk, cortactin and paxillin. Immunoblot analysis for total phosphotyrosine levels in FACS sorted control (C) and Csk-GEcre (M) $Gr1^{hi}$ bone marrow granulocytes (**A**) or total bone marrow leukocytes (**B**) before and after 5min culture in medium alone (med). Some cultures received either 100ng/ml LPS (LPS), 10ng/ml TNFα (TNFα), or 10μM PP2 (PP2), a specific inhibitor of Src-fk. SDS total cell lysates equivalent to 1 x 10^5 cells were subjected to immunoblot analysis with the anti-phosphotyrosine antibody (RC20). (**C**) Autoradiograph reveals Hck kinase activity against the Src-fk substrate enolase (top) and Hck protein levels after precipitation from purified control (C) and Csk-GEcre (M) granulocytes. Densitometric analysis revealed a 5.6-fold increase in Hck activity in Csk-deficient granulocytes when compared to controls. (**D**) Immunoblot analyses of phosphotyrosine (upper) or total protein levels (lower) in depletion purified bone marrow granulocytes before (0) and after 1min (1') or 5min (5') culture. The level of protein expression and the extent of specific tyrosine phosphorylation was determined using monoclonal antibodies against either cortactin, Syk and paxillin, or against cortactin Y421, Syk Y519/520 and paxillin Y31 respectively. Note the augmented phosphorylation of the integrin signalling associated proteins cortactin, Syk and paxillin in Csk-deficient granulocytes is apparent after as little as one minutes culture. Equivalent expression of CD11b in control and Csk-GEcre protein lysates was confirmed to exclude that increased tyrosine phosphorylation simply reflects differences in integrin expression.

conditional mutants most likely reflecting reduced Csk mediated phosphorylation of the C-terminal tyrosine residues in Src-fk. Culture in the presence of lipopolysaccharide did not further augment tyrosine phosphorylation, indicating that Csk represents a master regulator of Src-fk activity.

Due to the complex nature and associated time consumption of using flow cytometry to generate limited numbers of purified granulocytes, the following studies on total tyrosine phosphorylation levels were carried out upon unsorted bone marrow leukocyte suspensions.

Baseline phosphorylation in uncultured bone marrow leukocytes is again similar, however, the level of phosphorylation is much lower than that observed in granulocytes purified by flow cytometry, indicating that the process of flow sorting itself may partially activate granulocytes (figure 9.7b). Interestingly, phosphorylation of proteins in the 60kD range is absent in uncultured conditional mutants strengthening the previous hypothesis that Csk deficiency results in reduced C-terminal tyrosine phosphorylation of Src-fk.

Cell culture induces a rapid accumulation of tyrosine-phosphorylated proteins in both control and Csk-deficient cells. However, tyrosine phosphorylation of 68kD and 90-120kD proteins appears to be restricted to Csk-deficient cell lysates, while 85kD and 120-150kD proteins acquire increased tyrosine phosphorylation in Csk-deficient cells compared to controls (figure 9.7b). Notably, hyper-phosphorylated 120kD proteins observed in Csk-deficient bone marrow lysates are not observed in flow-sorted granulocyte lysates, possibly reflecting effects of cell processing, or perhaps the absence of a specific myeloid cell population which are responsible for tyrosine phosphorylation of these proteins, for example, macrophages (figures 9.7a and 9.7b). Culture in the presence of LPS or TNFα did not further augment tyrosine phosphorylation, and therefore all further studies were carried out in the absence of these pro-inflammatory mediators. Hyper-phosphorylation was fully sensitive to PP2, which completely abolished it in both controls and conditional mutants (figure 9.7b).

Concurrent with the increased tyrosine phosphorylation levels, the activity of Hck immuno-precipitated from depletion-purified bone marrow granulocytes against enolase, a commonly used Src-fk substrate (Nada *et al.*, 1993) (figure 9.7c) was markedly augmented (5.6 fold) in Csk deficient cells. Similar elevations in tyrosine kinase activity were reported for Lyn (8.5 fold increase) in cells derived from Csk null embryos (Nada *et al.*, 1993).

9.7.1 Hyperphosphorylation of Syk, a proximal event in β2-integrin signalling during granulocyte adhesion, is observed in Csk-deficient granulocytes.

Augmented β2-integrin cell surface expression, degranulation, spreading and reduced migratory capacity in cultured Csk-deficient granulocytes has been demonstrated. In human granulocytes, a proximal event of β2-integrin-mediated signalling is the activation of the non-Src tyrosine kinase $p72^{Syk}$ (Syk) (Yan *et al.*, 1997; Berton *et al.*, 1996; Dib K. 2000). Integrin mediated activation of Syk is critical for granulocyte respiratory burst, degranulation, and spreading in response to proinflammatory stimuli while adherent to immobilised integrin ligands or when stimulated by direct cross-linking of integrins (Mocsai *et al.*, 2002). It has been previously reported that Syk is stimulated by activation of Src-fk's (Mocsai *et al.*, 2002; Keshvara *et al.*, 1998). Indeed, macrophages lacking Hck and Fgr demonstrate hypophosphorylation of Syk (Suen *et al.*, 1999). Furthermore, inhibition of Src-fk's blocked Syk activation and inhibited phosphorylation of Syk substrates (Vav1, Vav3, SLP-76) implicated in cytoskeletal regulation in platelets (Obergfell et al., 2002). To establish whether deregulation of Src-fk activity associated with enhanced β2-integrin expression (figure 9.3a) and cluster formation (figure 9.6d) observed in Csk-deficient granulocytes is accompanied by hyperactivation of Syk, a central mediator of integrin signal transduction, the phosphorylatyion state of Syk was determined from depletion purified bone marrow granulocyte lysates. Using a phospho-specific antibody against tyrosines 519 and 520, the hyperphosphorylation state of Syk in Csk-deficient granulocytes was indeed confirmed (figure 9.7d).

This data demonstrates that Syk is hyperphosphorylated in Csk-deficient granulocytes independent of cell adhesion. In platelets, Csk is constitutively associated with integrins. Upon ligand binding, Csk dissociates from the integrin complex resulting in activation of Src-fk and Syk (Obergfell et al., 2002), thereby supporting a model in which Csk suppresses integrin signalling through constitutive suppression of integrin associated Src-fk kinase activity by default. In this model, Csk is critical for maintaining ligand dependence for initiation of integrin signalling and downstream cellular functions. In the absence of Csk, the requirement of ligand dependency would speculatively be removed resulting in adhesion independent initiation of integrin signalling leading to augmented phosphorylation of Syk, cell spreading and degranulation as observed in Csk-deficient granulocytes.

9.7.2 The focal adhesion component, paxillin, is hyperphosphorylated in Csk-deficient granulocytes.

Reduced migratory capacity associated with augmented cell surface expression of β2-integrin and adhesiveness has been observed in cultured Csk-deficient granulocytes. Paxillin, a multi-domain scaffold protein, represents a cellular target for protein tyrosine kinases activated as a result of integrin signalling after cell adhesion (Burridge *et al.*, 1992). Integrin clustering leads to autophosphorylation of focal adhesion kinase (FAK) upon tyrosine residue 397 (Calalb *et al.*, 1995; Eide *et al.*, 1995; Schaller *et al.*, 1994). Association of Src with FAK through an SH2-mediated interaction with tyrosine 397, forms a complex which is reportedly responsible for the phosphorylation of N-terminal residues residues 31 and 118 on paxillin which has been shown to permit the recruitment of CRK and p130Cas. Given that this complex formation is dependent on paxillin phosphorylation and furthermore, that the association of Crk with both p130Cas and paxillin is central to co-ordinating integrin-mediated cell motility (Klemke *et al.*, 1998; Petit *et al.*, 2000; Schaller and Parsons, 1995), the phosphorylation state of paxillin was determined from depletion purified bone marrow granulocyte lysates. Using a phospho-specific polyclonal antibody against tyrosine-31, the hyperphosphosphorylation state of paxillin was confirmed (figure 9.7d).

This data demonstrates that paxillin, a central scaffold component at the foundation of focal adhesion complexes for a wide range of proteins, including Src-fk's, phosphatases, and cytoskeletal structures (Turner, 2000), is hyperphosphorylated in cultured Csk-deficient granulocytes. This is likely to disrupt the regulated recruitment of specific proteins involved in the assembly and/or disassembly of focal adhesions resulting in impaired turnover of focal adhesions and ultimately cell migration.

9.7.3 Identification of the 85kD major tyrosine phosphorylated protein, cortactin, in Csk-deficient granulocytes.

An 85kD hyperphosphorylated protein is observed in cell lysates derived from cultured Csk-deficient granulocytes. Nada et al have previously identified an 85kD hyperphosphorylated protein in cell lysates derived from Csk-deficient fibroblasts as cortactin (Nada et al., 1994). Intriguingly, normal cortactin phosphorylation was restored in fibroblasts deficient for both Csk and Src (Thomas *et al.*, 1995), indicating that in fibroblastic cells Src directly phosphorylates cortactin. Fyn Src-fk has also been implicated in the phosphorylation

of cortactin in K-1735 murine melanoma cell lines (Huang *et al.*, 2003). Importantly, c-Src has been directly implicated in the tyrosine phosphorylation of cortactin in response to integrin-mediated cell adhesion and spreading (Vuori and Ruoslahti, 1995). Furthermore, given that it has been previously demonstrated that cortactin drives the reorganisation of the actin cytoskeleton via the actin related protein (Arp)2/3 complex (Uruno *et al.*, 2001), and therefore may represent a candidate for deregulation of cell migration, the phosphorylation state of cortactin was analysed in depletion purified bone marrow granulocyte lysates. Using a phospho-specific antibody against tyrosine-421, the hyperphosphorylation state of cortactin in Csk-deficient granulocytes was indeed confirmed (figure 9.7d).

This data demonstrates that cortactin is hyperphosphorylated on tyrosine-421 in Csk-deficient cells independent of cell adhesion. It has been previously demonstrated that Src phosphorylates murine cortactin in vitro on tyrosine residues 421, 466 and 482, which are also the major sites of tyrosine phosphorylation in v-Src transformed cells (Huang *et al.*, 1998). Mutation of tyrosine-421 to phenylalanine abolishes phosphorylation of tyrosine-466 (Head *et al.*, 2003) suggesting a processive phosphorylation model for cortactin. Therefore, enhanced tyrosine phsophorylation upon tyrosine-421 is likely to influence phosphorylation of other tyrosine residues which may provide additional binding sites for specific signalling proteins with SH2 domains, which connceivably may regulate the cellular functions performed by cortactin.

Cumulatively, these data show that Csk plays a central role in the negative control of degranulation and integrin release while negatively modulating cell activation and the activation of major pathways driving granulocyte recruitment and activation.

Chapter 10. Overcoming incomplete Cre mediated deletion of loxP flanked DNA sequences *in vivo*. Are introns the way forward?

A fundamental drawback of Cre/lox P technology has been demonstrated in our conditional inactivation of Csk in myeloid cells – incomplete deletion. Approximately 50% deletion is observed in both $Csk^{fl/+}$-$GE^{cre/+}$ (figure 8.1b). Incomplete deletion observed in our mouse model is not unique. In fact, incomplete deletion has also been observed in conditional mutants derived from lck-Cre and aP2-Cre mice (Barlow *et al.*, 1997; Hennet *et al.*, 1995). As outlined in the introduction (section 3.4.2), the efficiency of Cre-mediated deletion of a floxed allele and its relationship to the number of Cre molecules per cell has not been determined. However, it is conceivable that a threshold level of Cre molecules per cell is required to obtain complete deletion of the desired floxed allele within a cell population. Promoter activity governing Cre recombinase expression is important in establishing the level of Cre recombinase activity in a given cell type, and thus the efficiency of gene modification. Thus, it follows that the use of weak or transiently expressed promoters may result in reduced Cre recombinase activity accompanied by reduced gene modification efficiency. Increasing autonomous Cre recombinase expression may provide a solution to this problem. Here, a method is reported of increasing autonomous expression of both the Cre recombinase and green fluorescent protein (GFP) through insertion of two heterologous intron sequences directly into their open reading frames resulting in modified genes that yield a natural mammalian structure.

10.1 Construction of iCre and iGFP vectors.

Manipulation of EGFP was undertaken to generate unique restriction sites within the coding region to allow convenient intron insertion. Minigenes were then assembled via introduction of introns as described in tables 10.1.1-10.1.6. These cloning strategies produced a number of pairs of Cre recombinase coding sequences and a pair of GFP coding sequences that differed only by the presence or absence of two introns with expression of said genes under the control of the CMV promoter. Construction of eGFP, iGFP, CreX, and iCre vectors had been previously undertaken by Miss Aileen McDermott (eGFP, iGFP) and Dr Adam Lacy-Hulbert (CreX, iCre). Assembly tables for these vectors are given for completeness. It must be noted that the parental vectors eGFP and CreX do not contain any intronic sequence either in their open reading frames or their untranslated regions (UTR), and thus serve as intronless controls for the modified vectors in which introns have

been cloned directly into the open reading frame. No GFP or Cre vectors were available within the Roes lab. with intronic sequence cloned into the 5' or 3' UTR. Thus a comparison could not be made between the efficacy of introns placed into the UTR or directly into the ORF. It is important to stress, however, that the rational for cloning more than one intron directly into the ORF is to primarily take advantage of the co-operative effect between introns in enhancing gene expression (Neel *et al.*, 1993; Nesic and Maquat, 1994) and furthermore, to circumvent the possible negative effects of cloning an intron into either the 5' or 3' UTR (section 3.4.3).

10.1.1 Construction strategy for CreX vector

Vector name	Plasmid Backbone	Insert	Construction
pSP72creSB	pSP72	PCR amplifications of P1phage with primer pairs Cre1f/Cre1r and Cre2f/Cre2r ligated together and digested with SalI and BamHI.	SalI/BamHI fragment cloned into pSP72
pSP72creBC	pSP72	PCR amplifications of P1phage with primer pairs Cre2f/Cre2r and Cre3f/Cre3r ligated together and digested with BamHI and ClaI.	BamHI/ClaI fragment cloned into pSP72
pSP72creCX	pSP72	PCR amplifications of P1phage with primer pairs Cre3f/Cre3r and Cre4f/Cre4r ligated together and digested with ClaI and XhoI.	ClaI/XhoI fragment cloned into pSP72
PSP72creSC	pSP72	pSP72creBC digested with BamHI/ClaI	BamHI/ClaI fragment cloned into pSP72creSB digested with BamHI/ClaI.
pXcreB18.36A	pSP72	pSP72creSC digested with ClaI/XhoI.	ClaI/XhoI fragment cloned into pSP72creSC digested with ClaI/XhoI.
CreX	EGFP-N1	pXcreB18.36A digested with Sal/XhoI	SalI/XhoI fragment cloned into modified EGFP-N1.

10.1.2 Construction strategy for iCre vector

Vector name	Plasmid Backbone	Insert	Construction
pSP72-Eco.BglII	pSP72	N/A	pSP72 digested with EcoRI and BglII in the MCS and religated to remove EcoRV site used for subsequent cloning.
pSPCRE	pSP72	SalI/XhoI fragment derived from pXcreB18 (1060bp)	SalI/XhoI fragment cloned into identical sites of pSP72
pSPCREmi1	pSP72	PCR amplification of IgM intron (mi1) using primers mi1 and mi1r. (110bp) and template vector p1μCS	PCR fragment blunt ended, phosphorylated and cloned directly into the EcoRV site of pSPCRE within the Cre recombinase gene resulting in loss of said site.
pSPCREmi1 ei3	pSP72	PCR amplification of IgE intron (ei1) using primers ei3 and ei3r. (81bp) and template vector pB1-8ε	PCR fragment blunt ended, phosphorylated and cloned directly into the PvuII site of pSPCRE within the Cre recombinase gene retaining said site at the 5' end of the intron.

10.1.3 Construction strategy for iCre2 vector

Vector name	Plasmid backbone	Insert	Construction
iCre2	pCMV-CRE (from SCS110 cells)	PCR amplification of pCMV-CRE (iCre1) with primers Cre2f - 489Rmut and Cre141F - 489Rmut digested with BamHI/PvuI	BamHI/PvuI digested PCR products were inserted into BamHI/PvuI digested pCMV-CRE which had been passaged through SCS110 cells to ablate methylation in the DNA.

10.1.4 Construction strategy for iCre3 vector

Plasmid name	Vector backbone	Insert	Construction
pSPCrei2ei 3	pSP72	Amplified PCR fragment of pCreXS vector template using pfu polymerase and primers ei3F and βglobC2, then digested with EcoRI.	Cloned as blunt/EcoRI fragment into PvuII/EcoRI digested pSPCreI2 vector.
pSPiCre	pSP72	XhoI/PvuII fragment derived from pSPCremu1.	Cloned as XhoI/PvuII fragment into XhoI/Eco72I digested pSPCreI2ei3.
iCre3	EGFP-N1	AgeI/ClaI fragment derived from pSPiCre	Cloned as AgeI/Cla fragment into identically digested pCMV CRE.

10.1.5 Construction strategy for iCre4 vector

Vector name	**Plasmid Backbone**	**Insert**	**Construction**
pSPCre668 -839	pSP72	PCR amplification of pSPCre with primers Cre668f and Cre1045r using pfu polymerase, digested with ClaI.	ClaI digested PCR product inserted into SmaI/ClaI digested pSP72
pSPei3.668 -839	pSP72	PCR amplification of ei3 intron from pSPiCRE with primers ei3FPml and ei3r.	PCR product inserted into SmaI digested pSPCre668-839.
pSPniCRE	pSP72	PCR amplification of pCMV-iCRE with Cre141f and Cre667r with pfu polymerase, digested with BamHI.	BamHI digested PCR product inserted into BamHI/PmlI digested pSPei3.668-839.
iCre4	pCMV-iCRE	BamHI/ClaI fragment derived from pSPBCiCRE	Bam/Cla fragment inserted into similarly digested pCMV-iCRE.

10.1.6 Construction strategy for EGFP and iGFP vectors

Vector name	Plasmid Backbone	Insert	Construction
pSPeGFP-1	pSP72	PCR fragment (1) amplified with eGFP1 and eGFP1R incorporating a nuclear localisation signal and introducing a XhoI site at the 5' end and a SmaI site at the 3' end. (361bp)	XhoI and SmaI digested PCR fragment was cloned directly into pSP72 at identical sites.
pSPeGFP-12	pSP72	PCR fragment (2) amplified with eGFP2 and eGFP2R introducing a SmaI site at the 5' end and a PvuII and an EcoRI site at the 3' end. (236bp)	SmaI/EcoRI digested PCR fragment was cloned into identical sites of pSPeGFP-1
pSP1-3	pSP72	PCR fragment (3) amplified with eGFP3 and eGFP3R introducing a PvuII site at the 5' end and a BglII site at the 3' end. (236bp)	PvuII/BglII digested PCR fragment was cloned into identical sites of pSPeGFP-12
pSP1-3.mi1	pSP72	PCR amplification of IgM intron (mi1) using primers mi1 and mi1r. (110bp) and template vector p1μCS.	PCR fragment blunt ended, phosphorylated and cloned directly into the SmaI site of pSP1-3 within the GFP gene resulting in loss of said site.
pSP1-3 .mi1+ei3	pSP72	PCR amplification of IgE intron (ei1) using primers ei3 and ei3r. (81bp) and template vector pB1-8ε	PCR fragment blunt ended, phosphorylated and cloned directly into the PvuII site of pSP1-3 within the GFP gene retaining said site at the 5' end of the intron.
iGFP	EGFP-N1	XhoI/BsrGI fragment derived from pSP1-3.mi1+ei3 encompassing the iGFP gene. (~940bp)	XhoI/BsrGI fragment cloned into EGFP-N1
eGFP	EGFP-N1	XhoI/BsrGI fragment derived from pSP1-3 encompassing the GFP gene. (~740bp)	XhoI/BsrGI fragment cloned into EGFP-N1

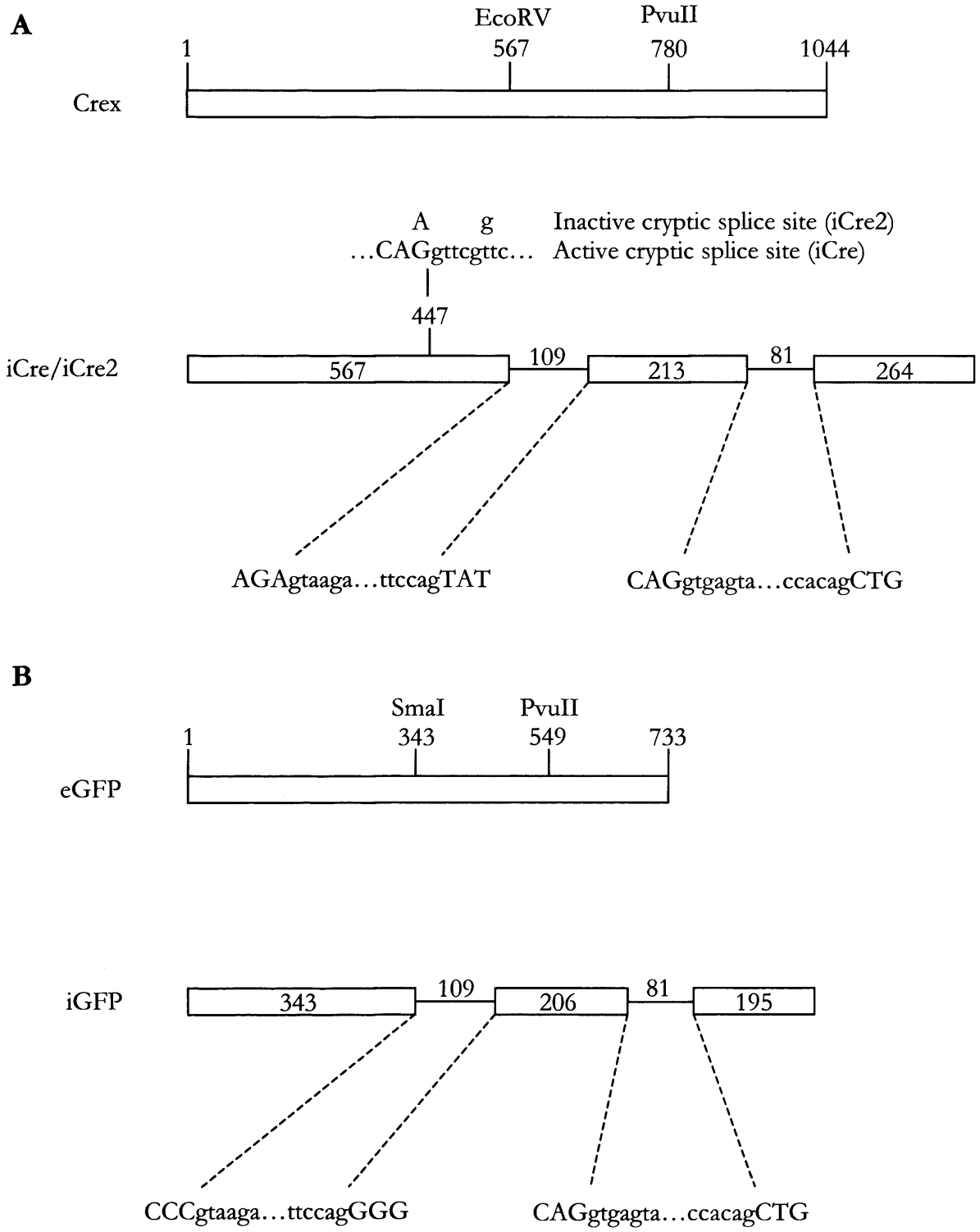

Figure 10.1.7. Artificial gene topologies. Open boxes represent either the intact intronless gene or exons generated via intron insertion (straight lines). Numbers indicate the position of natural or artificially generated restriction sites in the coding seqeunce or the length in base pairs of exons and introns generated by intron insertion. Upper case letters represent exonic sequence whilst lower case letters represent intronic sequence. The cryptic site at position 447 activated in iCre and the silent mutagenesis strategy employed to weaken this site to generate iCre2 are shown. Complete details for the construction of these artificial genes are found in Sections 10.1.1 - 10.1.6.

10.2 Intron mediated enhancement of gene expression.

Chinese hamster ovary (CHO) cells were stably transfected with constructs containing either the intronless or intron containing genes (See figure 10.1.7 – Artificial gene topologies). Drug resistant clones were pooled in order to reduce the variability of expression data due to possible site-specific integration effects, and passaged once before harvesting at mid-log phase for cytoplasmic RNA preparation.

10.2.1 Introduction of heterologous introns into the EGFP open reading frame results in a 30-fold increase in mRNA expression accompanied by a 5-fold increase in cellular fluorescence.

RT-PCR (described in full in figure legend) revealed a single amplification product of predicted size in cells transfected with eGFP or iGFP. Restriction digestion of RT-PCR products with SmaI and PvuII show reconstitution of the open reading frame confirming precise excision of introns through RNA splicing (Figure 10.2.1A), further supported by DNA sequencing.

Preparation of serial dilutions of cytoplasmic total RNA from eGFP and iGFP transfected cells, followed by hybridisation with sequence specific probes and phosphor-image analysis revealed an approximate 30-fold increase in steady-state iGFP mRNA level (Figure 10.2.1B).

Furthermore, flow cytometric analysis of randomly selected and expanded clones revealed an increase in protein expression in the iGFP population, concomitant with the elevated mRNA expression. Overall, a five-fold increase in mean level of FL1 fluorescence was observed for iGFP (n=23) over eGFP (n=24) transfected clones (Figure 10.2.1C). Moreover, increased homogeneity is observed within the iGFP population as indicated by the reduced co-efficient of variation (CV) values (148 ± 8.8 iGFP, 182 ± 11.9 eGFP) compared to eGFP, suggesting an increased uniformity of expression within clonal populations. Thus, the presence of introns in the coding sequence of GFP improves both levels and homogeneity of gene expression.

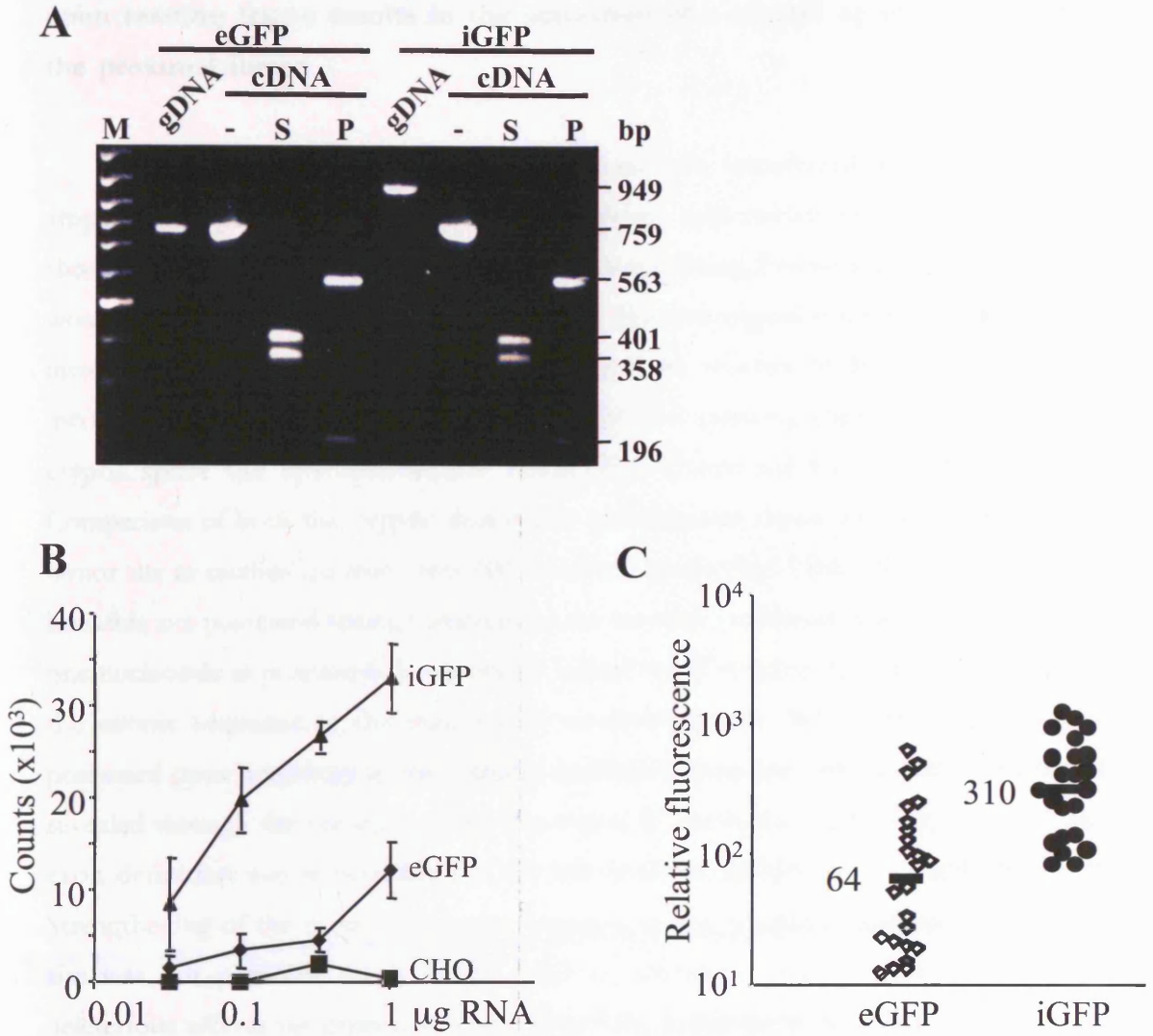

Figure 10.2.1: Creation of artificial exons through intron insertion into eGFP. A: rtPCR of mRNA from CHO cells transfected independently with eGFP and iGFP. GFP specific PCR of genomic DNA (gDNA) amplified with EGFP1 and EGFP3R shows the expected products of 759 bp for eGFP and 949 bp for iGFP including the two introns. cDNA amplification of iGFP and eGFP both reveal a 759 bp product indicative of removal of introns by RNA splicing. Digestion of the rtPCR products with Sma I (S) or Pvu II (P) leads to generation of 401/358 and 563/196 bp product pairs respectively, indicating the reconstitution of the ORF, which was further confirmed by DNA sequencing (data not shown). No PCR products were amplified in negative control samples lacking reverse transcriptase to exclude amplification from contaminating chromosomal DNA. **B:** GFP mRNA expression in pools of cells stably transfected with eGFP or iGFP expression vectors respectively. Signal intensity of slot blots was determined by phosporimage analysis of serial dilutions of mRNA and normalised to signals obtained with a GAPDH probe to adjust for mRNA loading. Relative expression levels of GAPDH and neo^r mRNA were identical in eGFP and iGFP expressing pools confirming the presence of equivalent GFP plasmid copy numbers in both pools of transfectants negating the requirement for Southern blot data. **C:** GFP expression in stable clones transfected with eGFP or iGFP. Mean green fluorescence of clones transfected with iGFP (closed symbols) or eGFP (open symbols). Geometric mean fluoresence of the population of eGFP and iGFP clones is indicated by a horizontal bar. Note the increased homogeneity observed within the iGFP population as indicated by the reduced co-efficient of variation (CV) values (148 ± 8.8 iGFP, 182 ± 11.9 eGFP) compared to eGFP, indicating an increased uniformity of expression within iGFP clonal populations. Untransfected CHO cells showed a background fluorescence of 3.2 relative fluorescent units (data not shown).

10.2.2 Introduction of heterologous introns into the modified Cre recombinase open reading frame results in the activation of a cryptic splice site upstream of the proximal intron

RT-PCR of cytoplasmic total RNA from cells transfected with CreX revealed an amplification product of predicted size. However, cells transfected with iCRE revealed a shorter than expected product suggesting incorrect splicing. Precise splicing of iCRE preRNA would reconstitute the open reading frame and thus the original restriction sites employed for intron insertion. Restriction digestion identified the absence of EcoRV, which suggested incorrect splicing of the IgM-derived intron. DNA sequencing confirmed the presence of a cryptic splice site upstream of the 'bonafide' 5' donor site for the IgM-derived intron. Comparison of both the cryptic donor site and bonafide donor site with the consensus 5' donor site as established from over 400 vertebrate genes (See Table 10.2.3) revealed that the bonafide site possessed strong homology to the intronic consensus sequence only differing by one nucleotide at position 6, but however lacked the 3' terminal G nucleotide which defines the exonic sequence in the majority of vertebrate genes. Whilst the cryptic splice site possessed poor homology to the intronic consensus sequence, strong exonic definition was revealed through the presence of the 3' terminal G nucleotide. This suggested that the poor exon definition was responsible for the incorrect recognition of the IgM-derived intron. Strengthening of the exonic consensus sequence at the bonafide IgM-derived intron donor site was not plausible for it would result in alteration of codon usage that may have deleterious effects on protein folding. Therefore, a mutagenesis strategy was employed to primarily weaken exon definition at the cryptic splice site, in addition to weakening further the intronic consensus sequence homology. The resultant construct was designated iCre2.

10.2.3 Modification of the cryptic splice site observed in iCre using silent mutagenesis results in correct splicing and is associated with a 30-fold increase on mRNA expression.

The identified cryptic splice site in the iCre construct was effectively disabled using PCR mutagenesis to weaken both cryptic exon definition, and the intron donor site consensus sequence whilst maintaining codon usage (Montell *et al.*, 1982; Nelson and Green, 1990; Nilsson and Magnusson, 1983; Reed and Maniatis, 1985; Treisman *et al.*, 1983; Treisman *et al.*, 1982). Two subtle mutations were introduced at nucleotide residue positions 454 G->A and 460 T->G (See table 10.2.3).

Table 10.2.3. Illustration of 5' splice sites

Consensus	-	A	G:	G	U	A	A	G	U	-	-
Bonafide	-	A	T:	G	U	A	A	G	A	-	-
Cryptic	-	A	G:	G	U	U	C	G	U	-	-
Cryptic^{Mt}	-	A	A:	G	U	U	C	G	G	-	-

RT-PCR analysis revealed the predicted single amplification product in cells transfected with CreX and iCre2 suggesting that aberrant splicing exhibited in the parent iCre construct had been abolished. Reconstitution of the open reading frame was confirmed by restriction analysis using EcoRV and PvuII indicating precise removal of introns (Figure 10.2.3A). DNA sequencing further corroborated this. Thus, in this instance, divergence from the exonic consensus sequence at the 3' terminal end of the primary exon results in attenuation of splicing at the bonafide site and activation of a cryptic splice site. Silent mutagenesis of the strong exonic sequence at the cryptic splice site abolishes splicing at that site and restores correct splicing at the bonafide site.

Again mRNA expression was analysed via serial dilutions of cytoplasmic total RNA from CreX and iCre2 transfected cells, followed by hybridisation of sequence specific probes generated by PCR. Signal intensities were quantitated using phosphor-image analysis. An approximate 30-fold increase in steady-state iCre mRNA levels was observed. (Figure 10.2.3B).

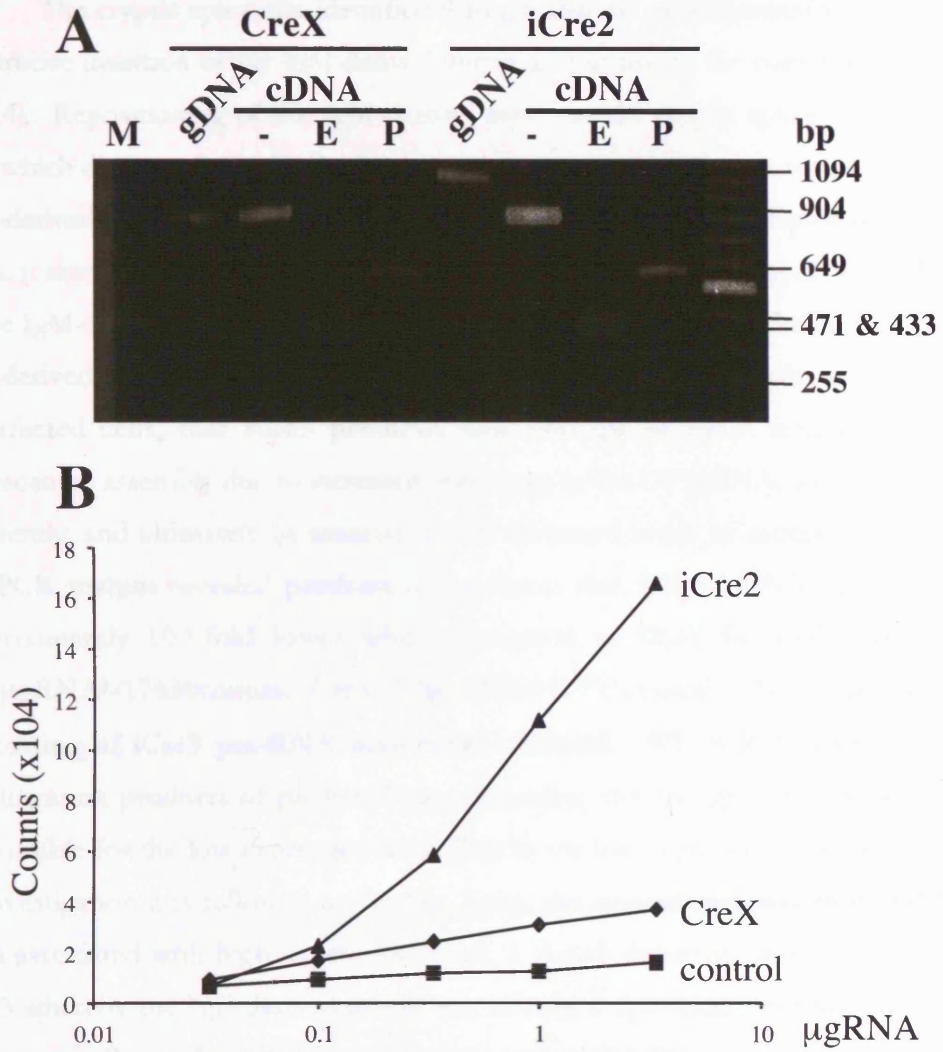

Figure 10.2.3: Creation of artificial exons through intron insertion into CreX. A: rtPCR of mRNA from CHO cells transfected independently with CreX and iCre2. Cre specific PCR of genomic DNA (gDNA) amplified with Cre 141F and Cre1045R shows the expected products of 904 bp for CreX and 1094 bp for iCre2. cDNA amplification of CreX and iCre2 both reveal a 904 bp product indicating precise removal of introns by RNA splicing. Digestion of CreX and iCre2 derived rtPCR products with EcoRV (E) or Pvu II (P) reveals 471/433 and 649/255 bp product pairs respectively, indicating the reconstitution of the ORF and supporting precise removal of introns. This was further confirmed by DNA sequencing (data not shown). No PCR products were amplified in negative control samples lacking reverse transcriptase to exclude amplification from contaminating chromosomal DNA. **B:** Cre mRNA expression pools of cells stably transfected with eGFP or iGFP expression vectors respectively. Signal intensities of serial diluted total cytoplasmic RNA were determined by phosphoimage analysis and normalised to signals obtained with a GAPDH probe to adjust for mRNA loading. An approximate 30-fold increase in Cre expression is observed in iCre2 transfected cells. Equivalent Cre vector copy numbers in both pools of transfectants was confirmed by identical levels of GAPDH and neoR mRNA expression negating the requirement for Southern blot

10.2.4 Other modifications – iCre3 and iCre4

The cryptic splice site identified through analysis of iCre transfected cells was utilised for precise insertion of the IgM-derived intron, giving rise to the construct iCre3 (see section 10.1.4). Repositioning of the IgM-derived intron at the cryptic splice site results in a donor site, which diverges from the donor consensus sequence at only one residue. Furthermore, the IgM-derived intron acceptor site shows no divergence from the acceptor consensus sequence. Thus, it seems reasonable to suggest that the presence of both strong donor and acceptor sites at the IgM-derived intron/exon boundaries, and in addition, that the current position of the IgE-derived intron has already been associated with increased levels of expression in iCre2 transfected cells, that iCre3 pre-RNA will perhaps be more readily recognised by the spliceosome assembly due to increased homology to the U1 snRNA, and thus processed more efficiently, and ultimately be associated with increased levels of expression. However, whilst RT-PCR analysis revealed products of predicted size, iCre3 mRNA expression levels were approximately 100-fold lower when compared to CreX by slot blot analysis (CreX: 0.03μgRNA=17630counts, iCre3: 3.3μgRNA=15771counts). This suggested that aberrant processing of iCre3 pre-RNA may have occurred. RT-PCR revealed correctly spliced amplification products of predicted size, discarding the thought that incorrect splicing was responsible for the low expression level. Due to the low expression levels of iCre3, this route of investigation was followed no further. Since, the internal exon size from iGFP had already been associated with high expression levels, a fourth construct was engineered based upon iCre3 whereby the IgE-derived intron was relocated upstream resulting in an internal exon size very similar to the iGFP construct (see section 10.1.5).

Repositioning of the 3' IgE-derived intron upstream towards the 5' IgM-derived intron in iCre3 generating iCre4 maintained a similar internal exon size as the high expression associated iGFP construct. iCre4 demonstrated similar mRNA expression levels as compared to CreX by slot blot analysis (CreX: 0.1μgRNA=30172counts, iCre3: 0.1μgRNA=28759counts). Thus, in relative terms, a 100-fold increase in iCre4 expression is observed over iCre3. The relative increase in expression maybe a direct consequence of the reduction of the internal exon size from 335bp in iCre3 to 213bp in iCre4. This supports previous observations that stable exon complexes will only be formed in the presence of a 3' and 5' splice sites in the correct orientation and within 300 base pairs of one another (Robberson *et al.*, 1990). The presence of introns in iCre4 were not associated with increased mRNA expression when compared to CreX. Intron positioning within the iCre4 construct

may have altered the phasing of nucleosomes relative to the CMV promoter element and may account for this observation (Brinster *et al.*, 1988).

DISCUSSION

Chapter 11 Myeloid Cell Specific Csk Deficiency in Mice

To assess the importance of Csk and its contribution to the negative regulation of Src-fk in myeloid cell function, the Cre/loxP recombination system (section 3.4) was utilised to inactivate Csk in a cell type specific manner. As outlined in section 3.4.2, identification and characterisation of a promoter are required to provide essential information regarding the onset and cell specificity of promoter driven expression. To target deletion to myeloid cells, primarily granulocytes, the granulocyte elastase promoter was utilised for the production of Cre transgenic mice.

Granulocyte elastase (GE) is a potent serine protease located on chromosome 19 in between proteinase 3 and azurozidin. Despite the term granulocyte elastase, GE has been recovered from other cell types other than granulocytes, including blood monocytes and alveolar macrophage (Harris and Ralph, 1985; Rodriguez *et al.*, 1977; Senior *et al.*, 1982). Paradoxically, in depth GE expression analyses revealed no mRNA expression in resting or stimulated blood monocytes, or alveolar macrophage. Indeed, another study using the immature myeloid cell line, HL-60 showed an accumulation of GE transcripts when differentiated towards the myelocytic lineage and not when differentiated towards the monocytic lineage (Takahashi *et al.*, 1988; Yoshimura and Crystal, 1992). Furthermore, Shapiro et al. reported that the low levels of GE found in monocyte subpopulations are generally lost upon differentiation into macrophage, superseded by macrophage–specific proteins (Shapiro *et al.*, 1991). These data are consistent with granulocyte elastase expression by bone marrow precursors with an emphasis towards the myelocytic and not monocytic lineages. In light of the above, the precise onset and termination of granulocyte elastase expression continues to be unclear, but it is almost certainly confined to cells of the myelocytic lineage and thus represented a good candidate for the generation of a Cre transgenic mouse for use in myeloid cell specific mutagenesis.

To define the role of Csk in myeloid cells, Csk^{flox} mice provided by Christian Schmedt (Schmedt *et al.*, 1998) were crossed with the GE^{cre} mice.

11.1 Csk-GEcre mice provide the foundation to study the role of Csk and its contribution to Src-fk regulation in myeloid cells *in vivo*.

We used a Southern blot strategy similar to Schmedt et al to determine the level of deletion and specificity in resting and inflammatory myeloid cell DNA (Schmedt *et al.*, 1998). $Csk^{fl/+}$-$GE^{cre/+}$ mice presented 55 ± 1% and 53 ± 3% somatic deletion of the *csk* allele in bone marrow derived and peritoneal exudate granulocytes respectively, evaluated by quantification of the acquisition of the Csk^{Δ} allele against the loss of the Csk^{fl} allele. In addition, 24 ± 3% deletion deletion was observed in inflammatory peritoneal exudate macrophage. Less than 5% deletion was observed in resident macrophage, splenocytes and thymocytes (Figure 8.1B). This demonstrates that deletion is restricted primarily to granulocytes, and furthermore, to a subpopulation of inflammatory macrophage.

Deletion in inflammatory macrophage is unexpected; however, whilst FACS analysis of the peritoneal exudate showed greater than 90% macrophage purity as assessed by F4/80 staining, cell-sorting techniques were not employed to enrich the macrophage population. Contamination of exudates with Csk-deficient granulocytes occupying the peritoneal compartment may account for the deletion observed. Indeed, since macrophages ingest granulocytes during resolution of the inflammatory response (Savill *et al.*, 2002), the apparent Csk deletion could be derived from ingested granulocyte DNA. Importantly, no deletion was detected in resident peritoneal macrophages, indicating that the elastase-Cre expressing precursor does not give rise to significant numbers of this macrophage subpopulation. Leakiness of the granulocyte elastase promoter under inflammatory conditions would provide another possibility for the deletion observed in inflammatory macrophages.

Why was complete deletion of *csk* exons 9 and 10 not obtained? Incomplete Cre mediated deletion may be a direct consequence of a short expression period dictated by the onset and termination of granulocyte elastase promoter driven expression. The longevity of specific promoter activity has previously been demonstrated to correlate with the level of Cre mediated deletion. For example, the $CD19^{cre}$ mouse strain when crossed with $pol\beta^{flox}$ mice revealed 80-85% deletion in bone marrow pre-B lymphocytes and 90-95% in splenic B-lymphocytes (Rickert *et al.*, 1997). This indicates that the level of Cre mediated deletion obtained in a specific cell population is dictated in part by the longevity of specific promoter activity within that cell population. Thus, as granulocyte elastase expression is terminated

early in myeloid cell development, it is perhaps not surprising that incomplete Cre mediated deletion is observed.

Activity of Src-fk Lyn and Fgr have been associated with inhibition of apoptosis in human peripheral blood granulocytes and retinoic acid induced granulocyte differentiation of the human promyelocytic leukaemia cell line HL-60 (Katagiri *et al.*, 1996; Wei *et al.*, 1996; Yousefi *et al.*, 1994). Given these observations, there exists a possibility that a lack of regulatory control in Csk-deficient granulocytes may exert a selective advantage over granulocytes that have not undergone somatic deletion, perhaps influencing the level of deletion observed in $Csk^{fl/fl}$-$GE^{cre/+}$ granulocytes. No difference in apoptosis is observed in in vitro cultured granulocytes in the absence of pro-inflammatory stimuli (figure 9.2G). Furthermore, $Csk^{fl/fl}$-$GE^{cre/+}$ mice show similar levels of deletion as $Csk^{fl/+}$-$GE^{cre/+}$ mice in all compartments examined (Personal communication J.Roes and figure 8.1B), demonstrating that there is no positive selection for Csk-deficient granulocytes.

To support the generation of Csk deficient cells, one *csk* allele was inactivated in the germline resulting in hemizygosity at the *csk* locus. In this genotype ($Csk^{fl/\Delta}$-$GE^{cre/+}$ referred to as Csk-GEcre), any cre-mediated deletion would give rise to a csk-deficient cell. Deletional analysis of bone marrow Csk-GEcre granulocytes demonstrated 79 ± 6% deletion. Interestingly, thioglycollate-induced peritoneal Csk-GEcre granulocytes showed 63 ± 5% deletion, indicating selective recruitment of granulocytes with a functional *csk* allele. However, the level of deletion demonstrates that peripheral granulocytes are indeed able to emigrate from the vascular space into the peritoneal cavity. This indicates that an absence of regulatory control in Csk deficient granulocytes impairs cell migration in a sterile peritonitis model. Peritoneal macrophage again demonstrated unexpected deletion at 59 ± 1%.

To determine whether somatic inactivation of the *csk* gene is accompanied by reduced protein expression, the level of Csk protein expression in bone marrow granulocytes was determined. Purified granulocyte populations subjected to anti-Csk immunoblotting revealed immunoreactive Csk in granulocytes derived from $Csk^{fl/\Delta}$-$GE^{+/+}$ bone marrow and a near absence in granulocytes derived from Csk-GEcre bone marrow. These data reveal a strict correlation between somatic gene inactivation and reduced Csk expression in purified granulocytes. Importantly, these data validate Csk-GEcre mice as an effective tool for studying deficiency of Csk in granulocytes.

Previous studies have shown a correlation between Csk inactivation and reduced expression of Src-fk (Section 2.4.1, Imamoto and Soriano, 1993; Nada *et al.*, 1993). To evaluate whether Csk deficiency in granulocytes is associated with reduced expression of myeloid cell Src-fk, Hck, Fgr and Lyn, SDS whole cell lysates were prepared from purified bone marrow granulocytes and were subjected to anti-Hck, anti-Fgr, and anti-Lyn immunoblotting. No differences in Hck, Fgr, or Lyn expression were observed between conditional mutants and controls from total cell (SDS) lysates (figure 9.1). However, cultured Csk-deficient granulocytes show a reduction in Hck expression compared to controls (figure 9.7c). Why is reduced expression of Src-fk observed in Csk-deficient embryo derived cells and cultured Csk-deficient granulocytes but not in quiescent Csk-deficient granulocytes? Reduced Src-fk expression may be a consequence of targeting the active Src-fk to ubiquitin-mediated degradation thus providing a physiological method of disposing of constitutively activated Src-fk. More provocatively, constitutively activated Src-fk may only be targeted to cellular degradation machinery when they interfere with normal cell development and homeostasis, thus explaining the difference in Hck expression profiles between quiescent uncultured granulocytes and spontaneously primed cultured granulocytes.

11.2 Csk is not involved in granulocyte development.

Previous studies have demonstrated a critical role for Csk in development of both the embryo (Section 2.4, Imamoto and Soriano, 1993; Nada *et al.*, 1993) and T-lymphocytes (Section 2.6, Schmedt *et al.*, 1998). In contrast, myeloid cell specific Csk deficient mice presented no overt phenotype in granulocyte development. Conditional mutants showed no significant difference compared to controls in relative numbers of immature ($Gr1^{lo}$) and mature ($Gr1^{hi}$) bone marrow granulocytes (Figure 8.3b) or total cell numbers in the bone marrow (Figure 8.3a). Furthermore, no difference in lifespan or turnover of Csk-deficient granulocytes was observed between conditional mutants and controls (Figure 8.3c). These data demonstrate that loss of regulatory control in the absence of Csk does not influence the development of granulocytes. Furthermore, this indicates that other unidentified regulatory molecules are most likely involved in granulopoiesis.

11.3 An important role for Csk in the regulation of phagocyte responsiveness.

Csk-GEcre mice maintained in conventional housing facilities display a diffuse and progressive inflammatory phenotype mediated by PMN/macrophage characterised by acute

perivascular pneumonia and microabsesses in the eyelids (figure 8.2). Microbiological analysis of lung tissue did not demonstrate any significant differences in microbial load between conditional mutants and controls (Personal communication J.Roes). These data indicate that either phagocyte microbicidal capacity is not compromised in the conditional mutants, or that a subpopulation of myeloid cells with a functional Csk allele is able to control the infection. Critically, the acute perivascular pneumonia appears to be driven by a bacterial organism that does not usually cause a sustained inflammatory response. Inappropriate mobilisation of innate defences towards an otherwise non-immunogenic stimulus, define a critical role for Csk in the negative regulation of phagocyte responsiveness.

A number of skin conditions of unknown etiology in humans show striking similarities to the inflammatory phenotype observed in Csk-GEcre mice. The localised form of granuloma annulare predominantly affects the extremities, such as the elbows, eyes and ears, though it can be restricted to the dorsum of the hands. Acute vasculitis and localisation of inflammatory cells to the deep dermis/subcutis has also been described in association with this condition (Weedon, 1997). Furthermore, acute febrile neutrophilic dermatosis (Sweet's Syndrome) is thought to represent an immunological hypersensitivity reaction, which affects the extremities and may be triggered by respiratory tract infection (Weedon, 1997) or treatment with GCSF (Johnson *et al.*, 1994). A form of atopic dermatitis that develops in the NC/Nga mouse, when maintained under non-SPF conditions (Vestergaard *et al.*, 2000), has been linked with the *csk* locus (Kohara *et al.*, 2001), but the nature of the defect remains unknown. The phenotypic similarities between the Csk-GEcre model and the human conditions suggest that impaired negative control of granulocyte activation, perhaps due to suboptimal Csk expression/activity and corresponding deregulation of Src-fk activity, may play a role in the development of these and similar acute inflammatory diseases.

Deregulation of Src-fk activity has previously been shown to contribute to the development of inflammatory disease in mice lacking SHP-1 (Src homology 2-containing tyrosine phosphatase 1), a tyrosine phosphatase that regulates Src-fk activity via dephosphorylation of regulatory tyrosine residues. Indeed, motheaten viable mice (mev/mev), which express catalytically inert SHP-1, manifest a strikingly similar phenotype, characterised by intra-alveolar accumulation of myeloid cells resulting in hemorrhagic interstitial pneumonitis and mortality at 4 months of age (Brumell *et al.*, 1997). This phenotype is completely driven by myeloid cells as rag-/-, mev/mev mice, which lack lymphocytes manifest the same disease characteristics as mev/mev mice alone (Yu *et al.*,

1996). Cumulatively, these data identify a critical requirement for precise regulation of Src-fk in myeloid cells to prevent inappropriate activation of phagocyte function.

The role for Csk in the negative regulation of phagocyte responsiveness was further defined in specific pathogen free Csk-GEcre mice challenged with endotoxin. Critically, SPF conditional mutants receiving lipopolysaccharide demonstrated hyper-responsiveness of the myeloid cell compartment to an inflammatory stimulus reflected by augmented sequestration of PMN to the liver parenchyma, augmented serum TNFα levels, acute hemorrhagic pneumonia and mortality (section 9.2). Importantly, further work carried out by colleague Ken Choi, demonstrated that this hypersensitivity does not seem to derive itself from a hypersensitivity of Csk-deficient macrophages to LPS as in vitro production of TNFα by LPS stimulated bone marrow derived macrophages did not differ significantly from the controls (Control, 839 ± 25; Csk-GEcre, 882 ± 69 pg/ml; p=0.58). This supports a predominant role for granulocytes in the LPS-induced pathogenesis.

The role of Src-fk in experimental endotoxemia remains unclear. Whilst mice lacking the myeloid restricted Src-fk, Hck and Fgr, are hypo-responsiveness to the high dose model of endotoxemia (Lowell and Berton, 1998) macrophages derived from Hck, Fgr, Lyn null mice show normal cytokine and nitrite production, and ERK1/2, JNK, and NF-kB activation in response to LPS (Meng and Lowell, 1997). This presents a paradox, why are mice lacking Hck and Fgr protected from endotoxic shock when LPS stimulated macrophage functions are essentially normal? A mechanistically distinct physiological process must exist to influence phagocyte responsiveness in an inflammatory environment.

Since, exposure of PMN to pro-inflammatory mediators, such as TNFα or LPS, has been shown to augment cell surface integrin expression (Condliffe *et al.*, 1996), transforming the neutrophil from a quiescent cell compatible with circulation, to a highly responsive cell primed for migration into tissues (Crockett-Torabi *et al.*, 1995; Pavalko and LaRoche, 1993; Simon *et al.*, 1995; von Andrian *et al.*, 1991), it is conceivable that enhanced phagocyte responsiveness in the conditional mutants may result from altered integrin expression.

11.4 Augmented spontaneous priming in Csk-deficient granulocytes is associated with augmented cellular responses.

Neutrophil priming represents one of the key processes regulating functional responsiveness both in vitro and in vivo (Smedly *et al.*, 1986; Worthen *et al.*, 1987). To determine whether Csk-deficient granulocytes exhibited altered priming characteristics, cell surface expression of CD11b and shape change was analysed. Flow cytometric analysis of cultured bone marrow leukocytes revealed a significant increase of granulocytes acquiring a $CD11b^{hi}$ phenotype indicative of spontaneous priming (figure 9.3a/b). It has been previously demonstrated that β2-integrins become incorporated into the plasma membrane through mobilisation and subsequent membrane fusion of the most rapidly mobilisable intracellular structure in neutrophils, the secretory vesicle (Borregaard *et al.*, 1987; Miller *et al.*, 1987) or through mobilisation of secondary granules (Sengelov *et al.*, 1993).

Mobilisation of secretory vesicles and resultant upregulation of cell surface CD11b occurs in granulocytes lacking Hck and Fgr, and in granulocytes treated with PP1 (a specific inhibitor of Src-fk), demonstrating that this process occurs independently of Src-fk activation (Lowell *et al.*, 1996; Mocsai *et al.* 2000). In contrast, release of secondary granules was defective in granulocytes lacking Hck, Fgr and Lyn, and in granulocytes treated with PP1 (Mocsai et al., 2000), demonstrating that exocytosis of secondary granules is dependent on Src-fk activation.

While suspension-cultured control granulocytes demonstrated a moderate increase in the number of cells expressing high levels of CD11b, approximately 75% of suspension-cultured Csk-deficient granulocytes demonstrated the $CD11b^{hi}$ phenotype (figure 9.3a). The susceptibility of the hyperinduction observed in Csk-deficient granulocytes to the Src-fk inhibitor PP2 demonstrates dependence on Src-fk activity (figure 9.3b), supporting a predominant role for mobilisation of secondary granules in the upregulation of cell surface CD11b. Indeed, an increase in the proportion of cells expressing CD51, a marker of secondary granule membranes, was identified in suspension-cultured Csk-deficient granulocytes, further supporting a role of secondary granule mobilisation in the hyperinduction of cell surface β2-integrin. Augmented mobilisation and corresponding exocytosis of secondary granules in suspension-cultured granulocytes is further verified by enhanced spontaneous adhesion-independent degranulation in culture alone measured by lactoferrin release (Control 1.00 ± 0.21, Csk-GEcre 1.42 ± 0.17 relative units, $p=0.02$; figure

9.5a). Together, these data support an essential role of Csk in the controlled, Src-fk-dependent insertion of integrins into the cell membrane through degranulation .

Granulocyte priming induces the transition of circulating neutrophils from a quiescent poorly adhesive state to a primed, strongly adhesive phenotype accompanied by a dramatic increase in the response of these cells to an activating agent such as the bacterial formylated peptide, N-formyl methionyl-leucyl-phenylalanine (fMLP). One principle effect of priming, aside from a direct effect on integrin/selectin expression is to permit degranulation (Condliffe *et al.*, 1999). Analysing degranulation in suspension assays, it was found that lactoferrin release by suspended Csk-GEcre granulocytes was augmented both in response to fMLP alone, and in conjunction with cytochalasin B, when compared to control granulocytes, providing functional evidence of enhanced spontaneous priming in Csk-deficient granulocytes. Mocsai and colleagues demonstrated that fMLP-induced exocytosis of lactoferrin containing secondary granules is mediated by Src-fk, and this has been confirmed in granulocytes lacking Hck, Fgr and Lyn (Mocsai *et al.*, 2000). The augmented degranulatory response observed in Csk-GEcre granulocytes is abolished by treatment with the Src-fk inhibitor PP2 demonstrating Src-fk dependence.

The hyper-responsiveness of Csk-deficient granulocytes is also apparent in an adhesion-dependent setting to the non-specific substrate, PVC, or by crosslinking of receptors, including both integrins and Fc-γ receptors (figure 9.5b). Notably, enhanced susceptibility of Csk-deficient granulocytes to Fc-γ receptor induced degranulation indicates an additional regulatory role for Csk aside from integrin signalling. Together, these data support an essential role for Csk in controlled secondary granule mobilisation and degranulation in both adhesion-dependent and independent settings.

Altered cell shape change (section 9.3) may also contribute to endotoxin susceptibility. Modifications in the actin cytoskeleton that result in shape change render neutrophils less deformable. Reduced deformabilty has been associated with increased sequestration of neutrophils within the pulmonary capillary bed (Haslett *et al.*, 1987; Worthen *et al.*, 1989). This phenomenon may contribute to the augmented recruitment of myeloid cells to the lung at LPS doses that do not usually precipitate a sustained inflammatory response. Indeed, prolonged retention of primed neutrophils within the pulmonary capillary bed in conjunction with augmented potential for degranulation may go

towards explaining the neutrophil mediated damage to the pulmonary vascular endothelium in endotoxin challenged conditional mutant mice (figure 9.2E/F).

Another possible contributory factor to endotoxin susceptibility in conditional mutant mice may result from augmented CD11b expression. It has been reported in macrophages that the CD11b subunit of β2 integrins acts together with CD14 and Toll-like receptor 4 (TLR4) to allow transcription of a full repertoire of LPS-inducible genes (Perera *et al.*, 2001). It is not known whether CD11b expression in response to LPS is also required in granulocytes for expression of a complete repertoire of LPS-inducible genes. However, it is conceivable that if indeed CD11b is required, then enhanced cell surface CD11b expression on Csk-deficient myeloid cells in response to LPS may together with CD14 and TLR4 lead to amplification of intracellular signals involved in mediating effector responses that contribute to endotoxemia exacerbating LPS-induced pathology.

The formation of integrin clusters with increased 'avidity' for ligand in central to effective cell adhesion and signalling (reviewed in Hogg *et al.*, 2002). Csk-deficient suspension cultured granulocytes demonstrate spontaneous upregulation of CD11b (figure 9.3a) accompanied by augmented actin polymerisation and formation of prominent integrin clusters not readily detectable in controls (figure 9.6d). Furthermore, culture of Csk-deficient granulocytes in an adhesion-dependent setting additionally displays the projection of filopodia on glass and lamellipodia on fibrinogen-coated glass, both of which are rich in polymerised actin and CD11b (figure 9.6e/f). The formation of these processes in Csk-deficient granulocytes, which are largely absent from the control population explains the hyper-adhesiveness of these cells (figure 9.6a/b). A critical role for integrin-mediated adhesion in PMN-mediated tissue injury has previously been demonstrated in experimental endotoxemia. Endotoxin challenged mice receiving anti-β1 or anti-β2 integrin monoclonal antibodies revealed dramatically reduced PMN induced tissue injury (Essani *et al.*, 1997; Jaeschke *et al.*, 1991). Furthermore, it has been shown that anti-β2 integrin monoclonal antibodies can also prevent autoimmune disease caused by SHP-1 deficiency in transplantation models (Koo *et al.*, 1993). These data support a critical role for β2-integrin dependent adhesion in the inflammatory process.

Genetic evidence for the involvement of integrin-mediated adhesion in the inflammation process was provided by crossing Hck, Fgr, or Lyn, mutations onto SHP-1 deficient mice (mev/mev). Spontaneous inflammation manifested in the absence of

catalytically active SHP-1 was partially ameliorated in mev/mev mice lacking Hck and Fgr, and completely ameliorated in mev/mev mice lacking Hck, Fgr, and Lyn (R.Holmes, G.Berton and C.A.Lowell, unpublished results). Furthermore, mice lacking Hck and Fgr, which are hypo-responsive to the effects of LPS, exhibited significantly reduced tissue damage (Lowell and Berton, 1998). Given these data, it is clear that Src-fk's, Hck, Fgr, and Lyn, are required for PMN adhesion-dependent activation *in vivo*. It is therefore conceivable that deregulated Src-fk activity in Csk-deficient granulocytes, accompanied by enhanced β2-integrin cell surface expression and formation of integrin clusters will lead to augmented cell adhesion which may result in increased adhesion-dependent activation of cellular responses including degranulation contributing to tissue damage in an inflammatory environment.

Spontaneous priming of Csk-deficient granulocytes may also have profound effects in recruitment to an inflammatory site. Interaction of β2 integrins with its vascular counter receptor ICAM-1 plays a major role in trans-endothelial migration from the periphery to a site of inflammation (Xie *et al.*, 1995). Furthermore, this interaction appears to be largely mediated by changes in β2-integrin receptor clustering (avidity modulation) as opposed to changes in receptor affinity (Stewart and Hogg, 1996). It is therefore plausible that upregulated β2-integrin cell surface expression and associated formation of integrin clusters in Csk-deficient granulocytes demonstrated *in vitro* may indeed enhance the avidity between these cells and the vascular endothelium *in vivo*. Furthermore, increased avidity of Csk-deficient granulocyte cell surface receptors towards their counter-receptors *in vivo* may in part explain the selective recruitment of granulocytes with a functional Csk allele in a sterile peritonitis model (figure 8.1c). Importantly, it must be noted that limited recruitment of Csk-deficient granulocytes to the peritoneum does occur during sterile peritonitis demonstrating that these cells retain some migratory capacity. This most likely reflects that multiple counter receptors for granulocyte cell surface adhesion molecules are present *in vivo*, which facilitate granulocyte recruitment despite defective β2-integrin function. This reduced migratory capacity would also be sufficient for extravasation of Csk-deficient granulocytes from the bloodstream before settling and accumulating in the perivasculature of the lung resulting in the profound inflammation observed in conventionally housed Csk-GEcre mice. Release of cellular and humoral factors at the inflamed site may additionally provide a positive feedback loop for the sustained recruitment of Csk-deficient granulocytes to the lung. Furthermore, increased functional longevity of Csk-deficient granulocytes as a result of the relative resistance of these cells to apoptosis (figure 9.2G) may further contribute to the profound perivascular inflammation. Importantly, the local accumulation of granulocytes was not

associated with significant tissue damage indicating a lack of secondary signals, which would normally be encountered in a full blown acute inflammatory response.

Interestingly, Ernst and colleagues reported a spontaneous pulmonary inflammation in mice expressing constitutively active Hck (Hck^{FF}) (Ernst *et al.*, 2002). However, in contrast to the Csk-GEcre model, the inflammation developed in a specific pathogen free environment and involved predominantly mononuclear cells, eosinophils and macrophages, suggesting that deregulation of Csk targets other than Hck may cause the acute granulocytic infiltrate in Csk-GEcre mice. To confirm this, it would be very interesting to elucidate whether mice expressing constitutively active forms of Fgr or Lyn would reflect the phenotype observed in Csk-GEcre mice. However, it must be noted that constitutively active forms of Src-fk's are not only uncoupled from Csk-mediated negative regulation but are also refractive to other regulatory protein tyrosine kinases and phosphatases, and thus the phenotype observed in the Hck^{FF} mice may reflect a cumulative deregulation of many regulatory pathways. This is supported by the fact that while deregulation of Src-fk in Csk-deficient fibroblasts does not result in cellular transformation, constitutive activation of Hck via direct mutagenesis of the C-terminal tyrosine to phenylalanine (Hck^{FF}) results in the ability to transform fibroblasts (Nada et al., 1994; Ziegler et al., 1989). Cumulative deregulation of Src-fk regulatory pathways in Hck^{FF} granulocytes may potentially explain the contrasting enhanced migratory capacity of these cells *in vitro*. However, it must be noted that the migration assay used included adhesion as a selecting parameter. Increased adhesiveness of Hck^{FF} granulocytes, which would be in line with data presented herein (figure 9.6a/b), may thus have contributed to the apparent migratory activity.

11.5 Identification of hyperphosphorylated integrin signalling components, Syk, paxillin and cortactin in Csk-deficient granulocytes. Further implications for cell migration.

The Syk tyrosine kinase plays a critical role in integrin signalling in granulocytes. Granulocytes lacking Syk kinase stimulated by direct crosslinking of integrins or by culturing upon immobilised integrin ligands showed defective respiratory burst, degranulation and spreading in response to proinflammatory stimuli (Mocsai *et al.*, 2002). It has been previously demonstrated that recruitment and subsequent activation of Syk is dependent upon its direct interaction with integrin beta cytoplasmic domains (Woodside *et al.*, 2001; Willeke *et al.*,

2003). Indeed, ligand binding of β2-integrins results in formation of protein complexes containing the β-subunit of β2-integrins, Syk kinase, and the Src-fk Fgr and Lyn (Yan *et al.* 1997; Yan *et al.*, 1996). Src-fk present in integrin-dependent protein complexes have been shown to be required for maximal integrin-dependent activation of Syk (Gao *et al.*, 1997). However, although initial tyrosine phosphorylation of Syk is mediated by Src-fk, subsequent tyrosine phosphorylation is likely to be mediated via transphosphorylation, a mechanism originally described for Syk-kinase mediated Fc-receptor signalling which involves a Src-fk-initiated Syk-activation loop phosphorylation chain reaction (El-Hillal *et al.*, 1997). This reaction requires Syk molecules to be in close proximity to one another. Integrin clustering as a consequence of β2-integrin-mediated adhesion provides the necessary accumulation of Syk molecules through its association with the β-subunits of β2-integrin for a transphosphorylation event to occur. In suspension-cultured Csk-deficient granulocytes, deregulated Src-fk activity is accompanied by the appearance of spontaneous β2-integrin clusters not readily detectable in controls. Thus, it is likely that the augmented phosphorylation upon tyrosine residues 518 and 520 is a consequence of not only direct phosphorylation mediated by deregulated Src-fk but also of augmented transphosphorylation mediated by the adhesion-independent clustering of β2-integrins. Given the role of Syk kinase in degranulation (Mocsai *et al.*, 2002), hyperactivation of Syk kinase through deregulated phosphorylation of tyrosine residues 518 and 520 in Csk-deficient granulocytes may contribute to the augmented capacity of these cells to degranulate in both adhesion-dependent and adhesion-independent settings. In contrast, deregulated Syk activity is unlikely to contribute to the impaired migratory capacity of Csk-deficient granulocytes since in vitro or in vivo migration of Syk-deficient granulocytes was not impaired (Mocsai *et al.*, 2002). Deregulated phosphorylation of other integrin signalling components, such as paxillin or cortactin, are more likely to contribute to the impaired migratory capacity of Csk-deficient granulocytes.

Phosphorylation of actin-associated and cytoskeletal-associated proteins, including paxillin, cortactin and p130Cas represents a proximal event in integrin signal transduction (Burridge *et al.*, 1992; Nojima *et al.*, 1995; Turner *et al.*, 1993; Vuori and Ruoslahti, 1995). To provide further evidence that deregulation of Src-fk in the absence of Csk is accompanied by deregulated integrin signal transduction, the phosphorylation state of focal adhesion components, paxillin and cortactin was determined. *In vitro* studies using Csk-deficient granulocytes demonstrated a profound increase in paxillin phosphorylation upon tyrosine residue 31 compared to control cells (figure 9.7d). Furthermore, a profound increase in

phosphorylation of cortactin upon tyrosine residue 421 was additionally identified (figure 9.7d). These data imply that negative regulation of Src-fk is required to prevent inappropriate tyrosine phosphorylation of focal adhesion components. The involvement of Src-fk in tyrosine phosphorylation of focal adhesion components has been confirmed in macrophages derived from mice lacking Hck and Fgr which showed reduced phosphorylation of paxillin, cortactin, and tensin after integrin ligation (Suen et al. Unpublished results). Importantly, phosphorylation of paxillin and cortactin in Csk-deficient myeloid cells occur in an adhesion-independent manner indicating that an impairment of negative regulatory control over Src-fk activity in the absence of Csk removes the requirement of integrin ligation for granulocyte priming. Association of constitutively active Src-fk with the autophosphorylation site, tyrosine 397, of focal adhesion kinase (FAK) may drive this process.

Conformationally active Src-fk restricted to Csk-deficient myeloid cells would be able to interact with phosphotyrosine 397 through an SH2-domain interaction. Interaction of Src with FAK leads to the phosphorylation of tyrosine residues 407, 576, and 577, which maximises the kinase activity of FAK in vitro (Calalb *et al.*, 1995). Moreover, association of Src with FAK drives phosphorylation of tyrosine 925, which provides a consensus motif for Grb2 SH2 binding. Grb2, an adaptor molecule connects activated receptor tyrosine kinases to the Ras/mitogen-activated protein kinase (MAPK) signalling pathway by binding to Sos, a guanine exchange factor for Ras (Schlaepfer *et al.*, 1994). Paxillin and p130Cas bind directly to FAK (Polte and Hanks, 1995; Schaller *et al.*, 1994; Turner and Miller, 1994). Interestingly, phosphorylation of N-terminal tyrosine residues 31 and 118 in paxillin generate SH2 binding sites for Csk (Sabe *et al.*, 1994). Thus, Csk may be targeted to the FAK/Src complex by its association with paxillin and function to inactivate Src through phosphorylation of the C-terminal tyrosine residue, allowing dissociation of Src from the complex, further allowing exposure of the FAK autophosphorylation site to cellular phosphatases, such as PEP or PTP-PEST, which have been reported to be constitutively associated with Csk via a SH3-domain interaction (Cloutier and Veillette, 1996; Davidson *et al.*, 1997). Thus, in the absence of Csk, it is conceivable that after the primary stimulus has been received, constitutive activation of the FAK/Src complex and its downstream events may occur.

Cell migration requires regulated assembly and disassembly of structural and signalling complexes at the plasma membrane to co-ordinate attachment and detachment of the cell from the extracellular matrix. The FAK/Src complex mediates phosphorylation of paxillin upon tyrosine residues 31 and 118. Two recent reports have underscored the requirement for

tyrosine phosphorylation upon both of these residues in focal adhesion disassembly, cell polarisation and motility through the construction of paxillin mutants where one or both of the tyrosine residues had been mutated to phenylalanine (Webb *et al.*, 2004; Romanova *et al.*, 2004). Phosphorylation of these sites allows the binding of Crk adaptor proteins, and subsequent binding of p130Cas (Bellis *et al.*, 1995; Schaller and Parsons, 1995). Association of Crk with both p130Cas and paxillin is important in co-ordinating integrin-mediated cell motility (Klemke *et al.*, 1998; Petit *et al.*, 2000). Constitutive phosphorylation of paxillin in Csk-deficient myeloid cells may thus affect the normal turnover of focal complexes or focal adhesions through deregulation of the Crk/p130Cas molecular switch. Indeed, a separate study revealed that the catalytic activity of Src controls the turnover of focal adhesions during cell motility (Fincham and Frame, 1998). It is thereby conceivable that impaired focal adhesion turnover may contribute to the reduced migratory capacity of Csk-deficient granulocytes towards fMLP *in vitro* (figure 9.6c).

Dynamic actin networks perform a critical role in a variety of cellular responses including cell migration (Ridley *et al.*, 2001). Initiation of cell migration requires cell polarisation and the formation of a leading edge at the migratory front composed primarily of lamellipodia. Remodelling of the actin cytoskeleton is mediated by Rho family GTPases, with Rac stimulating the formation of lamellipodia, Rho stimulating the formation of focal adhesions and stress fibres, and Cdc42 stimulating the formation of filopodia (Hall, 1998). Actin polymerisation can be initiated by *de novo* nucleation branched actin networks by the actin-related protein (Arp)2/3 complex (Cooper *et al.*, 2001). The activity of this complex is regulated by actin nucleation promoting factors (NPFs) of the WASP (Wiskott-Aldrich syndrome protein) and SCAR/WAVE (suppressor of cAMP receptor/WASP family verprolin homologous) family of proteins. Interaction of NPFs with the Arp2/3 complex leads to enhanced Arp2/3 complex activity, resulting in increased cortical actin polymerisation and formation of lamellipodia. (Borisy *et al.*, 2000).

Intriguingly, cortactin itself possesses NPF activity and interacts directly with the Arp2/3 complex and F-actin (Uruno *et al.*, 2001; Wu and Parsons., 1993; Weed *et al.*, 2000), stimulating Arp2/3 activity and preventing disassembly of Arp2/3-F-actin networks indicating that cortactin plays a central role in lamellipodia protrusion and integrity (Uruno *et al.*, 2001). Tyrosine phosphorylation of cortactin has been reported to be a consequence of Rac-1-mediated recruitment of Src and non-phosphorylated cortactin from their cytoplasmic compartments to the cortical actin cytoskeleton allowing for their compartmentalisation in

lamellipodia and subsequent Src-mediated phosphorylation of cortactin (Weed *et al.*, 1998; Timpson *et al.*, 2001). Indeed, cortactin phosphorylated on tyrosine 421 has been demonstrated to be enriched in lamellipodia where it co-localises with F-actin in fibroblasts (Head *et al.*, 2003). Thus, it is conceivable that deregulation of Src-fk activity in Csk-deficient granulocytes leads to Rac-1-independent Src-mediated cortactin phosphorylation and subsequent colocalisation with F-actin. Subcellular localisation of tyrosine-phosphorylated cortactin with F-actin may target cortactin to the Arp2/3 complex and may explain the formation of distinct lamellipodia in Csk-deficient granulocytes cultured upon fibrinogen-coated glass not observed in controls (figure 9.6F). Deregulated lamellipodial formation and their integrity in the absence of Csk may additionally affect the migratory capacity of Csk-deficient granulocytes.

Cumulatively, these data demonstrate a profound defect in the negative regulation of major activating pathways that drive granulocyte activation and recruitment.

11.6 Co-stimulation model for phagocyte responsiveness in Csk-GEcre mice.

The proximal events of an inflammatory response are characterised by margination of PMN in the microvasculature mediated initially by the selectin family of adhesion molecules, and subsequently by the interaction of integrins with their counter-receptors on endothelial cells. Once adherent, PMN transmigrate through the endothelial layer and migrate into the tissues, releasing granule constituents and reactive oxygen intermediates. Adhesion of PMN's to the vascular endothelium and susbsequent transmigration into the underlying tissue has been shown to contribute to tissue injury in experimental endotoxemia, since inhibition of β1-integrins or β2 integrins with specific antibodies markedly attenuates PMN-induced tissue damage (Jaeschke *et al.*, 1991; Morisaki *et al.*, 1991). Similarly, mice deficient for the β2-integrin counter-receptor ICAM-1, which is selectively upregulated on the surface of endothelial cells in response to LPS, TNFα and IL-1, are resistant to LPS. PMN from ICAM-1 deficient mice fail to transmigrate through the endothelium in response to LPS, and instead accumulate in the periphery demonstrating a marked neutrophilia (Xu *et al.*, 1994). This further supports the requirement of β2-integrin signalling in the extravasation process. Involvement of Src-fk in integrin mediated PMN activation and cell migration was demonstrated in Hck, Fgr null mice challenged with LPS. These mice present a strikingly similar phenotype to LPS challenged ICAM-1 deficient mice, characterised by LPS hypo-

responsiveness, reduced PMN migration and tissue injury, and a pronounced neutrophilia (Lowell and Berton, 1998).

In contrast, we have demonstrated that Csk-GEcre mice are hyper-responsive to the high dose model of experimental endotoxemia indicating that Csk-deficient granulocytes are constitutively primed. Myeloid Src-fk are not involved in LPS signalling (Meng and Lowell, 1997), therefore a signal transduction pathway functionally distinct from that initiated by LPS is responsible for the observed phenotype. Functional analyses of granulocytes lacking Hck and Fgr place these Src-fk downstream of β2-integrins and upstream of the signalling protein Syk and actin-cytoskeletal proteins, cortactin and paxillin (Lowell *et al.*, 1996; Mocsai *et al.*, 1999). In accord with this model, granulocytes lacking Hck and Fgr are defective in adhesion-dependent priming resulting in impaired degranulation and respiratory burst. *In vitro* studies using suspension cultured Csk-deficient granulocytes demonstrate a significant increase in spontaneous and pro-inflammatory induced priming compared to controls as assessed by cell surface CD11b staining. This phenotype was further accompanied by significantly augmented integrin clustering and actin polymerisation independent of cell adhesion (figure 9.6d) as assessed by confocal microscopy. Augmented cell surface expression of β2-integrin has been reported to transform the neutrophil from a quiescent cell compatible with circulation, to a highly responsive cell primed for migration into tissues (Crockett-Torabi *et al.*, 1995; Pavalko and LaRoche, 1993; Simon *et al.*, 1995; von Andrian *et al.*, 1991). Furthermore, the formation of integrin clusters with increased 'avidity' for ligand as been reported to be essential for effective cell adhesion and signalling (Hogg *et al.*, 2002). Therefore, it is conceivable that premature or inappropriate formation of β2-integrin clusters specifically in Csk-deficient granulocytes would through their associated increase in avidity for their counter receptor ICAM-1 lead to premature or inappropriate activation of cellular responses in vivo, including actin cytoskeleton rearrangement, migration, degranulation, and respiratory burst. To more directly determine the contribution of β2-integrin-mediated intracellular signals to the acute perivascular inflammation observed in conventionally housed Csk-GEcre mice and the enhanced susceptibility of specific pathogen free Csk-GEcre mice to LPS, mice lacking β2-integrins (Coxon *et al.*, 1996) could be breeded with Csk-GEcre mice to generate mice lacking both Csk and β2-integrin. Restoration of normal responses to experimental endotoxaemia and a lack of acute pulmonary inflammation in mice deficient for both Csk and β2-integrin would indeed confirm that deregulation of β2-integrin mediated signalling is responsible for these phenotypes in Csk-GEcre mice.

Taken together, the analysis of the murine model of myeloid cell-specific Csk deficiency outlined in this study identifies a critical contribution of Csk to the negative regulation of Src-fk in the control of granulocyte function, and identifies Csk as an important negative regulator of granulocyte responsiveness *in vivo* through regulation of cell surface integrin expression, clustering and signal initiation and propagation. This work was submitted and subsequently published in the February issue of Immunity, 2004 (Thomas *et al.*, 2004).

Chapter 12 Insertion of heterologous introns results in augmented gene expression.

The conclusion from these studies with matched pairs of genes with or without introns is that the introns improve transcriptional efficiency approximately 30-fold in the absence of cryptic splice sites and in the presence of suitable exon/intron architecture when transfected into Chinese hamster ovary cells.

The methodology described herein represents a novel approach to increase gene expression through insertion of heterologous introns directly into the open reading frame, in order to overcome the potential detrimental effects of intron insertion into the 5' or 3' untranslated regions. This may be partly due to previous reports that have stated that splicing of heterologous introns is associated with activation of cryptic splice sites (Nelson and Green, 1990). Whilst this did not occur in the case of iGFP, a cryptic splice site in the Cre recombinase gene was activated in iCre upon insertion of heterologous introns. This illustrates the requirement for thorough examination of candidate open reading frames for homology to splice consensus sequences, in order to allow appropriate measures to be taken, for example, insertion of an intron directly into the cryptic site, illustrated by iCre3 or a 'silent' mutagenesis approach to disable the cryptic site, illustrated by iCre2.

Increased gene expression was observed with the iGFP and iCre2 constructs at approximately 30-fold over their respective intron-less genes. The internal exon size for both these constructs are identical at 216bp. This suggests that the IgM and IgE constant region derived introns co-operate efficiently over this distance, and thus are associated with increased levels of expression. Repositioning of the 5'mu1 intron directly into the cryptic splice site increases the splice site consensus sequence homology, but extends the internal exon size to 335bp. The resultant iCre3 construct is associated with an approximate 100-fold lower level of expression than the intronless CreX, which is recovered by shortening the internal exon size to 213bp in iCre4. This may partly be explained by the finding that splicing precursor RNA's constructed to have elongated second exons spliced efficiently as long as the second exon was less than 300 nucleotides in length (Robberson *et al.*, 1990). This possibility is additionally supported by the observation that vertebrate internal exons rarely exceed 300bp (Hawkins, 1988; Naora and Deacon, 1982)

iGFP demonstrated a 30-fold increase in mRNA expression partnered with a modest 5-fold increase in fluorescence. High GFP concentrations inducing aggregation may account for this difference as GFP aggregates are mostly non-fluorescent (Tsien, 1998). A mechanistically different possibility is that the translational machinery may be saturated by GFP mRNA load. Another, more provocative, possibility is that high levels of GFP are cytotoxic, and thus cells would be selected against on the basis of their intracellular levels of GFP protein. Immunoblotting using specific anti-GFP antibodies would more accurately reflect the levels of GFP protein in transfected CHO cells.

It is clear that the presence of introns within the transcription unit is beneficial to expression. Importantly, the insertion of introns directly in the open reading frame has distinct advantages over single intron positioning in the UTR or the use of genomic/cDNA hybrid genes. Most significantly, introns can act co-operatively in enhancing mRNA production (Neel *et al.*, 1993), an effect that requires at least two introns. Furthermore, authentic introns present in genomic/cDNA hybrid genes can be very large presenting an unnecessary or unfeasible load for gene delivery systems. A novel approach of increasing gene expression is described herein through the introduction of heterologous introns directly into the open reading frames of two naturally intronless genes, the Cre recombinase and EGFP. Further work carried out by colleagues Rob Coffin and others demonstrated sustained long term expression of iGFP at increased levels in rat brain transduced with a herpes simplex virus-based vector. Importantly, this showed that intron-mediated enhanced expression could also attained *in vivo*. Whilst an *in vivo* study using iCre2 has not currently been undertaken, it is conceivable given the data presented here that introduction of introns into Cre recombinase open reading frame may result in enhanced expression, possibly overcoming the incomplete somatic deletion of genetic loci conditioned for Cre mediated deletion from weaker or transiently expressed promoters. Furthermore, this technology may be applied to gene therapy where expression of cDNA *in vivo* is often limited or shut down by poorly understood gene silencing mechanisms. In the first instance, application of our methodology may enhance gene expression of cDNA constructs *in vivo*. Moreover, the inclusion of introns may modulate the sensitivity of transgenes to positional effects by epigenetic silencing (Webster *et al.*, 1997). Additionally, it has been demonstrated that inactivation of the mouse $\psi\alpha 3$ globin gene is associated with loss of introns. This associates the presence of introns not only with increased expression but also with defence against gene silencing. The mechanisms by which the presence of introns precludes a gene from being silenced are not understood at present. Thus, more research is required into these mechanisms before this technology can be

implemented for the sustainable and enhanced expression of cDNA for gene therapy. This work was submitted and subsequently published in the volume 8 of Gene Therapy, 2001 (A.Lacy-Hulbert and R.Thomas – joint first author).

Chapter 13 Future directions

13.1 Reassessment of inflammatory macrophage deletion in a sterile model of peritonitis.

Unexpectedly, in a sterile peritonitis model, we observed approximately 20% deletion of csk exons 9 and 10 in inflammatory exudate at 4 days (mostly inflammatory macrophages) in our conditional mutants. At present, the contribution of granulocyte elastase promoter leakiness under inflammatory conditions or the recruitment and/or phagocytosis of Csk deficient granulocytes to the deletion levels observed has not been experimentally defined. In order to assess the impact, if any, of granulocyte recruitment and/or phagocytosis to the deletion levels observed, inflammatory macrophages would be purified by MACS using F4/80 as a cell-type identification marker. Deletion analysis would then be performed on a 'pure' population of inflammatory macrophages without contamination of other cells. However, this would not rule out a contribution from phagocytosed cells. Identification of phagocytosed granulocytes may be flow cytometrically defined via macrophage intracellular staining with an antibody against lactoferrin, a granulocyte secondary marker. Together, these data would formally demonstrate whether Csk deletion does in fact occur in inflammatory macrophages and that it is not due to persistent recruitment of Csk-deficient granulocytes.

13.2 Generation of an iCre *in vivo* model

Comparison between GFP and iGFP expression *in vivo* was carried out by Coffin et al. (Biovex). Briefly, both GFP and iGFP were cloned into a herpes simplex based vector, and administered through stereotaxic inoculation into the rat striatum. Four weeks post-inoculation, brains were removed and prepared for fluorescent microscopy. Mice that had received iGFP expression vectors revealed larger areas of fluorescence compared with GFP expression vector controls, which was associated with punctate areas of intense fluorescence deep into the axons. This data revealed that generation of artificial exon-intron structures through insertion of heterologous introns into the GFP open reading frame insertion could indeed boost expression levels *in vivo*. Currently, the impact of artificial exon-intron structures within the Cre recombinase open reading frame upon *in vivo* expression has not assessed. To address the contribution of insertion of short heterologous introns into the Cre coding sequence upon expression *in vivo*, it would be very interesting to take a known Cre transgenic mouse, which had been associated with incomplete Cre mediated deletion of a floxed genetic

locus, and 'replace' the Cre recombinase with the iCre recombinase and to reassess Cre mediated deletion in the new transgenic strain. To this end, the murine model of myeloid cell-specific Csk deficiency may serve as the perfect tool to address the efficiency of iCre mediated deletion. Generation of Csk $^{fl/fl}$-GE$^{cre/+}$ mice revealed approximately 50 % deletion of the floxed Csk locus in granulocytes. Through the generation of a GE iCre transgenic mouse strain, it will be possible to breed Csk$^{fl/fl}$-GE$^{icre/+}$ mice, allowing analysis of iCre mediated deletion of the floxed Csk locus in granulocytes. If indeed, greater deletions levels are observed in Csk$^{fl/fl}$-GE$^{icre/+}$ mice compared to Csk$^{fl/fl}$-GE$^{cre/+}$ mice, then we could through extrapolation argue that augmented expression of iCre had indeed occurred *in vivo*, providing a greater number of Cre recombinase molecules which would contribute to enhanced deletion of the target gene.

CONCLUSION

The primary purpose of this current study was to assess the contribution of Csk to the negative regulation of PMN responsiveness and function. Using conditional mutagenesis based upon the Cre/loxP system, embryonic lethality associated with germline mutagenesis of Csk was bypassed, and a model was generated to specifically address via a direct genetic approach, the role of Csk in the negative regulation of myeloid cell function. The data provided herein reveal roles of Csk in modulating PMN integrin expression, shape change, adhesion, degranulation and motility, all fundamental properties of phagocytic microbicidal function. Critically, a strict correlation between myeloid Csk deficiency and the development of inflammatory disease was observed. This is demonstrated both in the development of acute perivascular pneumonia observed in conventionally housed mice, and hemorrhagic interstitial pneumonia observed in endotoxin challenged SPF mice. Thus, the negative control that Csk exerts over Src-fk appears critical for integrin-mediated control of myeloid cell activation.

In a separate study, we have demonstrated that the generation of near-natural gene organisation through insertion of heterologous introns into two naturally intronless genes, the Cre recombinase and EGFP, resulted in considerably enhanced gene expression. Extending this study, enhanced EGFP protein expression both *in vitro* and *in vivo* was demonstrated. In principle, this method should be applicable where enhanced and sustained protein expression is required, for example, in cell type specific mutagenesis and perhaps more significantly in gene therapy.

Acknowledgements

This work is primarily dedicated to my father who was diagnosed with brain cancer during my PhD. His strength and determination to continue as his condition deteriorated provided me with the will and determination I required to complete my studies. I would also like to thank all other members of my family and friends who have supported me through this extremely difficult and emotional time and to particularly thank everyone who was there for me when my father eventually passed away in October, 2000. Without you, I will have never reached this point. Your love and friendship will never be forgotten.

I would also like to give particular thanks to my supervisor, Dr. Jurgen Roes, for giving me the opportunity to work in his laboratory, and to learn from his rigorous methods of data acquisition and analysis. Importantly, his essential criticism has demonstrated to me better approaches to solving experimental problems. I would also like to thank Professor Avrion Mitchison for his critical reading of this manuscript.

Furthermore, I would like to thank Dr. Christian Schmedt for the provision of the Csk^{flox} mice, Dr. Marco Novelli for his histopathalogical expertise. Finally, I would like to acknowledge the Wellcome Trust for funding this Prize studentship.

REFERENCES

Abbassi, O., Kishimoto, T.K., McIntire, L.V., Anderson, D.C. and Smith, C.W. (1993) E-selectin supports neutrophil rolling in vitro under conditions of flow. *J Clin Invest*, **92**, 2719-2730.

Abremski, K., Hoess, R. and Sternberg, N. (1983) Studies on the properties of P1 site-specific recombination: evidence for topologically unlinked products following recombination. *Cell*, **32**, 1301-1311.

Amrein, K.E. and Sefton, B.M. (1988) Mutation of a site of tyrosine phosphorylation in the lymphocyte- specific tyrosine protein kinase, p56lck, reveals its oncogenic potential in fibroblasts. *Proc Natl Acad Sci U S A*, **85**, 4247-4251.

Anderson, D.C. and Springer, T.A. (1987) Leukocyte adhesion deficiency: an inherited defect in the Mac-1, LFA-1, and p150,95 glycoproteins. *Annu Rev Med*, **38**, 175-194.

Appleby, M.W., Gross, J.A., Cooke, M.P., Levin, S.D., Qian, X. and Perlmutter, R.M. (1992) Defective T cell receptor signaling in mice lacking the thymic isoform of p59fyn. *Cell*, **70**, 751-763.

Arbones, M.L., Ord, D.C., Ley, K., Ratech, H., Maynard-Curry, C., Otten, G., Capon, D.J. and Tedder, T.F. (1994) Lymphocyte homing and leukocyte rolling and migration are impaired in L- selectin-deficient mice. *Immunity*, **1**, 247-260.

Archibald, A.L., McClenaghan, M., Hornsey, V., Simons, J.P. and Clark, A.J. (1990) High-level expression of biologically active human alpha 1-antitrypsin in the milk of transgenic mice. *Proc Natl Acad Sci U S A*, **87**, 5178-5182.

Bagrodia, S. and Cerione, R.A. (1999) Pak to the future. *Trends Cell Biol*, **9**, 350-355.

Barlow, C., Schroeder, M., Lekstrom-Himes, J., Kylefjord, H., Deng, C.X., Wynshaw-Boris, A., Spiegelman, B.M. and Xanthopoulos, K.G. (1997) Targeted expression of Cre recombinase to adipose tissue of transgenic mice directs adipose-specific excision of loxP-flanked gene segments. *Nucleic Acids Res*, **25**, 2543-2545.

Bellis, S.L., Miller, J.T. and Turner, C.E. (1995) Characterization of tyrosine phosphorylation of paxillin in vitro by focal adhesion kinase. *J Biol Chem*, **270**, 17437-17441.

Bergman, M., Mustelin, T., Oetken, C., Partanen, J., Flint, N.A., Amrein, K.E., Autero, M., Burn, P. and Alitalo, K. (1992) The human p50csk tyrosine kinase phosphorylates p56lck at Tyr-505 and down regulates its catalytic activity. *Embo J*, **11**, 2919-2924.

Berton G, Yan SR, Fumagalli L, Lowell CA. (1996) Neutrophil activation by

adhesion: mechanisms and pathophysiological implications. *Int J Clin Lab Res.* **26**, 160-77.

Berton, G. and Lowell, C.A. (1999) Integrin signalling in neutrophils and macrophages. *Cell Signal*, **11**, 621-635.

Borisy GG, Svitkina TM. (2000) Actin machinery: pushing the envelope. *Curr Opin Cell Biol.* **12**, 104-12.

Borregaard, N., Miller, L.J. and Springer, T.A. (1987) Chemoattractant-regulated mobilization of a novel intracellular compartment in human neutrophils. *Science*, **237**, 1204-1206.

Borregaard N, Christensen L, Bejerrum OW, Birgens HS, Clemmensen I. (1990) Identification of a highly mobilizable subset of human neutrophil intracellular vesicles that contains tetranectin and latent alkaline phosphatase. *J Clin Invest.* **85**, 408-16.

Borregaard, N., and Cowland, J.B. (1997) Granules of the neutrophilic polymorhonuclear leukocyte. *Blood*, **89**, 3503-3521.

Brdicka, T., Pavlistova, D., Leo, A., Bruyns, E., Korinek, V., Angelisova, P., Scherer, J., Shevchenko, A., Hilgert, I., Cerny, J., Drbal, K., Kuramitsu, Y., Kornacker, B., Horejsi, V. and Schraven, B. (2000) Phosphoprotein associated with glycosphingolipid-enriched microdomains (PAG), a novel ubiquitously expressed transmembrane adaptor protein, binds the protein tyrosine kinase csk and is involved in regulation of T cell activation. *J Exp Med*, **191**, 1591-1604.

Brinster, R.L., Allen, J.M., Behringer, R.R., Gelinas, R.E. and Palmiter, R.D. (1988) Introns increase transcriptional efficiency in transgenic mice. *Proceedings Of The National Academy Of Sciences Of The United States Of America*, **85**, 836-840.

Briskin, M.J., McEvoy, L.M. and Butcher, E.C. (1993) MAdCAM-1 has homology to immunoglobulin and mucin-like adhesion receptors and to IgA1. *Nature*, **363**, 461-464.

Brumell, J.H., Chan, C.K., Butler, J., Borregaard, N., Siminovitch, K.A., Grinstein, S. and Downey, G.P. (1997) Regulation of Src homology 2-containing tyrosine phosphatase 1 during activation of human neutrophils. Role of protein kinase C. *J Biol Chem*, **272**, 875-882.

Bullard, D.C., Kunkel, E.J., Kubo, H., Hicks, M.J., Lorenzo, I., Doyle, N.A., Doerschuk, C.M., Ley, K. and Beaudet, A.L. (1996) Infectious susceptibility and severe deficiency of leukocyte rolling and recruitment in E-selectin and P-selectin double mutant mice. *J Exp Med*, **183**, 2329-2336.

Burns, C.M., Sakaguchi, K., Appella, E. and Ashwell, J.D. (1994) CD45 regulation of tyrosine phosphorylation and enzyme activity of src family kinases. *J Biol Chem*, **269**, 13594-13600.

Burridge, K., Turner, C.E. and Romer, L.H. (1992) Tyrosine phosphorylation of paxillin and pp125FAK accompanies cell adhesion to extracellular matrix: a role in cytoskeletal assembly. *J Cell Biol*, **119**, 893-903.

Buss, J.E. and Sefton, B.M. (1985) Myristic acid, a rare fatty acid, is the lipid attached to the transforming protein of Rous sarcoma virus and its cellular homolog. *J Virol*, **53**, 7-12.

Cahir McFarland, E.D., Hurley, T.R., Pingel, J.T., Sefton, B.M., Shaw, A. and Thomas, M.L. (1993) Correlation between Src family member regulation by the protein-tyrosine-phosphatase CD45 and transmembrane signaling through the T- cell receptor. *Proc Natl Acad Sci U S A*, **90**, 1402-1406.

Calalb, M.B., Polte, T.R. and Hanks, S.K. (1995) Tyrosine phosphorylation of focal adhesion kinase at sites in the catalytic domain regulates kinase activity: a role for Src family kinases. *Mol Cell Biol*, **15**, 954-963.

Campbell, J.J., Hedrick, J., Zlotnik, A., Siani, M.A., Thompson, D.A. and Butcher, E.C. (1998) Chemokines and the arrest of lymphocytes rolling under flow conditions. *Science*, **279**, 381-384.

Carter, M.S., Li, S. and Wilkinson, M.F. (1996) A splicing-dependent regulatory mechanism that detects translation signals. *Embo J*, **15**, 5965-5975.

Cartwright, C.A., Eckhart, W., Simon, S. and Kaplan, P.L. (1987) Cell transformation by pp60c-src mutated in the carboxy-terminal regulatory domain. *Cell*, **49**, 83-91.

Chalfie, M., Tu, Y., Euskirchen, G., Ward, W.W. and Prasher, D.C. (1994) Green fluorescent protein as a marker for gene expression. *Science*, **263**, 802-805.

Cheng, J., Fogel-Petrovic, M. and Maquat, L.E. (1990) Translation to near the distal end of the penultimate exon is required for normal levels of spliced triosephosphate isomerase mRNA. *Molecular And Cellular Biology*, **10**, 5215-5225.

Choi, T., Huang, M., Gorman, C. and Jaenisch, R. (1991) A generic intron increases gene expression in transgenic mice. *Molecular And Cellular Biology*, **11**, 3070-3074.

Chow, L.M., Davidson, D., Fournel, M., Gosselin, P., Lemieux, S., Lyu, M.S., Kozak, C.A., Matis, L.A. and Veillette, A. (1994a) Two distinct protein isoforms are encoded by ntk, a csk-related tyrosine protein kinase gene. *Oncogene*, **9**, 3437-3448.

Chow, L.M., Jarvis, C., Hu, Q., Nye, S.H., Gervais, F.G., Veillette, A. and Matis, L.A. (1994b) Ntk: a Csk-related protein-tyrosine kinase expressed in brain and T lymphocytes. *Proc Natl Acad Sci U S A*, **91**, 4975-4979.

Chuah, M.K., Vandendriessche, T. and Morgan, R.A. (1995) Development and analysis of retroviral vectors expressing human factor VIII as a potential gene therapy for hemophilia A. *Hum Gene Ther*, **6**, 1363-1377.

Clemens, P.R., Krause, T.L., Chan, S., Korb, K.E., Graham, F.L. and Caskey, C.T. (1995) Recombinant truncated dystrophin minigenes: construction, expression, and adenoviral delivery. *Hum Gene Ther*, **6**, 1477-1485.

Cloutier, J.F. and Veillette, A. (1996) Association of inhibitory tyrosine protein kinase p50csk with protein tyrosine phosphatase PEP in T cells and other hemopoietic cells. *Embo J*, **15**, 4909-4918.

Cole, N.B., Smith, C.L., Sciaky, N., Terasaki, M., Edidin, M. and Lippincott-Schwartz, J. (1996) Diffusional mobility of Golgi proteins in membranes of living cells. *Science*, **273**, 797-801.

Condliffe, A.M., Chilvers, E.R., Haslett, C. and Dransfield, I. (1996) Priming differentially regulates neutrophil adhesion molecule expression/function. *Immunology*, **89**, 105-111.

Condliffe, A.M., Kitchen, E. and Chilvers, E.R. (1998) Neutrophil priming: pathophysiological consequences and underlying mechanisms. *Clin Sci (Lond)*, **94**, 461-471.

Connelly, S., Gardner, J.M., McClelland, A. and Kaleko, M. (1996) High-level tissue-specific expression of functional human factor VIII in mice. *Hum Gene Ther*, **7**, 183-195.

Cooper, J.A., Gould, K.L., Cartwright, C.A. and Hunter, T. (1986) Tyr527 is phosphorylated in pp60c-src: implications for regulation. *Science*, **231**, 1431-1434.

Cooper, J.A. and King, C.S. (1986) Dephosphorylation or antibody binding to the carboxy terminus stimulates pp60c-src. *Mol Cell Biol*, **6**, 4467-4477.

Cooper JA, Wear MA, Weaver AM. (2001) Arp2/3 complex: advances on the inner workings of a molecular machine. *Cell.* **107**, 703-5.

Courtneidge, S.A. (1985) Activation of the pp60c-src kinase by middle T antigen binding or by dephosphorylation. *Embo J*, **4**, 1471-1477.

Courtneidge, S.A., Fumagalli, S., Koegl, M., Superti-Furga, G. and Twamley-Stein, G.M. (1993) The Src family of protein tyrosine kinases: regulation and functions. *Dev Suppl*, 57-64.

Coxon, A., Rieu, P., Barkalow, F.J., Askari, S., Sharpe, A.H., von Andrian, U.H., Arnaout, M.A. and Mayadas, T.N. (1996) A novel role for the beta 2 integrin CD11b/CD18 in neutrophil apoptosis: a homeostatic mechanism in inflammation. *Immunity*, **5**, 653-666.

Craig, N.L. (1988) The mechanism of conservative site-specific recombination. *Annu Rev Genet*, **22**, 77-105.

Cramer E, Pryzwansky KB, Villeval JL, Testa U, Breton-Gorius J. (1985) Ultrastructural localization of lactoferrin and myeloperoxidase in human neutrophils by immunogold. *Blood.* **65**, 423-32.

Crameri, A., Whitehorn, E.A., Tate, E. and Stemmer, W.P. (1996) Improved green fluorescent protein by molecular evolution using DNA shuffling. *Nat Biotechnol*, **14**, 315-319.

Crockett-Torabi, E., Sulenbarger, B., Smith, C.W. and Fantone, J.C. (1995) Activation of human neutrophils through L-selectin and Mac-1 molecules. *J Immunol*, **154**, 2291-2302.

Cunningham, C.C. (1995) Actin polymerization and intracellular solvent flow in cell surface blebbing. *J Cell Biol*, **129**, 1589-1599.

Daar, I.O. and Maquat, L.E. (1988) Premature translation termination mediates triosephosphate isomerase mRNA degradation. *Molecular And Cellular Biology*, **8**, 802-813.

Daeron, M. (1997) Fc receptor biology. *Annu Rev Immunol*, **15**, 203-234.

Daniels, R.H. and Bokoch, G.M. (1999) p21-activated protein kinase: a crucial component of morphological signaling? *Trends Biochem Sci*, **24**, 350-355.

Davidson, D., Cloutier, J.F., Gregorieff, A. and Veillette, A. (1997) Inhibitory tyrosine protein kinase p50csk is associated with protein- tyrosine phosphatase PTP-PEST in hemopoietic and non-hemopoietic cells. *J Biol Chem*, **272**, 23455-23462.

Davidson, D., Fournel, M. and Veillette, A. (1994) Oncogenic activation of p59fyn tyrosine protein kinase by mutation of its carboxyl-terminal site of tyrosine phosphorylation, tyrosine 528. *J Biol Chem*, **269**, 10956-10963.

Davis, I., Girdham, C.H. and O'Farrell, P.H. (1995) A nuclear GFP that marks nuclei in living Drosophila embryos; maternal supply overcomes a delay in the appearance of zygotic fluorescence. *Dev Biol*, **170**, 726-729.

Detmers, P.A., Zhou, D., Powell, D., Lichenstein, H., Kelley, M. and Pironkova, R. (1995) Endotoxin receptors (CD14) are found with CD16 (Fc gamma RIII) in an intracellular compartment of neutrophils that contains alkaline phosphatase. *J Immunol*, **155**, 2085-2095.

Dib K. BETA 2 integrin signaling in leukocytes. (2000) *Front Biosci.* **5**, D438-51.

Dustin, M.L., Rothlein, R., Bhan, A.K., Dinarello, C.A. and Springer, T.A. (1986) Induction by IL 1 and interferon-gamma: tissue distribution, biochemistry, and function of a natural adherence molecule (ICAM-1). *J Immunol*, **137**, 245-254.

Dymecki, S.M., Niederhuber, J.E. and Desiderio, S.V. (1990) Specific expression of a tyrosine kinase gene, blk, in B lymphoid cells. *Science*, **247**, 332-336.

Eide, B.L., Turck, C.W. and Escobedo, J.A. (1995) Identification of Tyr-397 as the primary site of tyrosine phosphorylation and pp60src association in the focal adhesion kinase, pp125FAK. *Mol Cell Biol*, **15**, 2819-2827.

Eiseman, E. and Bolen, J.B. (1990) src-related tyrosine protein kinases as signaling components in hematopoietic cells. *Cancer Cells*, **2**, 303-310.

Eiseman, E. and Bolen, J.B. (1992) Engagement of the high-affinity IgE receptor activates src protein- related tyrosine kinases. *Nature*, **355**, 78-80.

Eissenberg, J.C., Cartwright, I.L., Thomas, G.H. and Elgin, S.C. (1985) Selected topics in chromatin structure. *Annu Rev Genet*, **19**, 485-536.

El-Hillal O, Kurosaki T, Yamamura H, Kinet JP, Scharenberg AM. (1997) Syk kinase activation by a src kinase-initiated activation loop phosphorylation chain reaction. *Proc Natl Acad Sci U S A.* **94**, 1919-24.

Elices, M.J., Osborn, L., Takada, Y., Crouse, C., Luhowskyj, S., Hemler, M.E. and Lobb, R.R. (1990) VCAM-1 on activated endothelium interacts with the leukocyte integrin VLA-4 at a site distinct from the VLA-4/fibronectin binding site. *Cell*, **60**, 577-584.

Ernst M, Inglese M, Scholz GM, Harder KW, Clay FJ, Bozinovski S, Waring P, Darwiche R, Kay T, Sly P, Collins R, Turner D, Hibbs ML, Anderson GP, Dunn AR. (2002) Constitutive activation of the SRC family kinase Hck results in spontaneous pulmonary inflammation and an enhanced innate immune response. *J Exp Med.* **196**, 589-604.

Essani, N.A., Bajt, M.L., Farhood, A., Vonderfecht, S.L. and Jaeschke, H. (1997) Transcriptional activation of vascular cell adhesion molecule-1 gene in vivo and its role in the pathophysiology of neutrophil-induced liver injury in murine endotoxin shock. *J Immunol*, **158**, 5941-5948.

Etzioni, A., Frydman, M., Pollack, S., Avidor, I., Phillips, M.L., Paulson, J.C. and Gershoni-Baruch, R. (1992) Brief report: recurrent severe infections caused by a novel leukocyte adhesion deficiency. *N Engl J Med*, **327**, 1789-1792.

Fawcett, J., Holness, C.L., Needham, L.A., Turley, H., Gatter, K.C., Mason, D.Y. and Simmons, D.L. (1992) Molecular cloning of ICAM-3, a third ligand for LFA-1, constitutively expressed on resting leukocytes. *Nature*, **360**, 481-484.

Fincham, V.J. and Frame, M.C. (1998) The catalytic activity of Src is dispensable for translocation to focal adhesions but controls the turnover of these structures during cell motility. *Embo J*, **17**, 81-92.

Fitzer-Attas, C.J., Lowry, M., Crowley, M.T., Finn, A.J., Meng, F., DeFranco, A.L. and Lowell, C.A. (2000) Fcgamma receptor-mediated phagocytosis in macrophages lacking the Src family tyrosine kinases Hck, Fgr, and Lyn. *J Exp Med*, **191**, 669-682.

Gao J, Zoller KE, Ginsberg MH, Brugge JS, Shattil SJ. (1997) Regulation of the pp72syk protein tyrosine kinase by platelet integrin alpha IIb beta 3. *EMBO J.* **16**, 6414-25.

Gerszten, R.E., Garcia-Zepeda, E.A., Lim, Y.C., Yoshida, M., Ding, H.A., Gimbrone, M.A., Jr., Luster, A.D., Luscinskas, F.W. and Rosenzweig, A. (1999) MCP-1 and IL-8 trigger firm adhesion of monocytes to vascular endothelium under flow conditions. *Nature*, **398**, 718-723.

Gjorloff-Wingren, A., Saxena, M., Williams, S., Hammi, D. and Mustelin, T. (1999) Characterization of TCR-induced receptor-proximal signaling events negatively regulated by the protein tyrosine phosphatase PEP. *Eur J Immunol*, **29**, 3845-3854.

Gopalan, P.K., Smith, C.W., Lu, H., Berg, E.L., McIntire, L.V. and Simon, S.I. (1997) Neutrophil CD18-dependent arrest on intercellular adhesion molecule 1 (ICAM-1) in shear flow can be activated through L-selectin. *J Immunol*, **158**, 367-375.

Grant, S.G., O'Dell, T.J., Karl, K.A., Stein, P.L., Soriano, P. and Kandel, E.R. (1992) Impaired long-term potentiation, spatial learning, and hippocampal development in fyn mutant mice. *Science*, **258**, 1903-1910.

Gu, H., Zou, Y.R. and Rajewsky, K. (1993) Independent control of immunoglobulin switch recombination at individual switch regions evidenced through Cre-loxP-mediated gene targeting. *Cell*, **73**, 1155-1164.

Hall, A. (1998) Rho GTPases and the actin cytoskeleton. *Science*, **279**, 509-514.

Harris, K.F., Shoji, I., Cooper, E.M., Kumar, S., Oda, H. and Howley, P.M. (1999) Ubiquitin-mediated degradation of active Src tyrosine kinase. *Proc Natl Acad Sci U S A*, **96**, 13738-13743.

Harris, P. and Ralph, P. (1985) Human leukemic models of myelomonocytic development: a review of the HL- 60 and U937 cell lines. *J Leukoc Biol*, **37**, 407-422.

Haseloff, J., Siemering, K.R., Prasher, D.C. and Hodge, S. (1997) Removal of a cryptic intron and subcellular localization of green fluorescent protein are required to mark transgenic Arabidopsis plants brightly. *Proceedings Of The National Academy Of Sciences Of The United States Of America*, **94**, 2122-2127.

Haslett, C., Guthrie, L.A., Kopaniak, M.M., Johnston, R.B., Jr. and Henson, P.M. (1985) Modulation of multiple neutrophil functions by preparative methods or trace concentrations of bacterial lipopolysaccharide. *Am J Pathol*, **119**, 101-110.

Haslett, C., Worthen, G.S., Giclas, P.C., Morrison, D.C., Henson, J.E. and Henson, P.M. (1987) The pulmonary vascular sequestration of neutrophils in endotoxemia is initiated by an effect of endotoxin on the neutrophil in the rabbit. *Am Rev Respir Dis*, **136**, 9-18.

Hattori, R., Hamilton, K.K., Fugate, R.D., McEver, R.P. and Sims, P.J. (1989) Stimulated secretion of endothelial von Willebrand factor is accompanied by rapid redistribution to the cell surface of the intracellular granule membrane protein GMP-140. *J Biol Chem*, **264**, 7768-7771.

Hawkins, J.D. (1988) A survey on intron and exon lengths. *Nucleic Acids Res*, **16**, 9893-9908.

Head JA, Jiang D, Li M, Zorn LJ, Schaefer EM, Parsons JT, Weed SA. (2003) Cortactin tyrosine phosphorylation requires Rac1 activity and association with the cortical actin cytoskeleton. *Mol Biol Cell.* **14**, 3216-29.

Heim, R., Prasher, D.C. and Tsien, R.Y. (1994) Wavelength mutations and posttranslational autoxidation of green fluorescent protein. *Proc Natl Acad Sci U S A*, **91**, 12501-12504.

Henderson, R.B., Lim, L.H., Tessier, P.A., Gavins, F.N., Mathies, M., Perretti, M. and Hogg, N. (2001) The use of lymphocyte function-associated antigen (LFA)-1-deficient mice to determine the role of LFA-1, Mac-1, and alpha4 integrin in the inflammatory response of neutrophils. *J Exp Med*, **194**, 219-226.

Hennet, T., Hagen, F.K., Tabak, L.A. and Marth, J.D. (1995) T-cell-specific deletion of a polypeptide N-acetylgalactosaminyl- transferase gene by site-directed recombination. *Proc Natl Acad Sci U S A*, **92**, 12070-12074.

Hensley, P., McDevitt, P.J., Brooks, I., Trill, J.J., Feild, J.A., McNulty, D.E., Connor, J.R., Griswold, D.E., Kumar, N.V., Kopple, K.D. and et al. (1994) The soluble form of E-selectin is an asymmetric monomer. Expression, purification, and characterization of the recombinant protein. *J Biol Chem*, **269**, 23949-23958.

Hentze, M.W. and Kulozik, A.E. (1999) A perfect message: RNA surveillance and nonsense-mediated decay. *Cell*, **96**, 307-310.

Hermand, P., Huet, M., Callebaut, I., Gane, P., Ihanus, E., Gahmberg, C.G., Cartron, J.P. and Bailly, P. (2000) Binding sites of leukocyte beta 2 integrins (LFA-1, Mac-1) on the human ICAM-4/LW blood group protein. *J Biol Chem*, **275**, 26002-26010.

Hibbs ML, Tarlinton DM, Armes J, Grail D, Hodgson G, Maglitto R, Stacker SA, Dunn AR. (1995) Multiple defects in the immune system of Lyn-deficient mice, culminating in autoimmune disease. *Cell.* **83**, 301-11.

Hoess, R.H., Ziese, M. and Sternberg, N. (1982) P1 site-specific recombination: nucleotide sequence of the recombining sites. *Proc Natl Acad Sci U S A*, **79**, 3398-3402.

Hogg N, Henderson R, Leitinger B, McDowall A, Porter J, Stanley P. (2002) Mechanisms contributing to the activity of integrins on leukocytes. *Immunol Rev.* **186**, 164-71.

Howe, A., Aplin, A.E., Alahari, S.K. and Juliano, R.L. (1998) Integrin signaling and cell growth control. *Curr Opin Cell Biol*, **10**, 220-231.

Hsu-Lin, S., Berman, C.L., Furie, B.C., August, D. and Furie, B. (1984) A platelet membrane protein expressed during platelet activation and secretion. Studies using a monoclonal antibody specific for thrombin- activated platelets. *J Biol Chem*, **259**, 9121-9126.

Huang C, Liu J, Haudenschild CC, Zhan X. (1998) The role of tyrosine phosphorylation of cortactin in the locomotion of endothelial cells. *J Biol Chem.* **273**, 25770-6.

Huang, C., Ni, Y., Wang, T., Gao, Y., Haudenschild, C.C. and Zhan, X. (1997) Down-regulation of the filamentous actin cross-linking activity of cortactin by Src-mediated tyrosine phosphorylation. *J Biol Chem*, **272**, 13911-13915.

Huang J, Asawa T, Takato T, Sakai R. (2003) Cooperative roles of Fyn and cortactin in cell migration of metastatic murine melanoma. *J Biol Chem.* **278**, 48367-76.

Imamoto, A. and Soriano, P. (1993) Disruption of the csk gene, encoding a negative regulator of Src family tyrosine kinases, leads to neural tube defects and embryonic lethality in mice. *Cell*, **73**, 1117-1124.

Jaeschke, H., Farhood, A. and Smith, C.W. (1991) Neutrophil-induced liver cell injury in endotoxin shock is a CD11b/CD18- dependent mechanism. *Am J Physiol*, **261**, G1051-1056.

Jesaitis AJ, Buescher ES, Harrison D, Quinn MT, Parkos CA, Livesey S, Linner J. (1990) Ultrastructural localization of cytochrome b in the membranes of resting and phagocytosing human granulocytes. *J Clin Invest.* **85**, 821-35.

Johnson ML, Grimwood RE. (1994) Leukocyte colony-stimulating factors. A review of associated neutrophilic dermatoses and vasculitides. *Arch Dermatol.* **130**, 77-81.

Johnson, R.C., Mayadas, T.N., Frenette, P.S., Mebius, R.E., Subramaniam, M., Lacasce, A., Hynes, R.O. and Wagner, D.D. (1995) Blood cell dynamics in P-selectin-deficient mice. *Blood*, **86**, 1106-1114.

Jones, D.A., Abbassi, O., McIntire, L.V., McEver, R.P. and Smith, C.W. (1993) P-selectin mediates neutrophil rolling on histamine-stimulated endothelial cells. *Biophys J*, **65**, 1560-1569.

Kalish, J.E., Keller, G.A., Morrell, J.C., Mihalik, S.J., Smith, B., Cregg, J.M. and Gould, S.J. (1996) Characterization of a novel component of the peroxisomal protein import apparatus using fluorescent peroxisomal proteins. *Embo J*, **15**, 3275-3285.

Katagiri, K., Yokoyama, K.K., Yamamoto, T., Omura, S., Irie, S. and Katagiri, T. (1996) Lyn and Fgr protein-tyrosine kinases prevent apoptosis during retinoic acid-induced granulocytic differentiation of HL-60 cells. *J Biol Chem*, **271**, 11557-11562.

Kawabuchi, M., Satomi, Y., Takao, T., Shimonishi, Y., Nada, S., Nagai, K., Tarakhovsky, A. and Okada, M. (2000) Transmembrane phosphoprotein Cbp regulates the activities of Src-family tyrosine kinases. *Nature*, **404**, 999-1003.

Keshvara LM, Isaacson CC, Yankee TM, Sarac **R**, Harrison ML, Geahlen RL. (1998) Syk- and Lyn-dependent phosphorylation of Syk on multiple tyrosines following B cell activation includes a site that negatively regulates signaling. *J Immunol.* **161**, 5276-83.

Kilby, N.J., Snaith, M.R. and Murray, J.A. (1993) Site-specific recombinases: tools for genome engineering. *Trends Genet*, **9**, 413-421.

Kjeldsen L, Sengelov H, Lollike K, Nielsen MH, Borregaard N. (1994) Isolation and characterization of gelatinase granules from human neutrophils. *Blood.* **83**, 1640-9.

Klemke, R.L., Leng, J., Molander, R., Brooks, P.C., Vuori, K. and Cheresh, D.A. (1998) CAS/Crk coupling serves as a "molecular switch" for induction of cell migration. *J Cell Biol*, **140**, 961-972.

Kmiecik, T.E. and Shalloway, D. (1987) Activation and suppression of pp60c-src transforming ability by mutation of its primary sites of tyrosine phosphorylation. *Cell*, **49**, 65-73.

Kohara Y, Tanabe K, Matsuoka K, Kanda N, Matsuda H, Karasuyama H, Yonekawa H. (2001) A major determinant quantitative-trait locus responsible for atopic dermatitis-like

skin lesions in NC/Nga mice is located on Chromosome 9 *Immunogenetics.* **53**, 15-21.

Koo, G.C., Rosen, H., Sirotina, A., Ma, X.D. and Shultz, L.D. (1993) Anti-CD11b antibody prevents immunopathologic changes in viable moth- eaten bone marrow chimeric mice. *J Immunol*, **151**, 6733-6741.

Kuhn, R., Schwenk, F., Aguet, M. and Rajewsky, K. (1995) Inducible gene targeting in mice. *Science*, **269**, 1427-1429.

Kuypers, T.W. and Roos, D. (1989) Leukocyte membrane adhesion proteins LFA-1, CR3 and p150,95: a review of functional and regulatory aspects. *Res Immunol*, **140**, 461-486.

Labow, M.A., Norton, C.R., Rumberger, J.M., Lombard-Gillooly, K.M., Shuster, D.J., Hubbard, J., Bertko, R., Knaack, P.A., Terry, R.W., Harbison, M.L. and et al. (1994) Characterization of E-selectin-deficient mice: demonstration of overlapping function of the endothelial selectins. *Immunity*, **1**, 709-720.

Lacy-Hulbert, A., Thomas, R., Li, X.P., Lilley, C.E., Coffin, R.S. and Roes, J. (2001) Interruption of coding sequences by heterologous introns can enhance the functional expression of recombinant genes. *Gene Ther*, **8**, 649-653.

Langlet, C., Bernard, A.M., Drevot, P. and He, H.T. (2000) Membrane rafts and signaling by the multichain immune recognition receptors. *Curr Opin Immunol*, **12**, 250-255.

Larsen, E., Palabrica, T., Sajer, S., Gilbert, G.E., Wagner, D.D., Furie, B.C. and Furie, B. (1990) PADGEM-dependent adhesion of platelets to monocytes and neutrophils is mediated by a lineage-specific carbohydrate, LNF III (CD15). *Cell*, **63**, 467-474.

Lowe, J.B., Stoolman, L.M., Nair, R.P., Larsen, R.D., Berhend, T.L. and Marks, R.M. (1990) ELAM-1--dependent cell adhesion to vascular endothelium determined by a transfected human fucosyltransferase cDNA. *Cell*, **63**, 475-484.

Lowell CA, Soriano P, Varmus HE. (1994) Functional overlap in the src gene family: inactivation of hck and fgr impairs natural immunity.
Genes Dev. **8**, 387-98.

Lowell, C.A. and Berton, G. (1998) Resistance to endotoxic shock and reduced neutrophil migration in mice deficient for the Src-family kinases Hck and Fgr. *Proc Natl Acad Sci U S A*, **95**, 7580-7584.

Lowell, C.A., Fumagalli, L. and Berton, G. (1996) Deficiency of Src family kinases p59/61hck and p58c-fgr results in defective adhesion-dependent neutrophil functions. *J Cell Biol*, **133**, 895-910.

Lowell, C.A., Soriano, P. and Varmus, H.E. (1994) Functional overlap in the src gene family: inactivation of hck and fgr impairs natural immunity. *Genes Dev*, **8**, 387-398.

Luscinskas, F.W., Cybulsky, M.I., Kiely, J.M., Peckins, C.S., Davis, V.M. and Gimbrone, M.A., Jr. (1991) Cytokine-activated human endothelial monolayers support enhanced neutrophil transmigration via a mechanism involving both endothelial- leukocyte adhesion molecule-1 and intercellular adhesion molecule-1. *J Immunol*, **146**, 1617-1625.

Marino, M.W., Dunn, A., Grail, D., Inglese, M., Noguchi, Y., Richards, E., Jungbluth, A., Wada, H., Moore, M., Williamson, B., Basu, S. and Old, L.J. (1997) Characterization of tumor necrosis factor-deficient mice. *Proc Natl Acad Sci U S A*, **94**, 8093-8098.

Marlin, S.D. and Springer, T.A. (1987) Purified intercellular adhesion molecule-1 (ICAM-1) is a ligand for lymphocyte function-associated antigen 1 (LFA-1). *Cell*, **51**, 813-819.

Marth, J.D., Peet, R., Krebs, E.G. and Perlmutter, R.M. (1985) A lymphocyte-specific protein-tyrosine kinase gene is rearranged and overexpressed in the murine T cell lymphoma LSTRA. *Cell*, **43**, 393-404.

Martin, M.U. and Wesche, H. (2002) Summary and comparison of the signaling mechanisms of the Tol/interleukin-1 receptor family. *Biochim. Biophys. Acta.* **1592**, 265-80.

Mayadas, T.N., Johnson, R.C., Rayburn, H., Hynes, R.O. and Wagner, D.D. (1993) Leukocyte rolling and extravasation are severely compromised in P selectin-deficient mice. *Cell*, **74**, 541-554.

McEver, R.P. (1994) Selectins. *Curr Opin Immunol*, **6**, 75-84.

Meng, F. and Lowell, C.A. (1997) Lipopolysaccharide (LPS)-induced macrophage activation and signal transduction in the absence of Src-family kinases Hck, Fgr, and Lyn. *J Exp Med*, **185**, 1661-1670.

Miller, L.J., Bainton, D.F., Borregaard, N. and Springer, T.A. (1987) Stimulated mobilization of monocyte Mac-1 and p150,95 adhesion proteins from an intracellular vesicular compartment to the cell surface. *J Clin Invest*, **80**, 535-544.

Miyamoto, S., Akiyama, S.K. and Yamada, K.M. (1995) Synergistic roles for receptor occupancy and aggregation in integrin transmembrane function. *Science*, **267**, 883-885.

Mocsai, A., Jakus, Z., Vantus, T., Berton, G., Lowell, C.A. and Ligeti, E. (2000) Kinase pathways in chemoattractant-induced degranulation of neutrophils: the role of p38 mitogen-activated protein kinase activated by Src family kinases. *J Immunol*, **164**, 4321-4331.

Mocsai, A., Ligeti, E., Lowell, C.A. and Berton, G. (1999) Adhesion-dependent degranulation of neutrophils requires the Src family kinases Fgr and Hck. *J Immunol*, **162**, 1120-1126.

Mocsai A, Zhou M, Meng F, Tybulewicz VL, Lowell CA. (2002) Syk is required for

integrin signaling in neutrophils. *Immunity.* **16**, 547-58.

Molina, T.J., Kishihara, K., Siderovski, D.P., van Ewijk, W., Narendran, A., Timms, E., Wakeham, A., Paige, C.J., Hartmann, K.U., Veillette, A. and et al. (1992) Profound block in thymocyte development in mice lacking p56lck. *Nature*, **357**, 161-164.

Monroe, R.J., Seidl, K.J., Gaertner, F., Han, S., Chen, F., Sekiguchi, J., Wang, J., Ferrini, R., Davidson, L., Kelsoe, G. and Alt, F.W. (1999) RAG2:GFP knockin mice reveal novel aspects of RAG2 expression in primary and peripheral lymphoid tissues. *Immunity*, **11**, 201-212.

Montell, C., Fisher, E.F., Caruthers, M.H. and Berk, A.J. (1982) Resolving the functions of overlapping viral genes by site-specific mutagenesis at a mRNA splice site. *Nature*, **295**, 380-384.

Moore, K.L., Eaton, S.F., Lyons, D.E., Lichenstein, H.S., Cummings, R.D. and McEver, R.P. (1994) The P-selectin glycoprotein ligand from human neutrophils displays sialylated, fucosylated, O-linked poly-N-acetyllactosamine. *J Biol Chem*, **269**, 23318-23327.

Morel F, Doussiere J, Vignais PV. (1991) The superoxide-generating oxidase of phagocytic cells. Physiological, molecular and pathological aspects. *Eur J Biochem.* **201**, 523-46.

Morisaki, T., Goya, T., Toh, H., Nishihara, K. and Torisu, M. (1991) The anti Mac-1 monoclonal antibody inhibits neutrophil sequestration in lung and liver in a septic murine model. *Clin Immunol Immunopathol*, **61**, 365-375.

Morrison, D.C. and Ryan, J.L. (1987) Endotoxins and disease mechanisms. *Annu Rev Med*, **38**, 417-432.

Muller, W.A. (1995) The role of PECAM-1 (CD31) in leukocyte emigration: studies in vitro and in vivo. *J Leukoc Biol*, **57**, 523-528.

Nada, S., Okada, M., Aizawa, S. and Nakagawa, H. (1994) Identification of major tyrosine-phosphorylated proteins in Csk- deficient cells. *Oncogene*, **9**, 3571-3578.

Nada, S., Okada, M., MacAuley, A., Cooper, J.A. and Nakagawa, H. (1991) Cloning of a complementary DNA for a protein-tyrosine kinase that specifically phosphorylates a negative regulatory site of p60c-src. *Nature*, **351**, 69-72.

Nada, S., Yagi, T., Takeda, H., Tokunaga, T., Nakagawa, H., Ikawa, Y., Okada, M. and Aizawa, S. (1993) Constitutive activation of Src family kinases in mouse embryos that lack Csk. *Cell*, **73**, 1125-1135.

Nakagawa, T., Tanaka, S., Suzuki, H., Takayanagi, H., Miyazaki, T., Nakamura, K. and Tsuruo, T. (2000) Overexpression of the csk gene suppresses tumor metastasis in vivo. *Int J Cancer*, **88**, 384-391.

Naora, H. and Deacon, N.J. (1982) Relationship between the total size of exons and introns in protein- coding genes of higher eukaryotes. *Proc Natl Acad Sci U S A*, **79**, 6196-6200.

Neel, H., Weil, D., Giansante, C. and Dautry, F. (1993) In vivo cooperation between introns during pre-mRNA processing. *Genes And Development*, **7**, 2194-2205.

Nelson, K.K. and Green, M.R. (1990) Mechanism for cryptic splice site activation during pre-mRNA splicing. *Proc Natl Acad Sci U S A*, **87**, 6253-6257.

Nesic, D. and Maquat, L.E. (1994) Upstream introns influence the efficiency of final intron removal and RNA 3'-end formation. *Genes Dev*, **8**, 363-375.

Newman, P.J., Berndt, M.C., Gorski, J., White, G.C., 2nd, Lyman, S., Paddock, C. and Muller, W.A. (1990) PECAM-1 (CD31) cloning and relation to adhesion molecules of the immunoglobulin gene superfamily. *Science*, **247**, 1219-1222.

Nilsson, S.V. and Magnusson, G. (1983) T-antigen expression by polyoma mutants with modified RNA splicing. *Embo J*, **2**, 2095-2101.

Nojima, Y., Morino, N., Mimura, T., Hamasaki, K., Furuya, H., Sakai, R., Sato, T., Tachibana, K., Morimoto, C., Yazaki, Y. and et al. (1995) Integrin-mediated cell adhesion promotes tyrosine phosphorylation of p130Cas, a Src homology 3-containing molecule having multiple Src homology 2-binding motifs. *J Biol Chem*, **270**, 15398-15402.

Obergfell A, Eto K, Mocsai A, Buensuceso C, Moores SL, Brugge JS, Lowell CA, Shattil SJ. (2002) Coordinate interactions of Csk, Src, and Syk kinases with [alpha]IIb[beta]3 initiate integrin signaling to the cytoskeleton.
J Cell Biol. **157**, 265-75.

Okada, M., Nada, S., Yamanashi, Y., Yamamoto, T. and Nakagawa, H. (1991) CSK: a protein-tyrosine kinase involved in regulation of src family kinases. *J Biol Chem*, **266**, 24249-24252.

Okada, M. and Nakagawa, H. (1989) A protein tyrosine kinase involved in regulation of pp60c-src function. *J Biol Chem*, **264**, 20886-20893.

Owen, C.A., Campbell, M.A., Sannes, P.L., Boukedes, S.S. and Campbell, E.J. (1995) Cell surface-bound elastase and cathepsin G on human neutrophils: a novel, non-oxidative mechanism by which neutrophils focus and preserve catalytic activity of serine proteinases. *J Cell Biol*, **131**, 775-789.

Palmiter, R.D., Sandgren, E.P., Avarbock, M.R., Allen, D.D. and Brinster, R.L. (1991) Heterologous introns can enhance expression of transgenes in mice. *Proceedings Of The National Academy Of Sciences Of The United States Of America*, **88**, 478-482.

Partanen, J., Armstrong, E., Bergman, M., Makela, T.P., Hirvonen, H., Huebner, K. and Alitalo, K. (1991) cyl encodes a putative cytoplasmic tyrosine kinase lacking the conserved tyrosine autophosphorylation site (Y416src). *Oncogene*, **6**, 2013-2018.

Patel, K.D., Zimmerman, G.A., Prescott, S.M., McEver, R.P. and McIntyre, T.M. (1991) Oxygen radicals induce human endothelial cells to express GMP-140 and bind neutrophils. *J Cell Biol*, **112**, 749-759.

Pavalko, F.M. and LaRoche, S.M. (1993) Activation of human neutrophils induces an interaction between the integrin beta 2-subunit (CD18) and the actin binding protein alpha- actinin. *J Immunol*, **151**, 3795-3807.

Pawson, T. and Gish, G.D. (1992) SH2 and SH3 domains: from structure to function. *Cell*, **71**, 359-362.

Pawson, T. and Scott, J.D. (1997) Signaling through scaffold, anchoring, and adaptor proteins. *Science*, **278**, 2075-2080.

Perera, P.Y., Mayadas, T.N., Takeuchi, O., Akira, S., Zaks-Zilberman, M., Goyert, S.M. and Vogel, S.N. (2001) CD11b/CD18 acts in concert with CD14 and Toll-like receptor (TLR) 4 to elicit full lipopolysaccharide and taxol-inducible gene expression. *J Immunol*, **166**, 574-581.

Petit, V., Boyer, B., Lentz, D., Turner, C.E., Thiery, J.P. and Valles, A.M. (2000) Phosphorylation of tyrosine residues 31 and 118 on paxillin regulates cell migration through an association with CRK in NBT-II cells. *J Cell Biol*, **148**, 957-970.

Petty, H.R. and Todd, R.F., 3rd. (1996) Integrins as promiscuous signal transduction devices. *Immunol Today*, **17**, 209-212.

Petty, H.R., Worth, R.G. and Todd, R.F., 3rd. (2002) Interactions of integrins with their partner proteins in leukocyte membranes. *Immunol Res*, **25**, 75-95.

Pfeffer, K., Matsuyama, T., Kundig, T.M., Wakeham, A., Kishihara, K., Shahinian, A., Wiegmann, K., Ohashi, P.S., Kronke, M. and Mak, T.W. (1993) Mice deficient for the 55 kd tumor necrosis factor receptor are resistant to endotoxic shock, yet succumb to L. monocytogenes infection. *Cell*, **73**, 457-467.

Picker, L.J., Warnock, R.A., Burns, A.R., Doerschuk, C.M., Berg, E.L. and Butcher, E.C. (1991) The neutrophil selectin LECAM-1 presents carbohydrate ligands to the vascular selectins ELAM-1 and GMP-140. *Cell*, **66**, 921-933.

Piwnica-Worms, H., Saunders, K.B., Roberts, T.M., Smith, A.E. and Cheng, S.H. (1987) Tyrosine phosphorylation regulates the biochemical and biological properties of pp60c-src. *Cell*, **49**, 75-82.

Pober, J.S., Gimbrone, M.A., Jr., Lapierre, L.A., Mendrick, D.L., Fiers, W., Rothlein, R. and Springer, T.A. (1986) Overlapping patterns of activation of human endothelial cells by interleukin 1, tumor necrosis factor, and immune interferon. *J Immunol*, **137**, 1893-1896.

Polte, T.R. and Hanks, S.K. (1995) Interaction between focal adhesion kinase and Crk-associated tyrosine kinase substrate p130Cas. *Proc Natl Acad Sci U S A*, **92**, 10678-10682.

Ponniah, S., Wang, D.Z., Lim, K.L. and Pallen, C.J. (1999) Targeted disruption of the tyrosine phosphatase PTPalpha leads to constitutive downregulation of the kinases Src and Fyn. *Curr Biol*, **9**, 535-538.

Rao, N., Miyake, S., Reddi, A.L., Douillard, P., Ghosh, A.K., Dodge, I.L., Zhou, P., Fernandes, N.D. and Band, H. (2002) Negative regulation of Lck by Cbl ubiquitin ligase. *Proc Natl Acad Sci U S A*, **99**, 3794-3799.

Reed, R. and Maniatis, T. (1985) Intron sequences involved in lariat formation during pre-mRNA splicing. *Cell*, **41**, 95-105.

Resh, M.D. (1994) Myristylation and palmitylation of Src family members: the fats of the matter. *Cell*, **76**, 411-413.

Richard-Foy, H. and Hager, G.L. (1987) Sequence-specific positioning of nucleosomes over the steroid-inducible MMTV promoter. *Embo J*, **6**, 2321-2328.

Rickert, R.C., Roes, J. and Rajewsky, K. (1997) B lymphocyte-specific, Cre-mediated mutagenesis in mice. *Nucleic Acids Res*, **25**, 1317-1318.

Ridley AJ. Rho GTPases and cell migration. (2001) *J Cell Sci.* **114**, 2713-22.

Rizzuto, R., Brini, M., De Giorgi, F., Rossi, R., Heim, R., Tsien, R.Y. and Pozzan, T. (1996) Double labelling of subcellular structures with organelle-targeted GFP mutants in vivo. *Curr Biol*, **6**, 183-188.

Robberson, B.L., Cote, G.J. and Berget, S.M. (1990) Exon definition may facilitate splice site selection in RNAs with multiple exons. *Mol Cell Biol*, **10**, 84-94.

Rodriguez, R.J., White, R.R., Senior, R.M. and Levine, E.A. (1977) Elastase release from human alveolar macrophages: comparison between smokers and nonsmokers. *Science*, **198**, 313-314.

Romanova LY, Hashimoto S, Chay KO, Blagosklonny MV, Sabe H, Mushinski JF. (2004) Phosphorylation of paxillin tyrosines 31 and 118 controls polarization and motility of lymphoid cells and is PMA-sensitive. J Cell Sci. 117, 3759-68.

Rossi GA, Hunninghake GW, Kawanami O, Ferrans VJ, Hansen CT, Crystal RG. (1985) Motheaten mice--an animal model with an inherited form of interstitial lung disease. Am Rev Respir Dis. **131**, 150-8.

Rothe, J., Lesslauer, W., Lotscher, H., Lang, Y., Koebel, P., Kontgen, F., Althage, A., Zinkernagel, R., Steinmetz, M. and Bluethmann, H. (1993) Mice lacking the tumour necrosis factor receptor 1 are resistant to TNF- mediated toxicity but highly susceptible to infection by Listeria monocytogenes. *Nature*, **364**, 798-802.

Rothlein, R., Dustin, M.L., Marlin, S.D. and Springer, T.A. (1986) A human intercellular adhesion molecule (ICAM-1) distinct from LFA-1. *J Immunol*, **137**, 1270-1274.

Sabe, H., Hata, A., Okada, M., Nakagawa, H. and Hanafusa, H. (1994) Analysis of the binding of the Src homology 2 domain of Csk to tyrosine- phosphorylated proteins in the suppression and mitotic activation of c- Src. *Proc Natl Acad Sci U S A*, **91**, 3984-3988.

Savill J, Dransfield I, Gregory C, Haslett C. (2002) A blast from the past: clearance of apoptotic cells regulates immune responses. *Nat Rev Immunol.* **2**, 965-75.

Schaller, M.D., Hildebrand, J.D., Shannon, J.D., Fox, J.W., Vines, R.R. and Parsons, J.T. (1994) Autophosphorylation of the focal adhesion kinase, pp125FAK, directs SH2-dependent binding of pp60src. *Mol Cell Biol*, **14**, 1680-1688.

Schaller, M.D. and Parsons, J.T. (1995) pp125FAK-dependent tyrosine phosphorylation of paxillin creates a high- affinity binding site for Crk. *Mol Cell Biol*, **15**, 2635-2645.

Scharffetter-Kochanek, K., Lu, H., Norman, K., van Nood, N., Munoz, F., Grabbe, S., McArthur, M., Lorenzo, I., Kaplan, S., Ley, K., Smith, C.W., Montgomery, C.A., Rich, S. and Beaudet, A.L. (1998) Spontaneous skin ulceration and defective T cell function in CD18 null mice. *J Exp Med*, **188**, 119-131.

Schlaepfer, D.D., Hanks, S.K., Hunter, T. and van der Geer, P. (1994) Integrin-mediated signal transduction linked to Ras pathway by GRB2 binding to focal adhesion kinase. *Nature*, **372**, 786-791.

Schmedt, C., Saijo, K., Niidome, T., Kuhn, R., Aizawa, S. and Tarakhovsky, A. (1998) Csk controls antigen receptor-mediated development and selection of T- lineage cells. *Nature*, **394**, 901-904.

Schoenwaelder, S.M., and Burridge, K. (1999) Bidirectional signaling between the cytoskeleton and integrins. *Curr. Opin. Cell Biol*, **11**, 274-286.

Sengelov H, Nielsen MH, Borregaard N. (1992) Separation of human neutrophil plasma membrane from intracellular vesicles containing alkaline phosphatase and NADPH oxidase activity by free flow electrophoresis.
J Biol Chem. **267**, 14912-7.

Sengelov H, Kjeldsen L, Diamond MS, Springer TA, Borregaard N. (1993) Subcellular localization and dynamics of Mac-1 (alpha m beta 2) in human neutrophils. *J Clin Invest.* **92**,

1467-76.

Senior, R.M., Campbell, E.J., Landis, J.A., Cox, F.R., Kuhn, C. and Koren, H.S. (1982) Elastase of U-937 monocytelike cells. Comparisons with elastases derived from human monocytes and neutrophils and murine macrophagelike cells. *J Clin Invest*, **69**, 384-393.

Shapiro, S.D., Campbell, E.J., Senior, R.M. and Welgus, H.G. (1991) Proteinases secreted by human mononuclear phagocytes. *J Rheumatol Suppl*, **27**, 95-98.

Shimomura, O., Johnson, F.H. and Saiga, Y. (1962) *J. Cell. Comp. Physiol.*, **59**, 223-239.

Simon, S.I., Burns, A.R., Taylor, A.D., Gopalan, P.K., Lynam, E.B., Sklar, L.A. and Smith, C.W. (1995) L-selectin (CD62L) cross-linking signals neutrophil adhesive functions via the Mac-1 (CD11b/CD18) beta 2-integrin. *J Immunol*, **155**, 1502-1514.

Simon, S.I., Cherapanov, V., Nadra, I., Waddell, T.K., Seo, S.M., Wang, Q., Doerschuk, C.M. and Downey, G.P. (1999) Signaling functions of L-selectin in neutrophils: alterations in the cytoskeleton and colocalization with CD18. *J Immunol*, **163**, 2891-2901.

Singer, II, Scott, S., Kawka, D.W. and Kazazis, D.M. (1989) Adhesomes: specific granules containing receptors for laminin, C3bi/fibrinogen, fibronectin, and vitronectin in human polymorphonuclear leukocytes and monocytes. *J Cell Biol*, **109**, 3169-3182.

Smedly, L.A., Tonnesen, M.G., Sandhaus, R.A., Haslett, C., Guthrie, L.A., Johnston, R.B., Jr., Henson, P.M. and Worthen, G.S. (1986) Neutrophil-mediated injury to endothelial cells. Enhancement by endotoxin and essential role of neutrophil elastase. *J Clin Invest*, **77**, 1233-1243.

Somani, A.K., Bignon, J.S., Mills, G.B., Siminovitch, K.A. and Branch, D.R. (1997) Src kinase activity is regulated by the SHP-1 protein-tyrosine phosphatase. *J Biol Chem*, **272**, 21113-21119.

Soriano, P., Montgomery, C., Geske, R. and Bradley, A. (1991) Targeted disruption of the c-src proto-oncogene leads to osteopetrosis in mice. *Cell*, **64**, 693-702.

Staunton, D.E., Dustin, M.L. and Springer, T.A. (1989) Functional cloning of ICAM-2, a cell adhesion ligand for LFA-1 homologous to ICAM-1. *Nature*, **339**, 61-64.

Stehelin, D., Varmus, H.E., Bishop, J.M. and Vogt, P.K. (1976) DNA related to the transforming gene(s) of avian sarcoma viruses is present in normal avian DNA. *Nature*, **260**, 170-173.

Stein, P.L., Lee, H.M., Rich, S. and Soriano, P. (1992) pp59fyn mutant mice display differential signaling in thymocytes and peripheral T cells. *Cell*, **70**, 741-750.

Sternberg, N. and Hamilton, D. (1981) Bacteriophage P1 site-specific recombination. I. Recombination between loxP sites. *J Mol Biol*, **150**, 467-486.

Stewart, M. and Hogg, N. (1996) Regulation of leukocyte integrin function: affinity vs. avidity. *J Cell Biochem*, **61**, 554-561.

Suen, P.W., Ilic, D., Caveggion, E., Berton, G., Damsky, C.H. and Lowell, C.A. (1999) Impaired integrin-mediated signal transduction, altered cytoskeletal structure and reduced motility in Hck/Fgr deficient macrophages. *J Cell Sci*, **112**, 4067-4078.

Takahashi, H., Nukiwa, T., Basset, P. and Crystal, R.G. (1988) Myelomonocytic cell lineage expression of the neutrophil elastase gene. *J Biol Chem*, **263**, 2543-2547.

Tate, R.M. and Repine, J.E. (1983) Neutrophils and the adult respiratory distress syndrome. *Am Rev Respir Dis*, **128**, 552-559.

Thermann, R., Neu-Yilik, G., Deters, A., Frede, U., Wehr, K., Hagemeier, C., Hentze, M.W. and Kulozik, A.E. (1998) Binary specification of nonsense codons by splicing and cytoplasmic translation. *Embo J*, **17**, 3484-3494.

Thomas, S.M., Soriano, P. and Imamoto, A. (1995) Specific and redundant roles of Src and Fyn in organizing the cytoskeleton. *Nature*, **376**, 267-271.

Tian, L., Kilgannon, P., Yoshihara, Y., Mori, K., Gallatin, W.M., Carpen, O. and Gahmberg, C.G. (2000) Binding of T lymphocytes to hippocampal neurons through ICAM-5 (telencephalin) and characterization of its interaction with the leukocyte integrin CD11a/CD18. *Eur J Immunol*, **30**, 810-818.

Timpson P, Jones GE, Frame MC, Brunton VG. (2001) Coordination of cell polarization and migration by the Rho family GTPases requires Src tyrosine kinase activity. *Curr Biol.* **11**, 1836-46.

Tkalcevic, J., Novelli, M., Phylactides, M., Iredale, J.P., Segal, A.W. and Roes, J. (2000) Impaired immunity and enhanced resistance to endotoxin in the absence of neutrophil elastase and cathepsin G. *Immunity*, **12**, 201-210.

Tracey, K.J., Beutler, B., Lowry, S.F., Merryweather, J., Wolpe, S., Milsark, I.W., Hariri, R.J., Fahey, T.J., 3rd, Zentella, A., Albert, J.D. and et al. (1986) Shock and tissue injury induced by recombinant human cachectin. *Science*, **234**, 470-474.

Treisman, R., Orkin, S.H. and Maniatis, T. (1983) Specific transcription and RNA splicing defects in five cloned beta- thalassaemia genes. *Nature*, **302**, 591-596.

Treisman, R., Proudfoot, N.J., Shander, M. and Maniatis, T. (1982) A single-base change at a splice site in a beta 0-thalassemic gene causes abnormal RNA splicing. *Cell*, **29**, 903-911.

Tsang, Y.T., Neelamegham, S., Hu, Y., Berg, E.L., Burns, A.R., Smith, C.W. and Simon, S.I. (1997) Synergy between L-selectin signaling and chemotactic activation during neutrophil adhesion and transmigration. *J Immunol*, **159**, 4566-4577.

Tsien, R.Y. (1998) The green fluorescent protein. *Annu Rev Biochem*, **67**, 509-544.

Turner CE. Paxillin interactions. (2000) *J Cell Sci.* **113**, 4139-40.

Turner, C.E., Brown, M.C., Perrotta, J.A., Riedy, M.C., Nikolopoulos, S.N., McDonald, A.R., Bagrodia, S., Thomas, S. and Leventhal, P.S. (1999) Paxillin LD4 motif binds PAK and PIX through a novel 95-kD ankyrin repeat, ARF-GAP protein: A role in cytoskeletal remodeling. *J Cell Biol*, **145**, 851-863.

Turner, C.E. and Miller, J.T. (1994) Primary sequence of paxillin contains putative SH2 and SH3 domain binding motifs and multiple LIM domains: identification of a vinculin and pp125Fak-binding region. *J Cell Sci*, **107**, 1583-1591.

Turner, C.E., Schaller, M.D. and Parsons, J.T. (1993) Tyrosine phosphorylation of the focal adhesion kinase pp125FAK during development: relation to paxillin. *J Cell Sci*, **105**, 637-645.

Urlaub, G., Mitchell, P.J., Ciudad, C.J. and Chasin, L.A. (1989) Nonsense mutations in the dihydrofolate reductase gene affect RNA processing. *Mol Cell Biol*, **9**, 2868-2880.

Uruno T, Liu J, Zhang P, Fan Yx, Egile C, Li R, Mueller SC, Zhan X. (2001) Activation of Arp2/3 complex-mediated actin polymerization by cortactin. *Nat Cell Biol.* **3**, 259-66.

Ushiyama, S., Laue, T.M., Moore, K.L., Erickson, H.P. and McEver, R.P. (1993) Structural and functional characterization of monomeric soluble P- selectin and comparison with membrane P-selectin. *J Biol Chem*, **268**, 15229-15237.

van Kooyk, Y. and Figdor, C.G. (2000) Avidity regulation of integrins: the driving force in leukocyte adhesion. *Curr Opin Cell Biol*, **12**, 542-547.

Vestergaard C, Yoneyama H, Matsushima K. (2000) The NC/Nga mouse: a model for atopic dermatitis. *Mol Med Today.* **6**, 209-10.

von Andrian, U.H., Chambers, J.D., McEvoy, L.M., Bargatze, R.F., Arfors, K.E. and Butcher, E.C. (1991) Two-step model of leukocyte-endothelial cell interaction in inflammation: distinct roles for LECAM-1 and the leukocyte beta 2 integrins in vivo. *Proc Natl Acad Sci U S A*, **88**, 7538-7542.

Vuori, K. and Ruoslahti, E. (1995) Tyrosine phosphorylation of p130Cas and cortactin accompanies integrin- mediated cell adhesion to extracellular matrix. *J Biol Chem*, **270**, 22259-22262.

Wall, R.J., Pursel, V.G., Shamay, A., McKnight, R.A., Pittius, C.W. and Hennighausen, L. (1991) High-level synthesis of a heterologous milk protein in the mammary glands of transgenic swine. *Proc Natl Acad Sci U S A*, **88**, 1696-1700.

Wang B, Lemay S, Tsai S, Veillette A. (2001) SH2 domain-mediated interaction of inhibitory protein tyrosine kinase Csk with protein tyrosine phosphatase-HSCF. Mol Cell Biol. **21**, 1077-88.

Wang, J.M., Zheng, H., Sugahara, Y., Tan, J., Yao, S.N., Olson, E. and Kurachi, K. (1996) Construction of human factor IX expression vectors in retroviral vector frames optimized for muscle cells. *Hum Gene Ther*, **7**, 1743-1756.

Webb DJ, Donais K, Whitmore LA, Thomas SM, Turner CE, Parsons JT, Horwitz AF. (2004) FAK-Src signalling through paxillin, ERK and MLCK regulates adhesion disassembly. *Nat Cell Biol.* **6**, 154-61.

Webster, J., Donofrio, G., Wallace, R., Clark, A.J. and Whitelaw, C.B. (1997) Intronic sequences modulate the sensitivity of beta-lactoglobulin transgenes to position effects. *Gene*, **193**, 239-243.

Weed SA, Du Y, Parsons JT. (1998) Translocation of cortactin to the cell periphery is mediated by the small GTPase Rac1. *J Cell Sci.* **111**, 2433-43.

Weed SA, Karginov AV, Schafer DA, Weaver AM, Kinley AW, Cooper JA, Parsons JT. (2000) Cortactin localization to sites of actin assembly in lamellipodia requires interactions with F-actin and the Arp2/3 complex. *J Cell Biol.* **151**, 29-40.

Weedon, D. (1997) Skin pathology (New York: Churchill Livingstone).

Wei, S., Liu, J.H., Epling-Burnette, P.K., Gamero, A.M., Ussery, D., Pearson, E.W., Elkabani, M.E., Diaz, J.I. and Djeu, J.Y. (1996) Critical role of Lyn kinase in inhibition of neutrophil apoptosis by granulocyte-macrophage colony-stimulating factor. *J Immunol*, **157**, 5155-5162.

Weitzman, J.B., Wells, C.E., Wright, A.H., Clark, P.A. and Law, S.K. (1991) The gene organisation of the human beta 2 integrin subunit (CD18). *FEBS Lett*, **294**, 97-103.

Whitelaw, C.B., Archibald, A.L., Harris, S., McClenaghan, M., Simons, J.P. and Clark, A.J. (1991) Targeting expression to the mammary gland: intronic sequences can enhance the efficiency of gene expression in transgenic mice. *Transgenic Research*, **1**, 3-13.

Willeke T, Schymeinsky J, Prange P, Zahler S, Walzog B. (2003) A role for Syk-kinase in the control of the binding cycle of the beta2 integrins (CD11/CD18) in human polymorphonuclear neutrophils. *J Leukoc Biol.* **74**, 260-9.

Woodside DG, Obergfell A, Leng L, Wilsbacher JL, Miranti CK, Brugge JS, Shattil SJ, Ginsberg MH. (2001) Activation of Syk protein tyrosine kinase through interaction with

integrin beta cytoplasmic domains. *Curr Biol.* **11**, 1799-804.

Worthen, G.S., Haslett, C., Rees, A.J., Gumbay, R.S., Henson, J.E. and Henson, P.M. (1987) Neutrophil-mediated pulmonary vascular injury. Synergistic effect of trace amounts of lipopolysaccharide and neutrophil stimuli on vascular permeability and neutrophil sequestration in the lung. *Am Rev Respir Dis*, **136**, 19-28.

Worthen, G.S., Schwab, B., 3rd, Elson, E.L. and Downey, G.P. (1989) Mechanics of stimulated neutrophils: cell stiffening induces retention in capillaries. *Science*, **245**, 183-186.

Wu H, Parsons JT. (1993) Cortactin, an 80/85-kilodalton pp60src substrate, is a filamentous actin-binding protein enriched in the cell cortex. *J Cell Biol.* **120**, 1417-26.

Xie, J., Li, R., Kotovuori, P., Vermot-Desroches, C., Wijdenes, J., Arnaout, M.A., Nortamo, P. and Gahmberg, C.G. (1995) Intercellular adhesion molecule-2 (CD102) binds to the leukocyte integrin CD11b/CD18 through the A domain. *J Immunol*, **155**, 3619-3628.

Xu, H., Gonzalo, J.A., St Pierre, Y., Williams, I.R., Kupper, T.S., Cotran, R.S., Springer, T.A. and Gutierrez-Ramos, J.C. (1994) Leukocytosis and resistance to septic shock in intercellular adhesion molecule 1-deficient mice. *J Exp Med*, **180**, 95-109.

Yamamoto, T., Yamanashi, Y. and Toyoshima, K. (1993) Association of Src-family kinase Lyn with B-cell antigen receptor. *Immunol Rev*, **132**, 187-206.

Yan SR, Fumagalli L, Berton G. (1996) Activation of SRC family kinases in human neutrophils. Evidence that p58C-FGR and p53/56LYN redistributed to a Triton X-100-insoluble cytoskeletal fraction, also enriched in the caveolar protein caveolin, display an enhanced kinase activity. *FEBS Lett.* **380**, 198-203.

Yan SR, Huang M, Berton G. (1997) Signaling by adhesion in human neutrophils: activation of the p72syk tyrosine kinase and formation of protein complexes containing p72syk and Src family kinases in neutrophils spreading over fibrinogen. *J Immunol.* **158**, 1902-10.

Yang, T.T., Cheng, L. and Kain, S.R. (1996) Optimized codon usage and chromophore mutations provide enhanced sensitivity with the green fluorescent protein. *Nucleic Acids Res*, **24**, 4592-4593.

Yew, N.S., Wysokenski, D.M., Wang, K.X., Ziegler, R.J., Marshall, J., McNeilly, D., Cherry, M., Osburn, W. and Cheng, S.H. (1997) Optimization of plasmid vectors for high-level expression in lung epithelial cells. *Hum Gene Ther*, **8**, 575-584.

Yokoe, H. and Meyer, T. (1996) Spatial dynamics of GFP-tagged proteins investigated by local fluorescence enhancement [see comments]. *Nat Biotechnol*, **14**, 1252-1256.

Yoshimizu, T., Sugiyama, N., De Felice, M., Yeom, Y.I., Ohbo, K., Masuko, K., Obinata, M., Abe, K., Scholer, H.R. and Matsui, Y. (1999) Germline-specific expression of the Oct-4/green fluorescent protein (GFP) transgene in mice. *Dev Growth Differ*, **41**, 675-684.

Yoshimura, K. and Crystal, R.G. (1992) Transcriptional and posttranscriptional modulation of human neutrophil elastase gene expression. *Blood*, **79**, 2733-2740.

Yousefi, S., Green, D.R., Blaser, K. and Simon, H.U. (1994) Protein-tyrosine phosphorylation regulates apoptosis in human eosinophils and neutrophils. *Proc Natl Acad Sci U S A*, **91**, 10868-10872.

Yu, C.C., Tsui, H.W., Ngan, B.Y., Shulman, M.J., Wu, G.E. and Tsui, F.W. (1996) B and T cells are not required for the viable motheaten phenotype. *J Exp Med*, **183**, 371-380.

Zheng, X.M., Wang, Y. and Pallen, C.J. (1992) Cell transformation and activation of pp60c-src by overexpression of a protein tyrosine phosphatase. *Nature*, **359**, 336-339.

Ziegler, S.F., Levin, S.D. and Perlmutter, R.M. (1989) Transformation of NIH 3T3 fibroblasts by an activated form of p59hck. *Mol Cell Biol*, **9**, 2724-2727.

Zolotukhin, S., Potter, M., Hauswirth, W.W., Guy, J. and Muzyczka, N. (1996) A "humanized" green fluorescent protein cDNA adapted for high-level expression in mammalian cells. *J Virol*, **70**, 4646-4654.

ADDITIONAL

MATERIAL

ADDENDUM

Richard Thomas

List of minor corrections

General comments

Paragraph 1 – This revised submission is much improved. It contains an increased analysis of the in-vivo and ex-vivo phenotype of the Csk conditional knockout mouse model, and in particular, the quality and depth of the discussion of these experiments is significantly improved.

Paragraph 2 – The discussion of signalling pathways and their manipulation is very clear and it is a shame that signalling events in the conditional Csk knockout were not explored more vigorously. However, we appreciate that the emphasis was on an in-vivo/ex-vivo functional examination. With this in mind, the introduction of innate immunity and specifically neutrophil function therein remains inadequate – a short section for insertion to the introduction should be included to correct this rather obvious omission for a thesis that claims an examination of phagocytic cell function in its title. Paradoxically, the discussion of the functional implications for master regulation of polymorphonuclear cell activation is extensive.

See altered original text in red, please refer to page 27 in revised PhD thesis for original text.

- **Chapter 3. Conditional mutagenesis of Csk in myeloid cells.**

3.1 Inflammation and the innate response – an introduction to neutrophil function.

Neutrophils represent the most common granulocyte subtype present in blood. Recruitment of these cells to the site of inflammation is one of the first lines of host defence against infection with microbial pathogens. Within minutes, these efficient phagocytes are recruited from the bloodstream into surrounding tissues where they engulf and kill the invading micro-organisms using a combination of oxidative and non-oxidative mechanisms. The oxidative killing mechanism involves the activation of the membrane-bound NADPH oxidase system, and is responsible for the production of large quantities of various highly reactive oxygen species that mediate the microbicidal action and destroy the pathogen (see section 3.1.4 Phagocytosis and the oxidative burst). The non-oxidative mechanisms involve various proteases, glycosidases, phospholipases, the defensins, bactericidal permeability inducing protein (BPI) and a variety of other bactericidal molecules. The importance of these neutrophilic functions are clearly demonstrated in individuals whom either lack neutrophils, have reduced neutrophil numbers, or have perturbations in neutrophil cell function. These individuals suffer from severe and recurrent infections involving usually innocuous pathogens (reviewed in Mills and Noya, 1993).

Once recruited to the site of infection, the inflammatory response maybe amplified by a positive feedback loop whereby recruited neutrophils release proinflammatory mediators which supports further recruitment of new phagocytic cells, and activation of cell function. These can include cytokines such as, IL-1, IL-6, IL-8, Il-12 and TNFα, and other mediators including nitric oxide (NO), leukotriene B4, prostaglandins, peroxides and oxygen radicals. The combined local effects of these mediators include activation of vascular endothelium, increase in vascular permeability, and activation of neutrophils, lymphocytes and natural killer cells. Thus, neutrophils can be considered as both inflammatory effector and immunoregulatory cells.

3.1.0 Neutrophil migration

Under normal conditions, resting post-capillary venule endothelium is relatively inert and does not recognise circulating leukocytes. Stimulation of endothelium with proinflammatory agents including IL-1, TNFα, or lipopolysaccharide (LPS), induces expression of endothelial cell surface molecules which specifically interact with counter-receptors upon activated leukocytes enhancing their interaction and migration across blood vessel walls into the surrounding tissues. The molecules involved in these events belong to three different structural groups; the immunoglobulin gene superfamily, the integrin family, and the selectin family.

3.1.5 Phagocytosis and the oxidative (respiratory) burst

While neutrophil migration occurs (section 3.1.0 – 3.1.4), invading microbes are opsonised, in effect, coated with antibodies and/or complement for recognition by the neutrophil. Neutrophils possess receptors specifically designed to bind the Fc fragment of the IgG molecule present on the surface of the opsonised microbe and other receptors designed to bind the activated complement factors. Binding of these receptors with their ligands stimulates phagocytosis and the microbe is internalised through a process involving de novo actin polymerisation and cytoskeletal remodelling, which results in the microbe become surrounded by pseudopodia resulting in a membrane bound vesicle known as the phagosome. Concurrently, secretory granules (lysosomes) found in the neutrophil cytoplasm fuse with the phagosome membrane to form the specialised compartment called the phagolysosome. It is here that the intracellularly sequestrated microorganism is killed and digested through a combination of oxidative and non-oxidative mechanisms.

The oxidative mechanism involves activation of the NADPH oxidase in the phagolysosomal membrane, which reduces molecular oxygen to superoxide by the following reaction (Yagisawa et al., 1996):

$$NADPH + 2O_2 \longrightarrow 2 \cdot O_2^- + NADP^+ + H^+$$

This represents the first step in a series of reactions that produces a variety of toxic oxygen species, including singlet oxygen, hydroxyl radicals ( ), hyperchlorous acid (HOCL), and chloramines (NH_2Cl, RNHCl, and $RNCl_2$) (reviewed in Verhoef and Visser 1993). To date, the exact contribution of each of these reactive oxygen species towards the killing of specific organisms is not entirely known, but together they provide an invaluable arm in the neutrophils microbicidal defence.

The critical requirement of this oxidative arm is perhaps best demonstrated in individuals with the rare condition named chronic granulomatous disease (CGD). Neutrophils of these individuals have a defective NADPH oxidase system due to mutations in one of the genes coding for the one of the NADPH subunits (reviewed in Roos *et al.*, 1996), which results in failure to generate reactive oxygen species and renders the cells profoundly ineffective in killing intracellular organisms. Consequently, this results in severe, recurrent bacterial and fungal infections (reviewed in Thrasher et al., 1996).

Neutrophil cytoplasmic granules contain many other antimicrobial agents that do not require reactive oxygen species for their activity. The fusion of the phagolysosome with these granules and the consequent release of proteases, other hydrolytic enzymes, such as glycosidases, phospholipases, and lysosymes, and other a variety of other bactericidal molecules, including the defensins, and bactericidal permeability inducing protein (BPI) serve as the non-oxidative arm of the neutrophils microbicidal defence.

The activity of these agents towards specific sequestrated microorganisms differs largely, for example, proteinase-3 is most active against gram-negative bacteria whilst cathepsin G (CLCP – chymotrypsin-like cationic protein) is more effective against gram-positive bacteria and fungi (reviewed by Gabay and Almeida, 1993). Indeed, it has been shown in this laboratory that mice deficient in both cathepsin G and elastase are more susceptible to fungal infections but also are more resistant to LPS-induced septic shock than their wild-type

counterparts (Tkalcevic *et al.* 2000). Furthermore, recent studies have demonstrated that it is these serine proteases, cathepsin G and elastase, and not the reactive oxygen species themselves that are primarily responsible for the killing of intracellularly sequestrated microorganisms (Reeves *et al.* 2002).

The action of other agents like BPI and the defensins result in a similar endpoint causing the loss of outer membrane integrity or the loss of both inner and outer membrane integrity respectively, resulting in microbial cell death. However, they are diverse in regards to their potency towards microbial targets. BPI is very potent against gram-negative bacteria, (Weiss *et al.*, 1992; Weise *et al.*, 1997), whereas defensins are potent against spirochetes, mycobacterium, fungi, and enveloped viruses (Lehrer et al., 1989).

Paragraph 3 – There is a lack of comment throughout as to the number of times an experiment has been performed – confirmation of data is clearly a basic activity in the lab and requires to be documented in the thesis. Perhaps mouse numbers have limited repetition – so be it but it is essential that a reader is aware of the confidence level for a given observation. Some of the 'differences' are modest and although of potential biological significance, one would wish to have some notion of reproducibility. Statistical analysis must be performed on all quantitative data with an indication of the number of times experiments have been repeated (or numbers of mice tested). If this has indeed been performed on all data, but p values only given when results are significant, this should be stated.

- The number of times each assay has been performed was included in the methods section of the revised thesis submission. However, I must acknowledge that the number of mice included per experimental group for each repetition had been omitted (as mouse records had been stored in the UK) and have now been included below for each methods section. The conditions for each experimental technique were metriculously titrated to give reproducible data sets. One representative experiment has been shown for each study in the results section.

    - Neutrophil apoptosis – this assay was performed in triplicate using 3 mice per experimental group (page 47).

- Neutrophil spontaneous priming (CD11b) – this assay was performed easily in excess of ten occasions using either 3 or 4 mice per experimental group. One representative experiment is shown (page 48).
- Neutrophil spontaneous priming (CD11b and CD62L) – this assay was performed in duplicate using 4 mice per experimental group (page 48).
- Mobilisation of secretory vesicles vs secondary granules – this assay was performed in duplicate using 4 mice per experimental group (page 48).
- Neutrophil degranulation – this assay was performed in quadruplicate using 4 mice per experimental group (page 49)
- Adhesion assay – this assay was performed in quaduplicate using 4 mice per experimental group (page 50).
- In vitro migration – this assay was performed in triplicate using 4 mice per experimental group (page 50).
- Confocal microscopy – this assay was performed in duplciate using 4 mice per experimental group (page 51)

- Statistical analyses (Students t-test) were performed on all quantitative data, but p-values only given when the results are significant, as was requested in the revised thesis submission.

Paragraph 3 continued: A section on statistical methods employed should be included in the methods chapter.

- **Statistical methods: The Student's *t*-test**

This test is used for comparing the means of two experimental populations, even if they have different numbers of replicates. The *t*-test compares the actual difference between two means in relation to the variation in the data (expressed as the standard deviation of the difference between the means).

$$t = \frac{\bar{x}_1 - \bar{x}_2}{\sigma_d}$$

The t-value will be positive if the first mean is larger than the second and negative if it is smaller. Manually, once the t-value is calculated, it needs to be looked up in a table of significance to test whether the ratio is large enough to say that the difference between the groups is not likely to have been a chance finding. To test the significance, the risk level (called the alpha level) needs to be set. In most experimental research, the "rule of thumb" is to set the alpha level at .05. This means that five times out of a hundred you would find a statistically significant difference between the means even if there was none (i.e., by "chance"). The degrees of freedom (df) also need to be determined for the test. In the t-test, the degrees of freedom is the sum of the persons in both groups minus 2. Given the alpha level, the df, and the t-value, the t-value can be looked up in a standard table of significance (available as an appendix in the back of most statistics texts) to determine whether the t-value is large enough to be significant. If it is, it can be concluded that the difference between the means for the two groups is significantly different (even given the variability). Fortunately, statistical computer programs routinely calculate the significance test results and circumvent the requirement for manually looking them up in a table.

Here, the statistical package provided in Microsoft Excel was used to calculate the significance levels. For our purposes, a two-tailed test was used as the direction of the test was not specified.

Paragraph 4 – With respect to the analysis of intron insertion, the introduction of this work explains far more clearly the constructs used and the rationale for their analysis. Since controls with introns placed outside the ORF were not available it remains difficult to conclude that the employed strategy is as beneficial as it is suggested, particularly given the problems encountered with some of the constructs. Inclusion in the discussion of a sentence qualifying the conclusions in this respect would be beneficial.

See altered text in red, please refer to page 126 in revised PhD thesis for original text.

- It is clear that the presence of introns within the transcription unit is beneficial to expression. Importantly, the insertion of introns directly in the open reading frame has distinct advantages over single intron positioning in the UTR or the use of genomic/cDNA hybrid genes. Most significantly, introns can act co-operatively in enhancing mRNA production (Neel *et al.*, 1993), an effect that requires at least two introns. Furthermore, authentic introns present in genomic/cDNA hybrid genes can be very large presenting an unnecessary or unfeasible load for gene delivery systems. However, it must be stated herein that due to an absence of controls with a single intron positioned within the UTR, it was not possible to make a direct comparison between these already established methods for gene expression enhancement and our novel technique. Thus, the potential benefit which our novel system may deliver over others still has to be determined experimentally. Given that, a novel approach of increasing gene expression is described herein through the introduction of heterologous introns directly into the open reading frames of two naturally intronless genes, the Cre recombinase and EGFP. Further work carried out by colleagues Rob Coffin and others demonstrated sustained long term expression of iGFP at increased levels in rat brain transduced with a herpes simplex virus-based vector. Importantly, this showed that intron-mediated enhanced expression could also attained *in vivo*. Whilst an *in vivo* study using iCre2 has not currently been undertaken, it is conceivable given the data presented here that introduction of introns into Cre recombinase open reading frame may result in enhanced expression, possibly overcoming the incomplete somatic deletion of genetic loci conditioned for Cre mediated deletion from weaker or transiently expressed promoters. Furthermore, this technology may be applied to gene therapy where expression of cDNA *in vivo* is often limited or shut down by poorly understood gene silencing mechanisms. In the first instance, application of our methodology may enhance gene expression of cDNA constructs *in vivo*. Moreover, the inclusion of introns may modulate the sensitivity of transgenes to positional effects by epigenetic silencing (Webster *et al.*, 1997). Additionally, it has been demonstrated that inactivation of the mouse ψα3 globin gene is associated with loss of introns. This associates the presence of introns not only with increased expression but also with defence against gene silencing. The mechanisms by which the presence of introns precludes a gene from being silenced are not understood at present. Thus, more

research is required into these mechanisms before this technology can be implemented for the sustainable and enhanced expression of cDNA for gene therapy. This work was submitted and subsequently published in the volume 8 of Gene Therapy, 2001 (A.Lacy-Hulbert and R.Thomas – joint first author).

Specific comments

Page 52 – it is surprising that the respiratory burst could not be measured using the described methodology – could an explanation be offered? Are there any negative data concerning phagocytosis results? It would be acceptable to show such negative outcomes if only to document the undertaken by the candidate in this area – or did the methodologies simply not succeed at all?

- The explanation for the failure of this particular experiment to yield effective results is almost certainly mechanical over biological. The experimental set up was repeated on many occasions with existing lab reagents and newly ordered reagents. Indeed, even the manufacturer of the tissue culture plates was changed in the extremely unlikely event that this would have an impact. Experiments were set up using both sorted and unsorted neutrophils to rule out the possibility of inactivation of neutrophils through the maintenance of cells on ice during the sorting procedure. The number of cells seeded into each well was also varied to ascertain whether this would have an effect. Despite these manipulations, a valid measurement of respiratory burst was not recorded. There was a reasonable chance that the spectrophotometer was not working properly as it was quite an old piece of laboratory equipment, and it was mentioned by a senior member of the institute that the filters may have needed replacing. When this subject was raised, it turned out that the replacement of the filters was a departmental cost, and there was a lack of funds at that time. Carrying out the experiment on a different spectrophotometer was not possible as this was the only apparatus at the time with a heated 37°C chamber to allow maintenance of plate temperature over the entirety of the experiment. Every attempt was undertaken to force this experimental procedure to give valid measurements with the experimental apparatus present at the time, but as stated none were obtained.

- There are no data for the measurement of phagocytosis. The methodology for the measurement of phagocytosis was provided to give the reader an overall account of the different methodologies that could be employed to monitor neutrophil activity as was requested for the revised thesis submission.

Page 66 – 67 – some further exploration of the means whereby cell numbers are reduced is an obvious conclusion from this experiment – could usefully link this to later chapters.

See altered text in red, please refer to page 67 in revised PhD thesis for original text.

- Previous studies have demonstrated the importance of Csk in development. Indeed, germline inactivation of Csk results in embryonic lethality in mice (Imamoto and Soriano, 1993; Nada *et al.*, 1993). Furthermore, using Cre/loxP technology, Csk has been implicated in the control of receptor-mediated development of T-lymphocytes (Schmedt *et al.*, 1998). To determine the role of Csk in myeloid cell development, bone marrow derived cell suspensions were analysed (figure 8.3). Total numbers of nucleated cells derived from SPF maintained control and Csk-GEcre mouse colonies showed no significant difference (figure 8.3a). Flow cytometric analysis for Gr1 cell surface expression showed no difference in either $Gr1^{hi}$, nor $Gr1^{lo}$ percentages demonstrating no difference in the mature or immature granulocyte populations respectively (figure 8.3b). To assess whether Csk played a role in myeloid cell lifespan and turnover, BrdU incorporation into leukocytes was measured in mice receiving BrdU in their drinking water. No difference was observed in granulocyte turnover between Csk-GEcre and control mice (figure 8.3c). Induction of sterile peritonitis revealed that granulocytes were recruited efficiently into the peritoneal cavity. However, in accordance with the apparent selection against Csk-deficient granulocytes demonstrated in the deletional analysis (figure 8.1c), Csk-GEcre granulocyte numbers were reduced compared to controls reaching significance at later stages of the inflammatory response (figure 8.3d). This counter-selection could be due to increased apoptosis and/or clearance of activated neutrophils within the inflammatory site, or impaired recruitment due to enhanced

adhesiveness and/or impaired migratory capacity, consequently leading to reduced recovery of Csk-deficient cells.

Page 72 – now much improved with a dose response – how did one achieve a >90% mortality with 3 mice per lowest dose group? Presume number is reference to overall groups – please clarify.

See altered text in red, please refer to page 72 in revised PhD thesis for original text.

- A strict correlation between myeloid Csk deficiency and an inappropriate sustained inflammatory response associated with acute perivascular pneumonia has been demonstrated (figure 8.2). This phenotype was abrogated upon embryo transfer of the mouse colony into a specific pathogen free environment. Mice deficient for the Src-fk Hck and Fgr are resistant to endotoxin (Lowell and Berton, 1998). If deregulated Src-fk activity caused granulocyte hyperresponsiveness observed in conventionally housed Csk-GEcre mice, this should also affect susceptibility to endotoxin (LPS, lipopolysaccharide). Indeed, Csk-GEcre mice proved hyper-responsive to the high dose model of endotoxemia (figure 9.2a-c). While intra-peritoneal administration of LPS at 10mg/kg induced lethal endotoxic shock in all Csk-GEcre mice (n=6), all control mice were fully protected (figure 9.2a). Extending this study, the rate of mortality at lower doses of LPS was assessed. While controls remained fully protected, Csk-GEcre mice remained hyperresponsive to LPS at 5mg/kg (n=6, figure 9.2b) and 2.5mg/kg (n=3, figure 9.2c), demonstrated by greater than 90% mortality rate over all groups. Both experimental groups showed characteristic symptoms of endotoxemia including shivering, piloerection, apathy, and eye secretion. However, these symptoms were more pronounced in the conditional mutants. No deaths were observed at 0.5mg/kg LPS (n=3) in either controls or Csk-GEcre mice indicating that the LD50 for Csk-GEcre mice lies between 0.5mg/kg and 2.5mg/kg. The availability of Csk-GEcre mice and the distress induced by endotoxic shock upon these mice prevented any further titration.

Figure 9.2 – what is the likely in-vivo significance of the relatively modest alteration in annexin V demonstrated after in-vitro culture over 48hrs? Why were no detailed studies of mechanisms of apoptosis in Csk-deficient cells undertaken – seems an obvious line of enquiry? Acknowledge the concerns expressed by some that annexin A is suboptimal for apoptosis measurement in neutrophils.

See altered text in red, please refer to page 72 in revised PhD thesis for original text.

- Acute lung injury, a symptom characteristic of acute respiratory distress syndrome (ARDS), develops from the release of proteases and reactive oxygen intermediates (ROI) from PMN sequestered in the pulmonary microvasculature and PMN infiltration into the alveolar airspace (Tate and Repine, 1983). To determine whether acute lung injury may have contributed to the mortality observed in the conditional mutants, lungs were removed from LPS challenged mice for histopathological analysis. Chronic vascular damage and hemorrhagic lesions were indeed observed in lung sections derived from Csk-GEcre mice receiving 10mg/kg LPS, which were not observed in the control group (figure 9.2e/f). Interestingly, LPS-stimulated Csk-GEcre granulocytes demonstrate delayed apoptosis after 48hr culture in vitro (controls 71 ± 5%, Csk-GEcre 59 ± 6% AnnV positive cells, p=0.01. Figure 9.2g). This subtle increase in resistance to apoptosis may contribute to the local accumulation of neutrophils in the pulmonary vasculature over time. This effect may potentially be further amplified by a positive feedback loop through the local release of inflammatory mediators (figure 9.2d). Notably, Csk-GEcre mice housed under normal conditions display a sustained local accumulation of neutrophils (figure 8.2) which is not associated with significant tissue damage observed in specific pathogen free Csk-GEcre mice challenged with endotoxin, indicating a lack of secondary signals necessary for the full-blown acute inflammatory response. This further illustrates the versatility of Csk as a master regulator of neutrophil function through the imposition of activation checkpoints.

- No detailed studies of mechanisms of apoptosis were undertaken because the increase in resistance to apoptosis between control and Csk-GEcre neutrophils

was small, and potential differences would almost certainly be masked. Additionally, whereas flow cytometric analysis requires relatively few cells to identify statistically relevant apoptotic populations, more detailed studies of the mechanisms of apoptosis in Csk-GEcre neutrophils would require not only much larger cell quantities which would be precluded by experimental mice numbers, but also would involve much more processing which could alter their apoptotic potential.

Flow cytometric detection of externalised phosphatidylserine expressed on apoptotic cells using fluorescein labelled Annexin V has been described (Vermes *et al.*, 1995) and has become a popular technique for apoptosis detection within mixed leukocyte populations. However, it must be noted that stimulation of neutrophils with pro-inflammatory mediators leads to the production of an oxidative burst (Hampton *et al.*, 1998) and an associated change in intracellular pH (Roos and Winterbourn, 2002), which has been documented to affect the intensity of fluorescein isothiocyanate (FITC) used in flow cytometry (Babcock, 1983). Thus caution should be employed when making statements concerning differences in apoptosis between cell populations when flow cytometry is the only method used, and ideally flow cytometric data should be supported with supplementary evidence provided from another technique for apoptosis detection.

Page 75 – hepatic histology better shown as table and perhaps some representative photos to orientate the reader as to the magnitude of changes reported.

Hepatic histology was assessed and scored independently by Dr Marco Novelli within the Histopathology department of University College Hospital. No photographic images were captured at that time. All of my histopathological slides were couriered to Australia for the acquisition and submission of new images for my revised thesis submission (seen in figure9.2e and 9.2f). These were unfortunately disposed of during my acrimonious break of which you have been made aware. As such, it is not possible for representative images requested to be submitted. Furthermore, in the absence of such images to necessitate an

accompanying hepatic data table, the presentation of the data in the current format demonstrates amply the magnitude of changes scored by the histopathologist.

Page 76 – negative controls should always be included (especially in a PhD) but we accept on this occasion that the candidate has acknowledged the omission in experimental design.

Page 76 – was shape change confirmed by simple phase microscopy or equivalent?

- Shape change was indeed confirmed by phase microscopy and confocal microscopy. Bone marrow leukocytes were collected and either fixed immediately in formalin, or cultured for 30 minutes at 37°C in DMEM, 5% heat-inactivated FCS, 20mM HEPES and fixed as described in section 4.10. Cells cultured in suspension were fixed with formalin and then adhered to poly-lysine coverslips before staining as described. In the first instance, cells were viewed with conventional phase contrast microscopy although no images were captured as it was thought that a better representation of the difference in cellular architecture would be best demonstrated with the specific stains for both CD11b and actin. These pictures can be viewed in section 9.6. Extensive staining for polymerised actin at the sites of β2-integrin clustering strongly indicate enhanced cytoskeletal remodelling in suspension cultured cells which would be reflected in the shift of forward scatter.

How reproducible are the various signalling data shown – has some quantification been attempted?

- The signalling data are extremely reproducible. Both experiments (a) and (b, upper panel) had been performed in excess of 5x and 10x respectively with identical results. Indeed, the abrogation of Src mediated tyrosine phosphorylation using PP2 in (b, lower panel) was again very reproducible, having observed this result or similar results in excess of three occasions. The phosphorylation of

enolase by immunoprecipitated Hck was repeated twice and demonstrated a similar fold increase in Hck activity in Csk-deficient cells. Panels revealed in (d) are representative of one of at least three independent experiments and show good reproducibility.

- Quantification was carried out on the activity of Hck only. The comments made for increased tyrosine phosphorylation of cellular protein in Csk-deficient cells, and for the augmented phosphorylation of integrin signalling proteins: cortactin, syk and paxillin are based purely on the qualitative assessment of the data. No densitometric quantifications were performed for these data.

Additional References

Babcock, D.F. (1983) Examination of the intracellular ionic environment and of ionophore action by null point measurements employing the fluorescein chromophore. *J. Biol. Chem.*, **258**, 6380-6389.

Gabay, I.E., and Almeida, R.P. (1993). Antibiotic peptides and serine protease homologs in human polymorphonuclear leukocytes: Defensins and azurocidin. *Curr. Opin. Immunol.* **15**, 97-102.

Hampton, M.B., Kettle, A.J., Winterbourn, C.C. (1998) Inside the neutrophil phagosome: oxidants, myeloperoxidase, and bacterial killing. *Blood*, **92**, 3007-3017.

Lehrer, R.I., Barton, A., Daher, K.A., Harwig, S.S., Ganz, T., Selsted, M.E. (1989). Interaction of human defensins with E. coli. Mechanismscof bactericidal activity. *J.Clin. Invest.*, **84**, 553-561.

Mills, E.L., and Noya, F.J. (1993) Congenital neutrophil deficiencies. Published in The Neutrophil (ed. Abramson, J.S. and Wheeler, J.G.) IRL press, Oxford. 183-215.

Reeves, E.P., Lu, H., Jacobs, H.L., Messina, C.G., Bolsover, S., Gabella, G., Potma, E.O., Warley, A., Roes, J., Segal, A.W. (2002) Killing activity of neutrophils is mediated through activation of proteases by K+ flux. *Nature*, **416**, 291-297.

Roos, D., Boer, M., Kuribayashi, F., Meischi, C., Weening, R.S., Segal, A.W., Ahlin, A., Nemet, K., Hossle, J.P., Bernatowska-Matuszkiewicz, E., Middleton-Price, H. (1996). Mutations in the X- linked and autosomal recessive forms of chronic granulomatous disease. *Blood*, **87**, 1663-1681.

Roos, D. and Winterbourne, C.C. (2002) Immunology: lethal weapons. *Science*, **292**, 669-671.

Thrasher, A.J., Keep, N.H., Wientjes, F., Segal, A.W. (1994). Chronic granulomatous disease. *Biochim. Biophys. Acta.* **1227**, 1-24.

Verhoef, J. and Visser, M.R. (1993) Neutrophil phagocytosis and killing: normal function and microbial evasion. Published in The Neutrophil (ed. Abramson, J.S. and Wheeler, J.G.) IRL press, Oxford. 109-131.

Vermes, I., Haanen, C., Steffens-Nakken, H. and Reutelingsperger, C. (1995) A novel assay for apoptosis. Flow cytometric detection of phosphatidylserine expression on early apoptotic cells using fluorescein labelled Annexin V. *J. Immunol. Methods*, **184**, 39-51.

Weise, A., Brandenburg, K., Carroll, S., et al. (1997). Mechanisms of action of bactericidal/permeability increasing protein BPI on reconstituted outer membranes of gram negative bacteria. *Biochemistry*, **36**, 10311-10319.

Weiss, J., Elsbach, P., Shu, C., Castillo, J., Grinna, L., Horwitz, A., Theofan, G. (1992). Human bactericidal/permeability increasing protein and a recombinant NH2 terminal fragment cause killing of serum resistant gram negative bacteria in whole blood and inhibit tumour necrosis factor release induced by the bacteria. *J. Clin. Invest.* 1122-1130.

Yagisawa, M., Yuo, A., Yonemaru, M., Imajoh-Ohmi, S., Kanegasaki, S., Yazaki, Y., Takaku, F. (1996). Superoxide release and NADPH oxidase components in mature human phagocytes: correlation between functional capacity and amount of functional proteins. *Biochem. Biophys. Res. Commun.* **228**, 510-516.